



University of
Stavanger

Faculty of Science and Technology

MASTER'S THESIS

Study program/ Specialization: Mechanical and Structural Engineering and Materials Science / Mechanical Engineering	Spring semester, 2016 Open access
Writer: Kristen Rege (Writer's signature)
Faculty supervisor: Dimitrios G. Pavlou External supervisor(s):	
Thesis title: Water Hammer Induced Vibration of Steel Pipelines Repaired with FRP Composites	
Credits (ECTS): 30	
Key words: Solid mechanics, thin-walled cylinders, pipe vibration, dynamic analysis, fibre-reinforced polymer, composite overwrap, pipeline repair, water hammer, fluid transients, pressure wave	Pages: 82 + enclosure: 26 Stavanger, 14.06.2016

Abstract

Since the 1990s, there has been an increasing trend to repair corroded or eroded pipelines, conveying oil, gas or water, by using fibre-reinforced polymer (FRP) composites. This relatively new repair technique involves wrapping the corroded part of the pipeline with a so-called FRP overwrap. FRP materials are lightweight, have high relative strength and do not corrode, making them an effective repair solution.

The viability of this repair technique has been proved by the numerous research programs which have been performed. However, most of the literature regarding the design of FRP overwraps does only consider a static internal pressure. In this thesis, the behaviour of steel pipelines, repaired with FRP overwraps, subjected to water hammer conditions, has been investigated. Water hammer is the occurrence of pressure waves in the conveyed liquid, due to abrupt changes to steady flow conditions, for example the rapid closure of a valve.

An approximate dynamic model, describing the radial vibration of steel pipes with a FRP overwrap, due to water hammer conditions, has been derived. The model is based on the theory of thin-walled cylinders, and the laminate stiffness matrix for a FRP laminate. In order to take the steel pipe into account, the laminate stiffness matrix was modified. Basic water hammer theory was used to find the magnitude and velocity of the water hammer-induced pressure wave. These properties defined the exciting load in the dynamic analysis of the repaired pipe wall. The derived governing equation was solved analytically by applying boundary conditions and utilising the properties of Fourier series. This resulted in series expressions for the radial deflection and the pipe wall stresses, as functions of the distance from the valve, and time since valve closure.

The model was also implemented on representative examples, with two different FRP materials; E-Glass/Epoxy and T300/5208 Carbon/Epoxy, and the influence of the thickness of the FRP overwrap was investigated. For both these materials, the model predicted the maximum radial deflection, due to the water hammer, to decrease if the overwrap was thin, and increase if the overwrap was thick. The reason was found to be that the natural frequency of the pipe is significantly altered when a thick FRP overwrap is applied, because of its low density, compared to the steel pipe. As the FRP overwrap gets thicker, the water hammer-induced vibration approaches a state of resonance, increasing the amplitude of the vibration. The rate, at which the amplitude increases, with respect to the thickness of the overwrap, will depend on the density and stiffness of the FRP material. The increased amplitude nevertheless causes an increased maximum radial deflection, and thereby increased stresses. During the design of a FRP overwrap for a pipe which is susceptible to water hammer conditions, it will therefore be important to ensure that the changed natural frequency does not lead to unacceptable stresses.

Table of Contents

Symbols and abbreviations	vii
Acknowledgements	xi
1. INTRODUCTION	1
1.1 Background	1
1.2 Purpose	2
1.3 Structure of the thesis	3
2. THEORY	5
2.1 Fibre-reinforced polymer (FRP) laminates	5
2.1.1 Materials and properties	5
2.1.2 Laminate nomenclature	6
2.1.3 The laminate stiffness matrix	8
2.1.4 Failure criterion for FRP laminae	10
2.2 Repair of pipelines	10
2.2.1 Conventional repair techniques	10
2.2.2 FRP overwraps	11
2.2.3 Repair techniques with FRP materials	12
2.2.4 Mechanics of the repaired pipe	13
2.3 Water hammer	14
2.3.1 General description	14
2.3.2 Effect of friction losses	17
2.3.3 Effect of valve closure time	17
2.3.4 Other causes of water hammer conditions	18
2.3.5 Brief history and fundamental equations	18
2.4 Vibration of pipelines due to water hammer conditions	19
2.4.1 Uncoupled models	19
2.4.2 The velocity of the pressure wave	20
2.4.3 Coupled models	21
2.4.4 Choice for this thesis	22
3. MODEL DEVELOPMENT	23
3.1 Equations of motion for a thin-walled axisymmetric cylinder	24
3.2 Relationships between internal forces, moments and the radial deflection	27
3.2.1 Relationships for a laminated FRP pipe	27
3.2.2 The stiffness matrix for a steel pipe repaired with a FRP overwrap	27
3.2.3 Relationships between strains, curvatures and the radial deflection	29
3.3 The governing equation of motion	30
3.3.1 The mean density of the pipe wall	31
3.3.2 The velocity of the pressure wave in a steel pipe with FRP overwrap	31
3.3.3 Mathematical formulation of the pressure wave	32
3.4 Analytical solution of the governing equation of motion	33

3.4.1	Convergence of the sum	37
3.5	Static pipe deformation.....	39
3.6	The critical velocity	40
3.7	The radial deflection during the wave of pressure unloading	42
3.8	Pipeline stresses	43
4.	RESULTS AND DISCUSSION.....	45
4.1	Immediate comments to the derived model.....	45
4.2	Implementation of the model	46
4.3	The behaviour of the pipeline under water hammer conditions	47
4.3.1	The deformed shape	47
4.3.2	The wave of pressure unloading	50
4.3.3	The wave of low pressure	52
4.3.4	The frequency of the vibration, and possibility for fatigue.....	53
4.4	The influence of the FRP overwrap	54
4.4.1	E-Glass/Epoxy laminate with fibre directions +/- 45°	55
4.4.2	E-Glass/Epoxy laminate, fibre directions +/- 45°, for a larger pipe	58
4.4.3	E-Glass/Epoxy laminate with fibre directions 90/90/0°	59
4.4.4	T300/5208 Carbon/Epoxy laminate with fibre directions +/- 45°	60
4.5	Recommendations for further research	63
5.	CONCLUSION	65
6.	REFERENCES.....	67

APPENDIX A. MATLAB PROGRAM

Symbols and abbreviations

The most important symbols and abbreviations which are used in this thesis are listed here alphabetically. Other symbols, which may be used in no more than one formula, are defined in the main text, where they are used.

A_{ij}, B_{ij}, D_{ij}	Components of the laminate stiffness (ABD) matrix
a_r, a_x	Acceleration component in directions r and x
b_n	Coefficient in the Fourier sine series for the dynamic pressure
DLF	Dynamic load factor
E_1	Elastic modulus of a FRP lamina, in its principal direction 1
E_2	Elastic modulus of a FRP lamina, in its principal direction 2
E_{st}	Elastic modulus for the steel pipe
F_i	Coefficients in the Tsai-Wu failure criterion
F_r, F_x	Force component in directions r and x
FRP	Fibre-reinforced polymer
FSI	Fluid-structure interaction
f_y	Yield strength of steel
G_{12}	Shear modulus of a FRP lamina
G_{st}	Shear modulus for steel
$H(\bullet)$	The Heaviside step function
h	Total thickness of a pipe wall
h_{la}	Thickness of one FRP lamina
h_{st}	Thickness of the steel pipe
IR	Inner radius of steel pipe
K	Elastic modulus of a liquid
k	Number of layer (steel layer or FRP lamina)
k_x^0, k_y^0	Mid-plane curvatures in directions x and y
k_{xy}^0	Mid-plane twisting curvature
L	Length of the pipe
M_x, M_y	Bending moments per unit length in directions x and y
M_{xy}	Twisting moment per unit length
MR	Outer radius of steel pipe
m	Cosine of the angle θ
m	Mass
N	Total number of laminae in a laminate
N_F	Number of terms of the Fourier series solution which should be calculated to ensure convergence

N_x, N_y	Normal forces per unit length along axes x and y
N_{xy}	Shear force per unit length
n	Sine of the angle θ
n	Number of a term in a Fourier series
OR	Outer radius of FRP overwrap
P	Internal gauge pressure
$p(x, t)$	Dynamic internal gauge pressure
$p_{tot}(x, t)$	Static + dynamic internal gauge pressure
p_0	Gauge pressure in pipe under steady-state fluid flow
p_n^*	Coefficient in term n of the Fourier sine solution
Q_{ij}	Reduced stiffnesses of a FRP lamina
\bar{Q}_{ij}	Transformed reduced stiffnesses of a FRP lamina
$\bar{Q}_{ij, st}$	Transformed reduced stiffnesses of a steel plate
R	Mean radius of a pipe
r	Radial coordinate in a cylindrical coordinate system
T_r	Duration of a round trip for the pressure wave
t	Time
u	Axial displacement
V	Steady-state flow velocity
V_i	Shear force per unit length with respect to the i -axis
V	Volume
W_n	Coefficient in term n of a Fourier series
w	Radial deflection/displacement
w_0	Static radial deflection/displacement
w_{mean}	Mean radial deflection
w_{st}	Equivalent static radial deflection, if the dynamic pressure had been static
X	Distance from the pressure wave front
x	Coordinate along a FRP laminate, or in the axial direction of a pipe
y	Coordinate across a FRP laminate, or in the circumferential direction of a pipe
z	Coordinate perpendicular to a composite plate or pipe wall
z_k	Distance from the mid-plane of a composite plate/pipe wall, to the top of layer k
α	Velocity of the pressure wave, also called the pressure wave speed or the wave propagation speed
α_{cr}	The critical velocity; i.e. the pressure wave speed which causes resonance
γ	Coefficient in the derivation of the critical velocity

γ_{12}	In-plane shear strain in a FRP lamina in principal directions 1,2
γ_{xy}	In-plane shear strain in directions x, y
γ_{xy}^0	Mid-plane shear strain in directions x, y
Δp	Pressure increase due to water hammer conditions, i.e. the magnitude of a pressure wave
ϵ_1, ϵ_2	Normal strains in the principal directions 1,2 of a FRP lamina
ϵ_x, ϵ_y	Normal strains in directions x and y
$\epsilon_x^0, \epsilon_y^0$	Mid-plane normal strains in directions x and y
θ	Angle between the x -axis, and the principal direction 1 (fibre direction) of a FRP lamina
Λ	Coefficient in the derivation of the critical velocity
λ_i	Coefficients for the governing equation of motion
ν_{12}, ν_{21}	Poisson's ratios for a FRP lamina
ν_{st}	Poisson's ratio for steel
ξ	Variable in the derivation of the critical velocity
ρ_f	Fluid density
ρ_{la}	Density of a FRP lamina
ρ_m	Mean density of a steel pipe fitted with a FRP overwrap
ρ_{st}	Density of steel
σ_1, σ_2	Normal stresses in the principal directions 1,2 of a FRP lamina
σ_e	von Mises equivalent stress
σ_x, σ_y	Normal stresses in directions x and y
σ_1^C	Compressive failure stress of a FRP lamina, in its principal direction 1
σ_2^C	Compressive failure stress of a FRP lamina, in its principal direction 2
σ_1^T	Tensile failure stress of a FRP lamina, in its principal direction 1
σ_2^T	Tensile failure stress of a FRP lamina, in its principal direction 2
τ_{12}	In-plane shear stress in a FRP lamina in principal directions 1,2
τ_{xy}	In-plane shear stress in directions x, y
τ_{12}^F	Shear failure stress of a FRP lamina
φ	Angular coordinate in a cylindrical coordinate system
Ω_n	Coefficient in term n of the Fourier sine solution
ω	Coefficient in the Fourier sine solution
ω_n	Coefficient in term n of the Fourier sine solution

Acknowledgements

This thesis is submitted in partial fulfilment of the requirements for the degree Master of Science in Mechanical and Structural Engineering and Materials Science, specialisation in Mechanical Engineering, at the University of Stavanger. The research presented has been carried out at the University of Stavanger during the spring semester of 2016.

The main findings of this work have been presented in an article, which has been submitted for publication in the scientific journal *Oil and Oil Products Pipeline Transportation: Science & Technologies*. As these two works have been written simultaneously by the same author, and neither of them is currently published, this thesis will not make further references to this article.

I would like to express my sincere gratitude to my supervisor, Professor Dimitrios G. Pavlou, for suggesting the topic of this thesis, and for his excellent guidance and advices throughout this semester. His previous works have also served as good sources for information and inspiration for this thesis.

I would also like to thank mathematics student Helge, for suggesting an excellent book on the solution of differential equations, which saved me a lot of time. Furthermore, I am grateful to Jørn Hansen and the rest of the fellows at the mechanical engineering students' room at the university, for great moral support and for providing a nice working environment.

Finally, I would like to thank my parents for their great encouragement and support.

Rege in Sola, 13.06.2016

Kristen Rege

1. Introduction

1.1 *Background*

The main material for pipeline manufacturing today is still carbon steel [1]. During their service life, carbon steel pipelines are subjected to various deterioration mechanisms, like corrosion and erosion. If unattended to, these mechanisms may lead to reduced pipe thickness and surface cracks, or in the worst case complete failure. However, pipeline monitoring and assessment are now in widespread use, which often makes repair or replacement prior to failure possible [2]. The use of fibre-reinforced polymer (FRP) composites to repair and strengthen such pipelines is increasing, both for onshore and offshore pipelines. Some advantages of using FRP for repairing the pipes are the possibility of repair without pipeline shut down, and the elimination of the explosion risk due to welding [3]. These attributes make the repair process simpler. Additionally, FRP is also made viable by its high-tensile strength, lightweight and non-corroding attributes [4].

When a pipe is subjected to the deterioration mechanisms mentioned above, its thickness will be reduced, either locally, or over a larger area. The reduced thickness leads to a reduced strength, which may drop below the required design strength. Stress and strain analyses of pipes which are repaired with FRP overwraps and subjected to a static pressure exist [3,5], but according to the author's knowledge, there have not been any theoretical analyses of how such pipelines behave under water hammer conditions.

Water hammer, also called fluid hammer, or fluid transient, is a phenomenon which is generated by abrupt changes to steady flow conditions, like the rapid closing of a valve in the end of a pipeline [6]. The liquid is locally compressed, causing a pressure wave, which travels up and down the pipe, alternating between higher and lower values than the steady-state pressure. This pressure wave causes the pipe to vibrate, leading to increased deformations and stresses in the pipe, which may result in catastrophic consequences to the pipeline integrity [1], if not taken into account in the design phase. The water hammer phenomenon is characterized by its familiar sound, which resembles the sound produced when a pipe is "hammered" [7:p45], hence its name. Even though it is normally called water hammer, the phenomenon can occur with any liquid [8:p559].

Water hammer is an important problem in the design of hydroelectric plants, where the flow of water needs to be rapidly varied [8], in order to maintain correct frequency for the produced electricity, when the electricity demand changes [9]. It may also be a problem in the design and operation of other types of hydraulic systems, like water-supply networks, irrigation systems, industrial conduits, distribution systems and waste piping, and cooling circuits of thermal and nuclear power stations [10:p21].

Water hammer may also occur in oil hydraulic systems [11:p80], and even in your own home, when valves in dishwashers or washing machines are closed [12], or when you quickly close the tap in a sink.

Several methods exist in order to protect a pipeline from damage by water hammer [6,7,8]. If there is no specific need for sudden changes to the steady flow, a slow-closing valve may be used to control the flow, thereby preventing water hammer from happening at all. If rapid valve motion is needed, a surge tank may be used. This is a long standpipe, which is connected to the pipeline directly upstream the valve in question. The surge tank is open in the top, thereby allowing the liquid to flow into the surge tank when the valve is closed, instead of being compressed in the pipe. Other damage-preventing devices are air chambers, flexible hoses, pump flywheels, relief valves and rupture disks.

As these damage-preventing devices are quite expensive, they are not necessarily always used in pipelines in which water hammer may occur. Water hammer analyses may be carried out to determine if the pipeline is strong enough on its own, or alternatively what the dimensions of these devices should be [6]. Additionally, these devices may not prevent water hammer to occur, instead only limiting its effect. There is therefore great reason to believe that many steel pipelines in need of repair are susceptible to water hammer conditions. If these pipelines are to be repaired with a FRP overwrap, it will be important to have knowledge about how the repaired pipeline will behave under water hammer conditions. This is necessary to ensure that the repaired pipeline will be able to survive such events.

1.2 Purpose

The goal of this thesis is to develop an analytical model for the dynamic response of a repaired pipeline due to water hammer conditions, i.e. an expression for the radial deflection of the pipe as a function of distance from the valve, and time since valve closure. The pipeline in question is made of steel (or any other isotropic metal), and repaired with an overwrap consisting of laminated fibre-reinforced polymer (FRP). When the radial deflection is known, the pipe wall stresses may easily be calculated. The model should then be applied to some examples, in order to investigate how the FRP overwrap influences the dynamic response of the pipe.

In order to limit the extents of the thesis, the same approximations and assumptions as Pavlou has used in his works on water hammer [1,13] have been adopted. This includes neglecting the effects of material damping and friction between the liquid and the pipe wall. The pipe is also assumed to be straight, thin-walled, and axially restricted throughout its length. Although this model is quite simplified, it captures the essential features of the pipeline behaviour [14], and may increase the qualitative understanding of the problem. This simplified model may also be used as a starting point for further research and development of more sophisticated models.

1.3 *Structure of the thesis*

Chapter 2 of this thesis covers much of the theory which is required to develop the desired analytical model. Material on FRP materials, pipe repair techniques and water hammer is provided, in order to give the reader the required knowledge to understand the model development. Additionally, a brief literature study on water hammer-induced vibration of pipelines is presented, and arguments for using the chosen simplifications are given.

In chapter 3, the analytical model for the dynamic radial vibration is derived. Some theory not included in chapter 2 is presented here instead, in order to avoid repeating it. The developed model is implemented on representative examples in chapter 4, and the model and its results are thoroughly discussed. Lastly, conclusions are given, before a MATLAB program for implementing the model is presented in the appendix.

2. Theory

2.1 *Fibre-reinforced polymer (FRP) laminates*

2.1.1 Materials and properties

The information presented in this subsection is taken from section 2.2 in "Composite Overwrap Repair System for Pipelines – Onshore and Offshore Application" by Saeed [3] and chapter 2 in *Composite Materials in Piping Applications* by Pavlou [15].

Fibre-reinforced polymer (FRP) laminates consist of multiple thin laminae, or layers. Each lamina is a composite, made by a polymer (plastic) matrix material, which is reinforced by fibres. In one single lamina, all the fibres are orientated in the same direction. As the fibres have much higher strength than the matrix, the mechanical properties of FRP materials are directionally dependent. FRP materials are thereby anisotropic. When multiple laminae are stacked on top of each other, one obtains a laminate.

Two main classes of resins are used for the polymer matrix; thermosets and thermoplastics. The main difference between these two classes is how they behave when heated. When thermosets are heated for the first time, their microstructure is irreversibly changed – they are cured. After curing, thermosets do not melt when heated, but will retain their shape until their thermal decomposition at very high temperatures. Examples of thermoset resins are polyesters, vinyl esters, epoxies and polyurethanes. Thermosets are the most common type of resin used for matrix fabrication for FRP composites, because of their mechanical stability in hot and moist conditions, good chemical resistance, good dimensional stability, low processing temperatures, excellent fibre impregnation, and low cost.

Thermoplastics on the other hand become malleable at high temperatures, and solidify when cooled. They can therefore be reshaped when heated, which allows them to be repaired. The manufacturing costs are lower for thermoplastics, and they have higher toughness than thermosets. Polypropylene and polyethylene are the most common thermoplastic resins used in FRPs.

The three common types of fibre materials are carbon (or graphite), glass and synthetics. E-glass is the most commonly used, as it is strong and has good heat resistance. If higher tensile strength or heat resistance is required, the more expensive S-glass may be used. Carbon fibres are lighter, have higher modulus of elasticity and strength, but at a higher cost.

The use of FRP materials is increasing, because of their many advantages compared to other materials, like steel. The advantages include good corrosion resistance, high

specific strength (strength-to-weight ratio), high dimensional stability and great flexibility in design. FRP materials are more expensive than steel per unit mass, but due to their high specific strength, their material cost per unit strength is lower [15]. It is therefore expected that it will be advantageous also to use FRP materials for pipeline repair purposes.

Typical mechanical properties of four common FRP materials, all with epoxy matrices are given in table 1. Please refer to the list of symbols after the table of contents, or the following sections, for an explanation of the symbols used.

Table 1. Material properties of widely used composites [15,16].

	E-Glass/Epoxy	S-Glass/Epoxy	AS/3501 Carbon/Epoxy	T300/5208 Carbon/Epoxy
E_1 (GPa)	39	43	138	181
E_2 (GPa)	8.6	8.9	8.96	10.3
G_{12} (GPa)	3.8	4.5	7.10	7.17
ν_{12}	0.28	0.27	0.30	0.28
σ_1^T (MPa)	1080	1280	1447	1500
σ_1^C (MPa)	620	690	1447	1500
σ_2^T (MPa)	39	49	51.7	40
σ_2^C (MPa)	128	158	206	246
τ_{12}^F (MPa)	89	69	93	68
ρ_{la} (kg/m ³)	2100	2000	1600	1600

2.1.2 Laminate nomenclature

This section is inspired by sections 1.2.2 and 1.2.7 in *Composite Materials in Piping Applications* by Pavlou [15].

As mentioned in the previous section, a FRP laminate consists of multiple laminae. Each lamina has all its fibres along its principal direction 1. When multiple laminae are stacked on top of each other in a laminate, the direction of the fibres may vary from one lamina to the next. The stacking sequence of the laminate will therefore influence its stiffness.

Let a global coordinate system have axes x and y in the length and width directions of a laminate plate respectively, while the z -axis is perpendicular to the laminate. See figure 1. The xy -plane is the midplane of the laminate, so that $z = 0$ in the middle of the laminate.

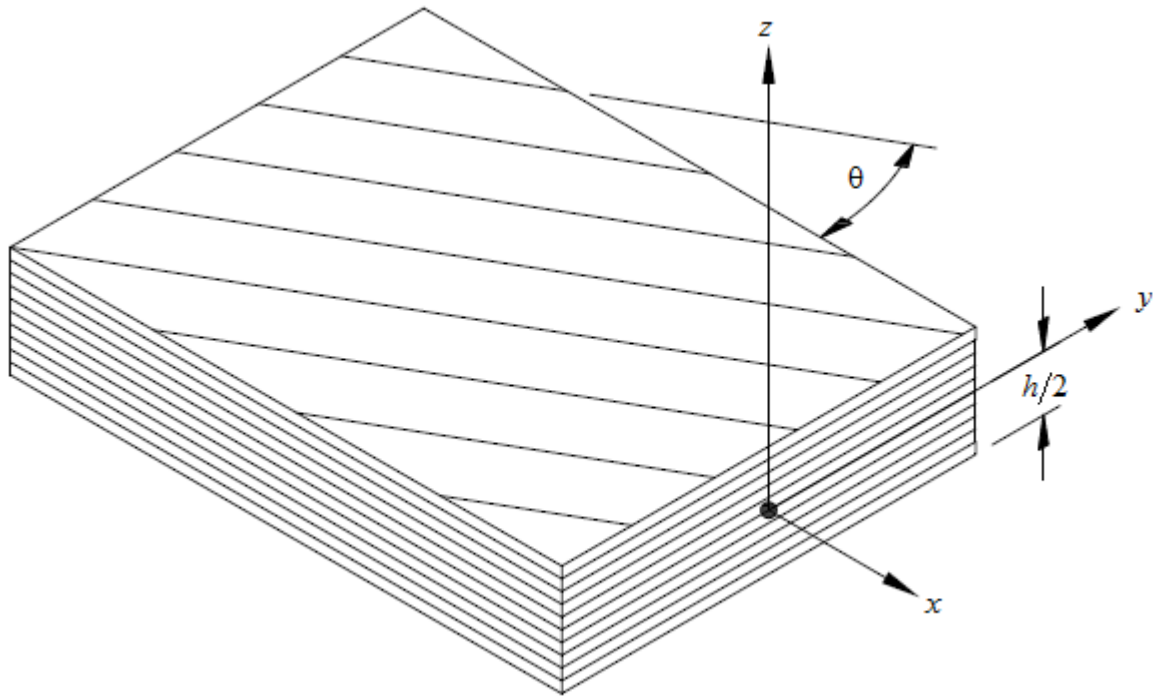


Figure 1: Global coordinate system for a FRP laminate.

The direction of the fibres is described by the angle θ for each lamina. The stacking sequence may then be described by a vector of these angles. For example, a laminate may be denoted as $[0/60/90/0]$. This means that the first (bottom) and last (top) lamina have their fibres along the global x-direction, while the fibres are directed 60° and 90° from the x-axis in the second and third lamina respectively. The fibres in the third lamina thereby run parallel to the global y-direction.

A laminate may be symmetric. This means that the stacking sequence above the midplane ($z > 0$) is a mirror image of the stacking sequence below ($z < 0$). Additionally, the thickness and material properties of a lamina at $z = +k$ must be equal to those of the lamina at $z = -k$, for all laminae, in order for the laminate to be symmetric. The s in the laminate notation $[\pm 45/0]_s$ means that it is symmetric, and it will therefore have the stacking sequence $[+45/-45/0/0/-45/+45]$.

A repeated group of laminae within the laminate may be denoted like $[(\pm 45/0)_2]_s$, which is a shortened notation for $[+45/-45/0/+45/-45/0/0/-45/+45/0/-45/+45]$.

The laminates which are considered in this thesis are balanced. A laminate is balanced if it for every lamina with orientation $+\theta$ also has another, equal lamina with orientation $-\theta$. The location of these two laminae in the laminate is arbitrary [17:p157]. The laminate $[(\pm 45/0)_2]_s$ is therefore a symmetric balanced laminate.

Normal stresses in x and y -directions will not introduce overall shear strains in the xy -plane if the laminate is balanced.

2.1.3 The laminate stiffness matrix

The relationship between stresses and strains in one single lamina, loaded in its principal directions under plane stress conditions may be expressed as [15:p11]:

$$\begin{Bmatrix} \sigma_1 \\ \sigma_2 \\ \tau_{12} \end{Bmatrix} = \begin{bmatrix} Q_{11} & Q_{12} & 0 \\ Q_{12} & Q_{22} & 0 \\ 0 & 0 & Q_{66} \end{bmatrix} \begin{Bmatrix} \varepsilon_1 \\ \varepsilon_2 \\ \gamma_{12} \end{Bmatrix} \quad (2.1)$$

where σ_1 and ε_1 are normal stress and strain along the fibres (principal direction 1), σ_2 and ε_2 are normal stress and strain in-plane, perpendicular to the fibres (principal direction 2), and τ_{12} and γ_{12} are in-plane shear stress and shear strain, respectively.

The parameters Q_{ij} are called reduced stiffnesses, and are given by the following expressions:

$$Q_{11} = \frac{E_1}{1 - \nu_{12}\nu_{21}} \quad (2.2)$$

$$Q_{12} = \frac{\nu_{12}E_2}{1 - \nu_{12}\nu_{21}} = \frac{\nu_{21}E_1}{1 - \nu_{12}\nu_{21}} \quad (2.3)$$

$$Q_{22} = \frac{E_2}{1 - \nu_{12}\nu_{21}} \quad (2.4)$$

$$Q_{66} = G_{12} \quad (2.5)$$

where E_1 and E_2 are the moduli of elasticity in the principal directions, ν_{12} and ν_{21} are the Poisson's ratios, and G_{12} is the shear modulus in the principal directions 1, 2 of the FRP material. Please note that the second Poisson's ratio may be found from the Maxwell-Betti Reciprocal Theorem to be [15:p5]:

$$\nu_{21} = \frac{E_2}{E_1} \nu_{12} \quad (2.6)$$

Often, a lamina is loaded in another direction than its principal directions. Let x and y be global coordinates, where the angle between the x -axis and principal axis 1 is θ , as shown in figure 1. Let $m = \cos \theta$ and $n = \sin \theta$. The relationship between stresses and strains in the lamina under plane stress conditions, expressed in the global xy -coordinate system, may be expressed by the transformed reduced stiffness matrix [15:p15]:

$$\begin{Bmatrix} \sigma_x \\ \sigma_y \\ \tau_{xy} \end{Bmatrix} = \begin{bmatrix} \bar{Q}_{11} & \bar{Q}_{12} & \bar{Q}_{16} \\ \bar{Q}_{12} & \bar{Q}_{22} & \bar{Q}_{26} \\ \bar{Q}_{16} & \bar{Q}_{26} & \bar{Q}_{66} \end{bmatrix} \begin{Bmatrix} \varepsilon_x \\ \varepsilon_y \\ \gamma_{xy} \end{Bmatrix} \quad (2.7)$$

where the transformed reduced stiffnesses \bar{Q}_{ij} are given as:

$$\bar{Q}_{11} = Q_{11}m^4 + 2(Q_{12} + 2Q_{66})n^2m^2 + Q_{22}n^4 \quad (2.8)$$

$$\bar{Q}_{12} = (Q_{11} + Q_{22} - 4Q_{66})n^2m^2 + Q_{12}(n^4 + m^4) \quad (2.9)$$

$$\bar{Q}_{16} = (Q_{11} - Q_{12} - 2Q_{66})nm^3 + (Q_{12} - Q_{22} + 2Q_{66})n^3m \quad (2.10)$$

$$\bar{Q}_{22} = Q_{11}n^4 + 2(Q_{12} + 2Q_{66})n^2m^2 + Q_{22}m^4 \quad (2.11)$$

$$\bar{Q}_{26} = (Q_{11} - Q_{12} - 2Q_{66})n^3m + (Q_{12} - Q_{22} + 2Q_{66})nm^3 \quad (2.12)$$

$$\bar{Q}_{66} = (Q_{11} + Q_{22} - 2Q_{12} - 2Q_{66})n^2m^2 + Q_{66}(n^4 + m^4) \quad (2.13)$$

Using the stiffness matrices established so far, the stiffness matrix for both in-plane loading, bending and twisting of a multi-layered laminate may be derived [15]. The derivation results in the following relationship [15:p35]:

$$\begin{Bmatrix} N_x \\ N_y \\ N_{xy} \\ M_x \\ M_y \\ M_{xy} \end{Bmatrix} = \begin{bmatrix} A_{11} & A_{12} & A_{16} & B_{11} & B_{12} & B_{16} \\ A_{12} & A_{22} & A_{26} & B_{12} & B_{22} & B_{26} \\ A_{16} & A_{26} & A_{66} & B_{16} & B_{26} & B_{66} \\ B_{11} & B_{12} & B_{16} & D_{11} & D_{12} & D_{16} \\ B_{12} & B_{22} & B_{26} & D_{12} & D_{22} & D_{26} \\ B_{16} & B_{26} & B_{66} & D_{16} & D_{26} & D_{66} \end{bmatrix} \begin{Bmatrix} \varepsilon_x^0 \\ \varepsilon_y^0 \\ \gamma_{xy}^0 \\ k_x^0 \\ k_y^0 \\ k_{xy}^0 \end{Bmatrix} \quad (2.14)$$

where N_x and N_y are normal forces per unit length in x - and y -direction, N_{xy} is the shear force per unit length, and M_x , M_y and M_{xy} are bending moments per unit length. Please refer to section 3.1 for a further explanation of these quantities. ε_x^0 , ε_y^0 and γ_{xy}^0 are mid-plane strains (at $z=0$ in figure 1), k_x^0 and k_y^0 are the curvatures of the mid-plane, and k_{xy}^0 is the twisting curvature of the mid-plane.

The 6x6 matrix in equation (2.14) is called the laminate stiffness matrix or ABD matrix. Its components may be found from the following expressions:

$$A_{ij} = \sum_{k=1}^N \bar{Q}_{ijk} (z_k - z_{k-1}) \quad (2.15)$$

$$B_{ij} = \frac{1}{2} \sum_{k=1}^N \bar{Q}_{ijk} (z_k^2 - z_{k-1}^2) \quad (2.16)$$

$$D_{ij} = \frac{1}{3} \sum_{k=1}^N \bar{Q}_{ijk} (z_k^3 - z_{k-1}^3) \quad (2.17)$$

In these equations, k is the number of the lamina, N is the total number of laminae, and \bar{Q}_{ijk} are the transformed reduced stiffnesses of lamina k . z_k is the distance from the mid-plane, to the top of lamina k , which means that $z_0 = -h/2$ and $z_N = h/2$, if h is the thickness of the whole laminate. Equation (2.14) will be used later in this thesis.

2.1.4 Failure criterion for FRP laminae

A failure criterion is needed for the FRP material, in order to check whether it is overloaded or not. The most popular failure criterion for design purposes is the Tsai-Wu failure criterion [15:p40]. Under plane stress conditions, this criterion states that failure occurs if the following condition is fulfilled:

$$F_1\sigma_1 + F_2\sigma_2 + F_{11}\sigma_1^2 + F_{22}\sigma_2^2 + F_{66}\tau_{12}^2 - \sqrt{F_{11}F_{22}}\sigma_1\sigma_2 \geq 1 \quad (2.18)$$

where

$$F_1 = \frac{1}{\sigma_1^T} + \frac{1}{\sigma_1^C} \quad (2.19)$$

$$F_2 = \frac{1}{\sigma_2^T} + \frac{1}{\sigma_2^C} \quad (2.20)$$

$$F_{11} = -\frac{1}{\sigma_1^T\sigma_1^C} \quad (2.21)$$

$$F_{22} = -\frac{1}{\sigma_2^T\sigma_2^C} \quad (2.22)$$

$$F_{66} = \left(\frac{1}{\tau_{12}^F}\right)^2 \quad (2.23)$$

σ_1^C and σ_1^T are the compressive and tensile failure stresses, respectively, of the material in its principal direction 1. σ_2^C and σ_2^T are the failure stresses in principal direction 2, and τ_{12}^F is the shear failure stress in the 12-plane. Their values are given in table 1, page 6 for common FRP materials.

2.2 Repair of pipelines

2.2.1 Conventional repair techniques

When a pipeline has been damaged to the extent that its integrity no longer is intact, the owner must consider whether a portion of the pipeline should be replaced, or repaired to allow further service. In many cases, the replacement of a damaged steel pipe with a new one is expensive and time-consuming, and not easily accommodated [4]. Especially if the damage is far away from the pipe's connections (flanges or similar), either a section of the pipe must first be cut out, before a new one is welded back on, or the whole pipe must be replaced. The last option is unnecessarily costly, while the first one also is time-consuming, and is difficult to perform subsea or in hazardous areas (explosive atmospheres, etc.). In both cases, the pipeline must be shut down and emptied, possibly leading to a long downtime, which also may cause revenue losses.

In the early 1970s, full encirclement steel sleeves for pipeline repair were developed [18]. These may be made by taking a length of pipe of equal diameter, wall thickness

and grade as the pipe to be repaired, splitting it along its length, and then wrapping it around the pipe to be repaired. The split is then butt welded, making a type A sleeve. In addition to the butt weld, the steel sleeve may also be fillet welded to the steel pipe in both ends, giving a pressure containing type B sleeve. Type A sleeves may be installed while the pipeline is under internal pressure, as the butt weld is not considered to be an "in-service" weld according to API 1104 [18]. However, type A sleeves may not be used to repair through-thickness defects, or defects which are deeper than 80% of the pipe's wall thickness, as they are not pressure containing. In these cases, type B sleeves have to be used instead, but those require the pipe to be drained/depressurized, in order to allow welding of the fillet weld.

Other conventional methods of repair include weld overlays, fillet welded patches, flush welded patches and welded leak box mechanical clamps [3].

2.2.2 FRP overwraps

From the 1950s and 1960s, there has been an interest in using FRP materials for structural purposes, due to their high specific strength [19]. One of their earliest uses was in fighter aircraft. In the 1980s and 1990s, a pipeline repair system using FRP-materials was developed [18,19]. Multiple different systems are now in commercial use [19-21], both for internal and external pipeline repair, and new systems are still developed and enhanced.

The main advantages of using FRP materials for pipeline repair are their low weight, flexibility, and the fact that they do not corrode [3,4,22]. If the environment of the pipeline is corrosive, a steel sleeve will just delay the problem, while a FRP overwrap will fix it. Furthermore, some pipes, like offshore risers, are designed to be able to support their own weight. These pipes may not have sufficient strength to support a heavy steel sleeve, while a FRP overwrap may be sufficiently light. Additionally, FRP overwraps may be installed while the pipeline is in service [3,18], but as stated in the last section, so may type A steel sleeves too. In hazardous areas however, the use of FRP overwraps will be preferred, as the explosion risk due to welding then may be avoided. FRP overwraps may even be installed underwater [20], where the installation of a steel sleeve would be very challenging.

One shortcoming of commercial FRP overwraps is that they are not pressure containing. They can therefore not be used to repair defects with a wall loss of 80% or more [18,21]. Type B steel sleeves may be used in such applications. However, Shamsuddoha et.al. report that pressure containing FRP overwraps, called stand-off sleeves, have been developed [20]. They do not seem to have reached commercial use yet, but may solve this shortcoming in the future.

One of the disadvantages of using FRP materials for pipe repair is that their modulus of elasticity is lower than steel. Because of this, some types of defects will not be

sufficiently restricted by a FRP overwrap, instead allowing them to grow and possibly fail due to fatigue [18]. Another main disadvantage is that the long term performance of FRP overwraps beyond 20-25 years has not yet been demonstrated [18], so that the life time of a FRP repair cannot be predicted [22]. Other disadvantages of FRP materials include susceptibility to damage from vandalism, impact and fire, and that the resin matrix may exhibit degradation when exposed to moisture, high temperature and UV rays [3].

2.2.3 Repair techniques with FRP materials

In general, there are two types of composite repair systems in common use; wet lay-up systems and layered systems [3,4,19,20]. Both systems can be used for either internal (wet lay-up mostly for large pipes) or external pipe repair, but neither of these systems provides pressure containment.

Wet lay-up systems involve a cloth which is cured in the field. The cloth can either be a fibreglass or carbon fibre cloth which is saturated in the field, or a pre-impregnated cloth that is activated by water in the field [19]. These systems are flexible, and can be used to cover a range of different geometries like elbows, tees and valves. Pictures of this repair system used in practice may be found at www.premier-florida.com [23]. If straight pipe sections are repaired, the cloth fabrics are typically cut in lengths equal to the circumference of the pipe, plus a necessary overlap length, in order to ensure development of the full strength of the fibres in this direction [4]. Other cloth fabrics are applied in the longitudinal direction, also with sufficient overlap, in order to also provide axial strength to the repaired pipe.

Wet lay-up systems can also be applied and cured underwater [20].

On the other hand, layered systems use pre-fabricated laminate coils, which are wrapped around the pipe. The laminate may be produced as a large plate, which then is coiled, so that it runs multiple times around the pipe, in order to achieve proper circumferential strength. The coil is pre-cured, and held together with an adhesive applied in the field. Before the laminate is installed, any defects in the steel pipe are filled with an adhesive filler to assist with support and load transfer. As the laminates are manufactured in plants, the quality of the FRP material is higher, and the repair may be completed much faster in the field. Additionally, the strength of the laminates can be tested prior to installation. The main disadvantage of layered systems is that they in general are limited to repair of straight pipe sections. Furthermore, underwater application of layered systems is challenging, due to the need to apply the adhesive.

Interested readers may refer to Ehsani [4] for detailed descriptions of these two techniques.

2.2.4 Mechanics of the repaired pipe

Previous studies of the mechanical behaviour of steel pipelines repaired with FRP materials are generally limited to static loads. Toutanji and Dempsey have provided equations describing the maximum stress in the steel pipe, after reparation, due to internal pressure, and due to the mass of soil and traffic atop of a buried pipe [5]. If the steel pipe has thickness t_{st} , and defects with maximum depth d , they implement an "effective thickness" t_{eff} , which is considered to represent the remaining strength of the pipe:

$$t_{eff} = t_{st} - d \quad (2.24)$$

The stress in the pipe, prior to reparation, will then be:

$$\sigma = \frac{pr}{t_{st} - d} \quad (2.25)$$

where p is the internal pressure and r is the radius of the pipe. Using compatibility, the stress in the steel pipe after the reparation has been found to be [5,19]:

$$\sigma = \frac{pr}{(t_{st} - d) \left[1 + \frac{E_{FRP} t_{FRP}}{E_{st} (t_{st} - d)} \right]} \quad (2.26)$$

where E_{FRP} and E_{st} are the moduli of elasticity of the FRP material in the hoop direction, and the steel, respectively, and t_{FRP} is the thickness of the overwrap. As the variation of the circumferential strain over the wall thickness of a thin-walled cylinder is very small [24:p202], the stress in the steel pipe may be related to its strain, which then may be related to the stress in the FRP material. Expression (2.26) can therefore be used to check the suitability of the repair.

Saeed has provided different equations, where the strain in the FRP material is found, and where the internal pressure at the time of repair application has been included [3]. These models do also only consider constant internal pressures.

As this thesis considers the vibrations of repaired steel pipelines, a dynamic model for the behaviour of the repaired pipeline is required, but has not been found in the current literature. Such a model must therefore be developed. This is done in chapter 3.

2.3 Water hammer

2.3.1 General description

Water hammer is a phenomenon happening when a steady-state flow is abruptly changed. The main principles and physics of water hammer are found in section 12.6 of the book by Finnemore and Franzini [8]. Their description is presented here in a shortened form. More advanced and thorough descriptions may be found in the books by Massey and Ward-Smith [25] and Wylie and Streeter [26], and some of their details are also included here.

In the current discussion, damping in the pipe material, and the friction between the liquid and the pipe wall are neglected. Furthermore, instantaneous valve closure is considered to be possible, even though it is physically impossible.

Consider a large storage tank, filled with a liquid, for example water. At the bottom of the storage tank, a horizontal pipe is leading away from it. At a length L from the storage tank, a valve is fitted to the pipe, see figure 2. Any piping system at the other side of the valve is not of importance to the current discussion. Due to the pressure from the water column in the storage tank, water is flowing out from the storage tank, through the pipe and the open valve. The flow is steady at velocity V , and the steady-state gauge pressure in the pipe is p_0 . The water hammer conditions are described by the following list of events, which correspond to the numbers shown in figure 2.

1. The valve is closed completely and instantaneously, stopping the lamina of liquid next to it. The rest of the liquid column in the pipe is still flowing against this lamina, increasing the pressure in the lamina by Δp . This pressure increase compresses the lamina, while also stretching the walls of the pipe surrounding this lamina of liquid. When the lamina has been compressed, the next upstream lamina of liquid will also be brought to rest at increased pressure.

2. As time goes by, a larger section of the liquid column will be brought to rest at increased pressure. This phenomenon is called a pressure wave. α is the velocity of the pressure wave (also called the pressure wave speed or the wave propagation speed), which may be explained as the length of liquid brought to rest per unit time. Note that no fluid particles move at velocity α ; α is rather just a measurement for the pressure propagation in the pipe. Expressions for the values of Δp and α , which define the pressure wave, are given in subsections 2.3.5 and 2.4.2.

3. At last, the pressure wave reaches the far end of the pipe. Now, all the liquid in the pipe AB is at rest, but the liquid is compressed and under increased pressure. The storage tank is assumed to be very large, so that the pressure in the storage tank is independent of the flow through the pipe AB. Therefore, the pressure inside the

storage tank will be constant, and given by the liquid depth in the storage tank. It is impossible for a pressure to exist at point A that is greater than that due to the liquid depth. When the pressure wave arrives at point A, the pressure at A therefore drops instantly to the value it would have for zero flow. Due to the elevated pressure in the pipe, liquid will start flowing from the pipe, and back into the storage tank. This will cause a wave of pressure unloading.

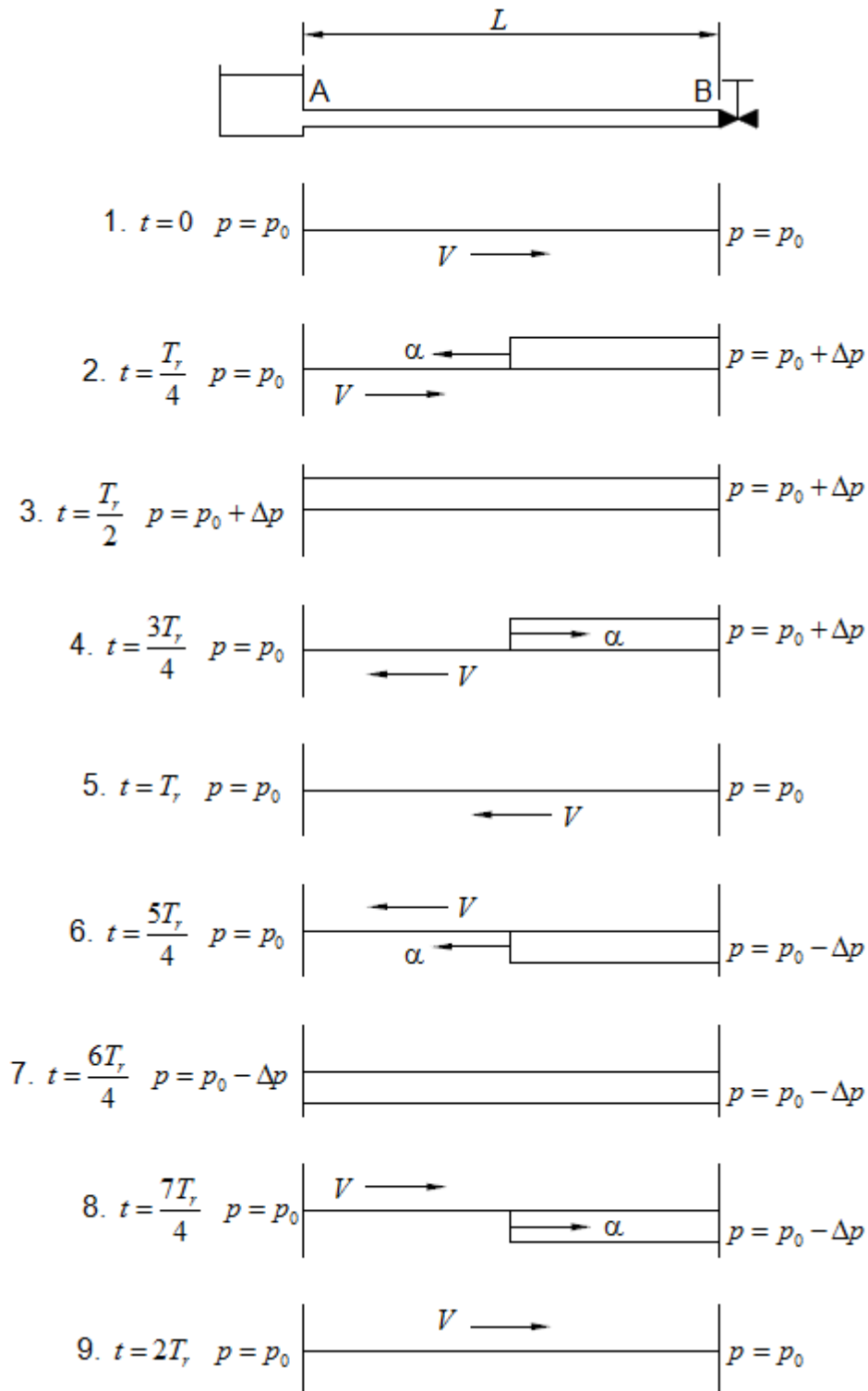


Figure 2: Pressure diagrams for nine time steps after instantaneous valve closure.

4. Because of the liquid leaving the pipe, the wave of pressure unloading travels from the storage tank (point A), towards the valve (point B). The liquid flows at velocity V in one direction, while the pressure wave travels at velocity α in the opposite direction.

5. When the pressure wave has returned to the valve, all the liquid in the pipe has returned to its initial pressure p_0 , and is not compressed anymore. The time required for the pressure wave to travel from the valve, to the storage tank, and back to the valve again, is given as:

$$T_r = 2 \frac{L}{\alpha} \quad (2.27)$$

However, at $t = T_r$, liquid is still flowing from the pipe and into the storage tank, causing a suction/pressure drop at the valve. The pressure at point B will then ideally become equal to $p_0 - \Delta p$.

6. A wave of low pressure travels from B to A, stopping the liquid flow towards the storage tank.

7. When the wave of low pressure reaches point A, the liquid in the pipe is once more at rest. However, it is now at rest at a lower pressure than the pressure in the storage tank, and liquid will start to flow into the pipe again.

8. As more liquid flows into the pipe, the pressure in the pipe returns to its original value once more.

9. At $t = 2T_r$, all the liquid in the pipe has returned to its original pressure. However, liquid is still flowing into the pipe at velocity V , and we have therefore returned to the situation we were in at step 1. A series of pressure waves will therefore travel back and forth, alternating between high and low pressures. The amplitude of the pressure wave will gradually decrease however, because of damping due to fluid friction and imperfect elasticity of liquid and pipe.

Please note that the duration of elevated/reduced pressure at a point at distance x_1 from the storage tank is given by $2x_1/\alpha$. This means that the pressure at point B (at the valve) will alternate between $p_0 + \Delta p$ and $p_0 - \Delta p$, with a rapid change from the high to the low pressure. The pressure at point A on the other hand, will normally be equal to p_0 , with only a very fast pressure spike each time the pressure wave reaches this point.

In the preceding discussion, it is assumed that the pressure at all times remains higher than the vapour pressure of the liquid. If the low pressure becomes lower than the vapour pressure, cavitation will occur, causing a discontinuity and implosion

damage to the valve and or/pipe. Piping systems are generally designed so that cavitation does not occur.

2.3.2 Effect of friction losses

If friction losses are included in the water hammer analyses, the pressure at the valve will rise a bit as the pressure wave travels towards the storage tank, becoming larger than if friction losses are not included [25:p568]. The reason is that the liquid which has travelled the length L has lost more of its energy to friction than the liquid which only has travelled $L/2$ when the valve has stopped. The liquid far from the valve thereby contains more energy, which is transformed to higher pressure when it stops. Values "on the safe side" for the pressure may be obtained by assuming that the initial pressure energy at the valve is equal to the initial energy at the storage tank, thereby neglecting the frictional effects both prior to and during water hammer conditions.

The effects of friction, fluid gravity, bends etc. may be included in the analysis, but makes the problem very complex. Such problems are therefore solved by using numerical methods, like the finite difference method [25:p575].

2.3.3 Effect of valve closure time

As previously stated, the preceding discussion is based on instantaneous valve closure, even though it is not realistic. In real life, the valve closure will either be rapid or slow.

If the valve is subjected to rapid closure, the closure time t_c is less than $T_r = 2L/\alpha$. The pressure will then not change instantly between different levels, but instead take some time to do so. For example, the pressure at the valve will rise during the time t_c , and then remain at its maximum value for $T_r - t_c$. The maximum pressure obtained in the pipe will still be the same as for instantaneous valve closure however.

If $t_c > T_r$, the closure of the valve is said to be slow. In this case, the wave of pressure unloading reaches the valve before the pressure has reached the maximum value from instantaneous closure, $p_0 + \Delta p$. It is possible to calculate how the pressure will change because of slow valve closure, but this is beyond the scope of this thesis.

2.3.4 Other causes of water hammer conditions

Water hammer may also occur if the valve in figure 2 only partially is closed, but also if it is rapidly opened. The pressure may also be provided by other means than a storage tank filled with liquid. The following list of common events that may introduce water hammer conditions has been given by Wylie and Streeter [26:p11]:

- Changes in valve settings, accidental or planned
- Starting or stopping of pumps
- Changes in power demand in turbines
- Action of reciprocating pumps
- Changing elevation of a reservoir
- Waves on a reservoir
- Turbine governor hunting
- Vibration of impellers or guide vanes in pumps, fans, or turbines
- Vibration of deformable appurtenances such as valves
- Draft-tube instabilities due to vortexing
- Unstable pump or fan characteristics

2.3.5 Brief history and fundamental equations

Research on water hammer started in Europe in the late nineteenth century [27]. Hydroelectric generation was the principal supply of electrical power, and incidents and failures caused by overpressure due to rapid valve closure in power plants was therefore a considerable problem. Two of the best known researchers on water hammer from this time were Joukowsky and Allievi. Joukowsky derived the equation for the pressure increase due to water hammer, which is known as the fundamental equation of water hammer [6,27]:

$$\Delta p = \pm \rho_f \alpha \Delta V \quad (2.28)$$

where ρ_f is the density of the liquid, α is the acoustic/water hammer wave speed, and ΔV is the change to the steady-state velocity through the pipe, because of valve motion. An expression for the speed of sound through a fluid in a pipe had been derived by Korteweg earlier, in 1878 [6], and Joukowsky adapted this expression for α .

Allievi developed a mathematical model for the water hammer-induced pressure wave. His mathematical solution method was used, until the more practical graphical method was developed in the 1920s and 1930s [6]. When the digital computers were introduced in the early 1960s, solution by the method of characteristics, a finite difference method, became the standard numerical approach for solving the water hammer equations. The equations in question (the two-equation model) may be expressed as [26:p32]:

$$\frac{1}{\rho_f} \frac{\partial p}{\partial x} + \frac{\partial V}{\partial t} + \frac{fV|V|}{2 \cdot ID} = 0 \quad (2.29)$$

$$\frac{1}{\rho_f} \frac{\partial p}{\partial t} + \alpha^2 \frac{\partial V}{\partial x} = 0 \quad (2.30)$$

In these equations, ρ_f is the density of the liquid, $p(x,t)$ is the pressure inside the pipe, x is position along the pipe, $V(x,t)$ is the liquid velocity, t is time, f is the friction factor, ID is the inner diameter of the pipe, and α is the speed of sound through the liquid. These equations may be solved to find how the pressure field and velocity field inside the pipe varies during water hammer conditions, when fluid friction is taken into account. In case of sloped pipes, the gravity of the liquid may also be included, as shown in [25:p576].

2.4 Vibration of pipelines due to water hammer conditions

Most of the information in this section has been found in the reviews by Tijsseling [6] and Shepherd and Inaba [14]. The use of other sources is indicated.

The theory covered in the last section describes the behaviour of the liquid under water hammer conditions. However, when the pressure is suddenly increased, the pipe wall will start to vibrate. Each time the pipe wall retracts, it exerts an additional pressure to the fluid. There will therefore be a fluid-structure interaction (FSI).

There are two different ways that the vibration of the pipelines under water hammer conditions may be calculated. One way is to perform an uncoupled calculation, in which the pressure history from a water hammer analysis, as described in the last section, is used as the exciting load in a structural dynamics analysis of the pipe wall. This type of model is called uncoupled, as the calculated structural response does not influence the predicted liquid pressures. Thus, FSI is not taken into account. The other type of model, which takes FSI into account, is called coupled models.

2.4.1 Uncoupled models

Uncoupled models do not take the effect of pipe wall vibration on the fluid pressure into account. This is an appropriate assumption if the pipe is very stiff, compared to the fluid, in which case the motion of the pipe wall does not influence the velocity of the pressure wave. This is normally true for pressure waves in gas-filled pipes, because gases are very compressible. Uncoupled models have therefore been used to estimate the radial deflection of a gun tube, in the wake of the projectile [28]. If the pipe is filled with liquid however, the wall thickness needs to be roughly equal to the diameter of the pipe, in order for this assumption to be appropriate. However, Tijsseling suggests that uncoupled models still are acceptable for rigidly anchored liquid-filled pipe systems [6].

Even though uncoupled analyses are said to be dubious and quite simplified, they are not unusual to perform. Their simplicity makes it possible to obtain analytical solutions, while still capturing the essential features of dispersive waves and a critical speed. Uncoupled analyses are available for steel pipes, both with pipe material damping neglected [13,29] and taken into account [29]. Uncoupled water hammer analyses for laminated FRP pipes have also been conducted, both with damping neglected [1], and included [30]. In all these four papers, liquid friction has not been taken into account.

2.4.2 The velocity of the pressure wave

In uncoupled calculations, the previously mentioned Korteweg approximation is used to estimate the velocity of the pressure wave (the wave propagation speed), α . This velocity is estimated by considering one-dimensional continuity across the wave front. The details of the derivation may be found in [25:p561-563]. In this derivation, a relationship between the pressure change and the change in the cross-sectional area of the pipe is required. The Korteweg approximation is to neglect the inertia and bending stiffness of the pipe in this matter. The pipe is then considered as a series of massless rings expanding and contracting in accordance with the internal pressure.

The velocity of the pressure wave depends on how the pipe is supported in its axial direction. Three different support conditions are standard in theoretical water hammer analyses:

- (a) The pipe is anchored with expansion joints throughout its length, in which case its axial stresses may be neglected.
- (b) The pipe is anchored throughout against axial motion, in which case the axial displacements, and hence strains, may be neglected.
- (c) The pipe is anchored at its upstream end only.

For an isotropic pipe subjected to support condition (a) (no axial support), the velocity of the pressure wave may be found to be [25:p563]:

$$\alpha = \sqrt{\frac{1}{\rho_f \left(\frac{1}{K} + \frac{2R}{hE} \right)}} \quad (2.31)$$

where ρ_f is the density of the liquid, K is the modulus of elasticity of the liquid, R is the mean radius of the pipe, h is the thickness of the pipe wall, and E is the modulus of elasticity for the pipe wall.

The velocity of the pressure wave for an isotropic pipe subjected to support condition (b) (axially restricted) is [26:p6]:

$$\alpha = \sqrt{\frac{1}{\rho_f \left(\frac{1}{K} + (1-\nu^2) \frac{2R}{hE} \right)}} \quad (2.32)$$

where ν is Poisson's ratio for the isotropic pipe material.

In a similar way, the Korteweg approximation may be applied to a pipe made of a balanced symmetric FRP laminate. With support condition (a) (no axial support), the velocity of the pressure wave may be found to be:

$$\alpha = \sqrt{\frac{1}{\rho_f \left(\frac{1}{K} + \frac{2R\rho_f}{A_{22} - \frac{A_{12}^2}{A_{11}}} \right)}} \quad (2.33)$$

where A_{ij} is given by equation (2.15). With support condition (b) (axially restricted), the velocity of the pressure wave may be found to be [1]:

$$\alpha = \sqrt{\frac{1}{\rho_f \left(\frac{1}{K} + \frac{2R}{A_{22}} \right)}} \quad (2.34)$$

2.4.3 Coupled models

Coupled models take fluid-structure interaction into account. This is required when less restrained liquid-filled piping systems are to be analysed for water hammer conditions. In general, there are three liquid-pipe interaction mechanisms; friction coupling, Poisson coupling and junction coupling. Friction coupling takes the mutual friction between liquid and pipe into account. Poisson coupling is more important, and relates the radial motion of the pipe wall to axial motions of the pipe wall. Because of Poisson's ratio, the pipe will shorten when it is radially expanded, if it is not anchored against axial motion throughout. This will cause precursor waves, which are disturbances in the liquid which travel faster than the classical water hammer pressure waves. The last mechanism is junction coupling, which occurs if there are unsupported bends, tees or other deviations from straight and uniform pipes. If a pressure wave hits a bend, for example, it will exert an impulse to the bend, causing it to vibrate, introducing additional pressure waves to the liquid. Junction coupling has to be considered on a case-to-case basis, and is normally modelled by applying continuity and equilibrium principles to a control volume enclosing the entire junction.

In many cases, the effects of fluid friction are neglected, and only Poisson coupling is considered for straight pipes. The resulting model is two-dimensional, with equations both for the radial and axial movement of the liquid. An approximate analytical solution of this model has been derived by Skalac [31], but the expressions are very complex. Therefore, either his simplified "four-equation" model or numerical solutions are normally used. Interested readers may refer to Shepherd and Inaba [14] for the details regarding this model. In short, it is made up of four differential equations, which may be used to find the internal pressure and axial velocity fields, in addition to the radial and axial displacement of the pipe wall, as functions of the distance x along

the pipe and time t . These equations are either solved by the method of characteristics (a finite difference method), or the complicated analytical solution provided by Tijsseling [32]. This model has successfully been applied to both thin-walled and thick-walled pipes subjected to water hammer conditions [14,33].

2.4.4 Choice for this thesis

As no earlier studies on water hammer-induced vibration of steel pipes with a FRP overwrap have been found in available literature, it has been chosen to study the problem using an uncoupled model of a straight, thin-walled pipeline, neglecting liquid friction and pipe material damping. As discussed above, this kind of model has its weaknesses. It neglects fluid-structure interaction, and assumes the pipeline to be anchored against axial motion, which rarely is the case in real-life. The calculated pipe wall deformations may therefore not correspond to physical values.

Despite its weaknesses, the proposed model may give interesting results, which can tell something about the qualitative behaviour of pipes repaired with a FRP overwrap, subjected to water hammer conditions. Additionally, it is often desirable to make a simpler model before more advanced models are developed. The intention is therefore that the model developed in this thesis may be used as a starting point for further research and development of more sophisticated models.

3. Model development

In this section, an analytical model for the radial vibration of a steel pipe, repaired with a FRP overwrap, subjected to water hammer conditions will be derived. The steel pipe with its FRP overwrap is modelled as a thin-walled cylinder, where material damping is neglected. The pipe is assumed to be straight, and the thickness of both the steel pipe and the FRP overwrap is assumed to be constant along its length. The derived model is an uncoupled model, in which the pressure history from a water hammer analysis is used as the exciting load in the analysis of the pipe. The pipe is as such considered to be anchored against axial motion throughout, and to be simply supported against radial deflection in each end. Furthermore, the effects of liquid friction are neglected, and the internal absolute pressure is assumed to stay above the saturation pressure of the liquid, so that cavitation does not occur. The valve closure causing the water hammer conditions is modelled to be instantaneous. These approximations and assumptions are the same as Pavlou has used in his works on water-hammer induced pipe vibration [1,13]. Furthermore, it is assumed that the pipe will be free from stress when the FRP overwrap is applied, and that the resulting composite pipe may be considered to be axisymmetric. The discussion will be limited to pipes whose full length has been repaired with a FRP overwrap.

The derivation starts by considering a small element of a thin-walled axisymmetric cylinder, and deriving its equations of motion with respect to internal forces and bending moments. These forces and bending moments are then related to pipe wall strains and curvatures by using the stiffness matrix for a FRP laminate, which is modified to take the steel pipe into account. Next, the strains and curvatures are related to the radial deflection w using Flügge's shell theory. In addition, a mathematical expression for the water hammer pressure wave is stated. The resulting governing equation for $w(x,t)$ is a partial differential equation, which is transformed into an ordinary differential equation, by taking boundary conditions into account and utilizing the properties of Fourier sine series. This equation is solved, giving a series solution for $w(x,t)$.

As the solution is an infinite series, recommendations about when it should be truncated are given. A similar solution is also derived for the static response of the pipe due to a steady state pressure. Additionally, an expression for the pressure wave speed which predicts the largest pipeline vibration is derived. Lastly, an expression for the vibration due to the reflected pressure wave is stated, and the radial deflections are related to pipe wall stresses.

3.1 Equations of motion for a thin-walled axisymmetric cylinder

The derivation of the equilibrium differential equation for a thin-walled, isotropic cylinder is quite straight forward, and may be found in the books by R.T. Fenner [24:p200] and Timoshenko and Woinowsky-Krieger [34:p466]. However, as the internal pressure during water hammer conditions will vary with time, inertia forces must be taken into account. Additionally, the anisotropic nature of the fibre-reinforced plastic (FRP) material further complicates the matter. The corresponding governing differential equation for laminated FRP pipes has been derived by Pavlou [1,13]. A complete derivation is conducted in this section for the sake of clarity, and to establish the notation used throughout this thesis. Positive directions are chosen to match those used by Fenner, to enable a smooth application of laminate mechanics.

Thin-walled cylinders, or pipes, may be regarded as axisymmetric shells. If the pipe is made of laminated FRP, the laminate needs to be symmetric balanced, in order for the condition of axial symmetry to be fulfilled. If the laminate is not symmetric balanced, the pipe will twist when subjected to internal pressure.

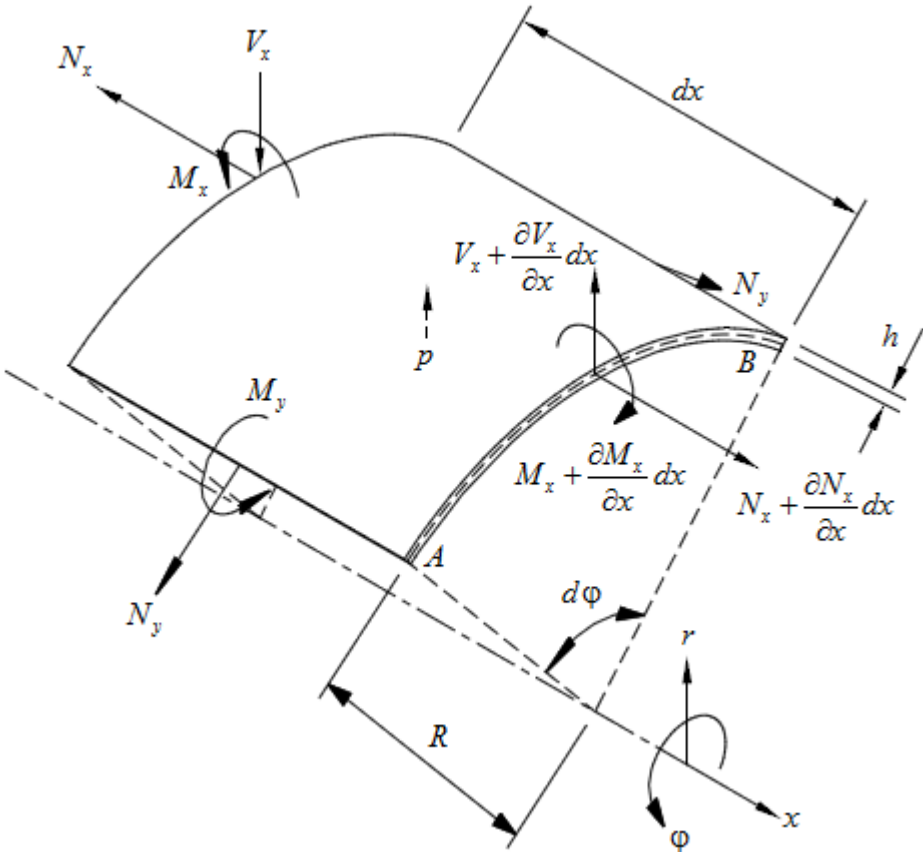


Figure 3: Moments and forces acting on a small element of a cylindrical shell in equilibrium.

Figure 3 shows a small element of a circular cylindrical shell, together with the moments and forces acting on it. Its size is exaggerated for illustrative purposes. Cylindrical coordinates r , ϕ , x are used. The pressure, p , acts in the outward radial direction. In the current discussion, the pressure is assumed to act axisymmetrically,

i.e. it does not vary with φ . This means that the weight of the fluid in a horizontal pipe is not taken into account in this model. This is a reasonable neglect for pipes of normal size, in which the fluid pressure will be considerable higher than that due to the mass of the fluid in the pipe.

The length of the element in the axial direction is dx , and its angle of revolution is $d\varphi$. R is the mean radius of the cylinder, while h is its thickness. M_x and M_y are the bending moments per unit length in the axial and circumferential directions, while N_x and N_y are the tensile membrane forces per unit length in the axial and circumferential directions, respectively. Because of the axial symmetry, V_x is the only non-zero shear force acting on the edges of the element. V_x is also given as force per unit length. The axial symmetry also means that the moments and forces are independent of φ , and that there are no twisting moments. The theory of thin-walled cylinders is generally applicable when $R > 20h$ [35:p381].

Axial equilibrium of the shell element may be stated as:

$$\Sigma F_x = \left(N_x + \frac{\partial N_x}{\partial x} dx \right) R d\varphi - N_x R d\varphi = 0 \quad (3.1)$$

When the internal pressure p is varying with the time, the pipe wall will vibrate, and inertia forces must be taken into account. For the shell element, the inertia force in radial direction may be stated as:

$$ma_r = (\rho_m \cdot h \cdot R d\varphi \cdot dx) \cdot \frac{\partial^2 w}{\partial t^2} \quad (3.2)$$

Similarly, in axial direction:

$$ma_x = (\rho_m \cdot h \cdot R d\varphi \cdot dx) \cdot \frac{\partial^2 u}{\partial t^2} \quad (3.3)$$

where ρ_m is the density of the pipe material, w is the radial displacement/deflection of the pipe wall, and u is its axial displacement. According to Newton's second law, $\Sigma F_x = ma_x$, and combining equation (3.1) and (3.3) yields:

$$\begin{aligned} \frac{\partial N_x}{\partial x} R dx d\varphi &= \rho_m h \frac{\partial^2 u}{\partial t^2} R dx d\varphi \\ &\Downarrow \\ \frac{\partial N_x}{\partial x} &= \rho_m h \frac{\partial^2 u}{\partial t^2} \end{aligned} \quad (3.4)$$

As discussed in earlier sections, the pipeline is assumed to be anchored against axial motion throughout. The axial deformation u and all its derivatives are therefore equal to zero. Introducing this assumption into equation (3.4) yields:

$$N_x = \text{constant} \quad (3.5)$$

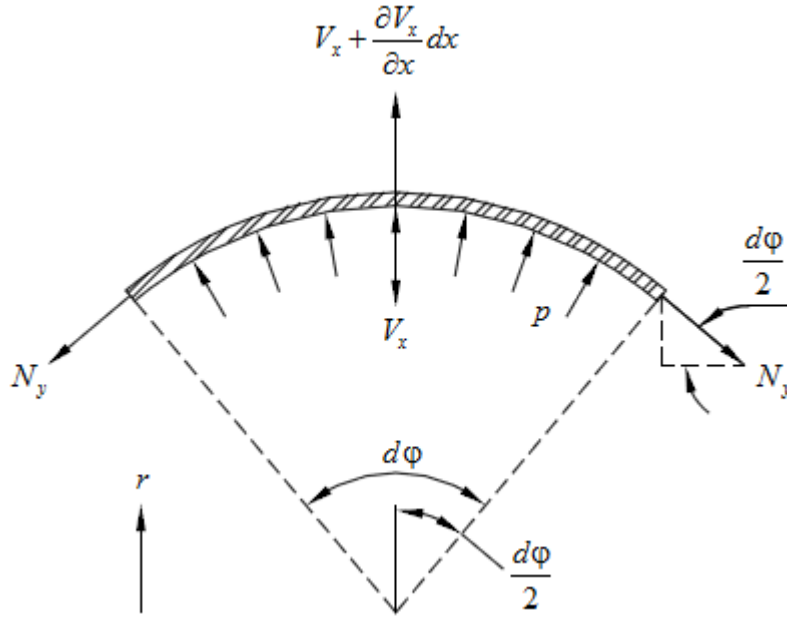


Figure 4: Equilibrium of shell element, seen from the end.

In figure 4, the shell element is seen from the end. From the geometry, it is observed that the radial component of N_y (the component acting downwards in figure 4) is equal to $N_y \sin(d\phi/2)$. The element is considered to be very small, in which case the approximation $N_y \sin(d\phi/2) \approx N_y d\phi/2$ can be adopted. The sum of forces acting in the r -direction on the small element of the cylindrical shell may now be written as:

$$\Sigma F_r = \left(V_x + \frac{\partial V_x}{\partial x} dx \right) R d\phi - V_x R d\phi + p \cdot R d\phi \cdot dx - 2 \cdot N_y \frac{d\phi}{2} \cdot dx \quad (3.6)$$

According to Newton's second law, $\Sigma F_r = ma_r$, and combining equation (3.6) and (3.2) yields:

$$\frac{\partial V_x}{\partial x} R dx d\phi + p R dx d\phi - N_y dx d\phi = \rho_m h \frac{\partial^2 w}{\partial t^2} R dx d\phi \quad (3.7)$$

Dividing all terms by $R dx d\phi$, and reordering the terms yields:

$$\frac{N_y}{R} - \frac{\partial V_x}{\partial x} + \rho_m h \frac{\partial^2 w}{\partial t^2} = p(x, t) \quad (3.8)$$

Consider now the rotational equilibrium about the side AB of the element. The following equation of motion may be obtained:

$$\begin{aligned} \Sigma M_{AB} &= \left(M_x + \frac{\partial M_x}{\partial x} dx \right) R d\phi - M_x R d\phi - V_x dx R d\phi + p dx R d\phi \cdot \frac{dx}{2} \\ &= \rho_m h R d\phi dx \frac{\partial^2 w}{\partial t^2} \cdot \frac{dx}{2} \end{aligned} \quad (3.9)$$

The terms containing dx^2 are neglected, because dx is very small. Equation (3.9) may then be shortened, giving:

$$\frac{\partial M_x}{\partial x} = V_x \quad (3.10)$$

Equations (3.8) and (3.10) may now be combined:

$$\frac{N_y}{R} - \frac{\partial^2 M_x}{\partial x^2} + \rho_m h \frac{\partial^2 w}{\partial t^2} = p(x,t) \quad (3.11)$$

We now have an equation which relates the internal pressure $p(x,t)$ to the hoop force N_y and bending moment M_x acting on the small element of the pipe. One term also includes the radial deflection $w(x,t)$. In order to solve the equation, the hoop force and bending moment should also be related to the radial deflection.

3.2 Relationships between internal forces, moments and the radial deflection

3.2.1 Relationships for a laminated FRP pipe

If the pipe is solely made of laminated FRP, the laminate stiffness matrix given in equation (2.14) may be used to relate the internal forces and moments to the strains and curvatures [1]. x is simply taken to be the axial direction of the cylinder, while y is taken to be the circumferential direction. In equations (2.15)-(2.17), z_k is taken to be the distance from the mean radius R of the pipe to the top of lamina k , which means that $z_0 = -h/2$ and $z_N = h/2$, as shown in figure 5.

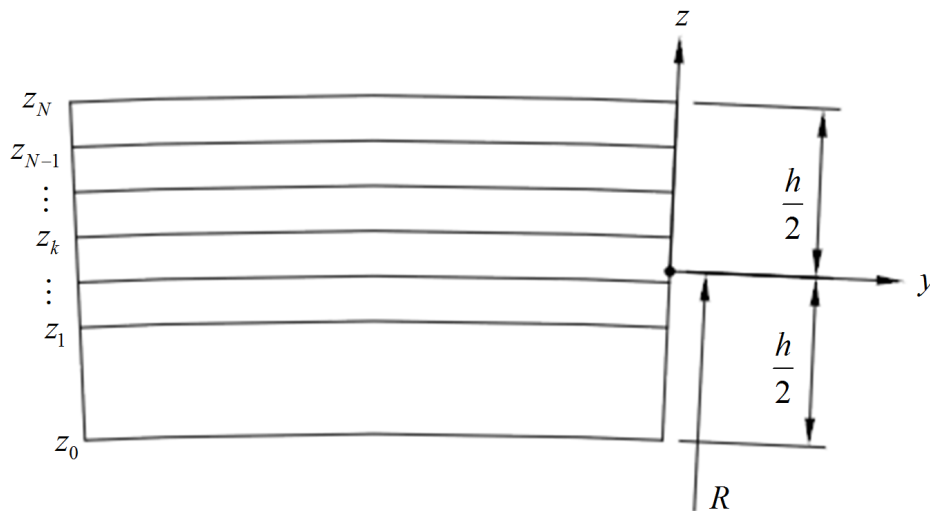


Figure 5: Definition of coordinate system for a cylinder consisting of N layers [36].

3.2.2 The stiffness matrix for a steel pipe repaired with a FRP overwrap

When a layered FRP system is applied to a steel pipe, the behaviour of the FRP overwrap is assumed to be reasonably well modelled by the equations for a laminated FRP pipe. Ehsani also describes wet lay-up systems to be built up of layers [4]. If the cloth fabrics are properly overlapped and installed, it is assumed that

also the behaviour of wet lay-up systems may be modelled by classical lamination theory.

Furthermore, it is assumed that the pipeline is free from stress when it is repaired. This may not always be the case, as in-service repair is possible. However, when the pipeline is exposed to large pressure decreases during water hammer conditions, the adhesive between the steel and the FRP will be subjected to considerable forces, if applied in-service. The behaviour of this adhesive is hard to predict, and it is also rigorous to model the difference in stress between pipe and overwrap due to in-service repair analytically. This assumption is therefore considered to be reasonable for a first dynamic model, as many pipelines are repaired while being pressure-free.

Taking these two assumptions into account, it should be possible to model the wrapped pipe using the same laminate stiffness matrix as for a laminated FRP pipe, equation (2.14). It is assumed that the steel pipe acts just like any other lamina in the laminate, but with different thickness and material properties. Metals like steel are isotropic, in which case the stiffnesses under plane stress conditions are given as [35:p87]:

$$\bar{Q}_{11,st} = \bar{Q}_{22,st} = \frac{E_{st}}{1 - \nu_{st}^2} \quad (3.12)$$

$$\bar{Q}_{12,st} = \frac{\nu_{st} E_{st}}{1 - \nu_{st}^2} \quad (3.13)$$

$$\bar{Q}_{16,st} = \bar{Q}_{26,st} = 0 \quad (3.14)$$

$$\bar{Q}_{66,st} = G_{st} = \frac{E_{st}}{2(1 + \nu_{st})} \quad (3.15)$$

In these equations, E_{st} is the modulus of elasticity, G_{st} is the shear modulus and ν_{st} is Poisson's ratio for the steel pipe (the equations may also be used for any other isotropic pipe material). The steel pipe is as such considered to be the first layer in the composite pipe, extending from z_0 to z_1 in figure 5. Equations (3.12)-(3.15) should therefore be used for the first layer when the coefficients of the ABD matrix are calculated, using expressions (2.15)-(2.17). If N is the total number of FRP laminae in the overwrap, N in expressions (2.15)-(2.17) and figure 5 must be replaced with $N+1$, in order to also include the steel pipe. This means that a pipe which consists of one layer of steel and $N = 20$ FRP laminae, consists of $N+1 = 21$ layers in total, and all those 21 layers must be included when calculating the ABD matrix.

The same model may also be used if the pipe is internally repaired with a FRP laminate. The steel pipe will then be the outermost layer, extending from z_N to z_{N+1} . The rest of this thesis will only consider external reparation however.

3.2.3 Relationships between strains, curvatures and the radial deflection

The laminate stiffness matrix relates the internal forces and moments in the pipe to its mid-plane strains and curvatures. These strains and curvatures then need to be related to the radial deflection of the pipe.

Expressions for the axial and circumferential strains, and the shear strain, in cylindrical coordinates, in the case of axial symmetry, may be found in the book by Fenner [24:p67], and adapted to the notation used here:

$$\varepsilon_x^0 = \frac{\partial u}{\partial x} \quad (3.16)$$

$$\varepsilon_y^0 = \frac{w}{r} \Big|_{r=R} = \frac{w}{R} \quad (3.17)$$

$$\gamma_{xy}^0 = 0 \quad (3.18)$$

The curvatures are measurements for how much the strains vary over the thickness of the shell. Timoshenko shell theory assumes the variation of the hoop strain to be negligible in thin-walled cylinders [24:p202], which means that $k_y^0 = 0$. This assumption could probably give sufficiently accurate results for composite pipes too, but both Kollár and Springer [16:p371] and Pavlou [1] have chosen to use Flügge's shell theory, in which the variation of the hoop strain is taken into account. The reason for this may be to better estimate the resulting stress in each lamina. The associated curvatures may be found in the book by Kollár and Springer [16:p371]:

$$k_x^0 = -\frac{\partial^2 w}{\partial x^2} \quad (3.19)$$

$$k_y^0 = -\frac{w}{R^2} \quad (3.20)$$

$$k_{xy}^0 = -\frac{2}{R} \frac{\partial v}{\partial x} \quad (3.21)$$

When the steel pipe is included as a "layer" in the laminate, the full laminate (steel and FRP) will not be symmetric. Therefore, axial symmetry is no longer entirely fulfilled, as the twisting curvature k_{xy}^0 will not be equal to zero, unless all fibres are orientated at either 0° or 90° (or a combination of these two directions). However, if the FRP overwrap is balanced, calculations have shown that k_{xy}^0 will be very small compared to $k_x^0 + k_y^0$, typically $k_{xy}^0 \leq (k_x^0 + k_y^0) \cdot 5\%$ for thin laminae. The deviation from axial symmetry is therefore considered to be very small, and thereby neglected in the current model.

In the case of axial symmetry, u , v and their derivatives are equal to zero, causing ε_x^0 and k_{xy}^0 to be equal to zero. Implementing this observation with expressions (3.16)-(3.21) to equation (2.14) gives:

$$\begin{Bmatrix} N_x \\ N_y \\ N_{xy} \\ M_x \\ M_y \\ M_{xy} \end{Bmatrix} = \begin{bmatrix} A_{11} & A_{12} & A_{16} & B_{11} & B_{12} & B_{16} \\ A_{12} & A_{22} & A_{26} & B_{12} & B_{22} & B_{26} \\ A_{16} & A_{26} & A_{66} & B_{16} & B_{26} & B_{66} \\ B_{11} & B_{12} & B_{16} & D_{11} & D_{12} & D_{16} \\ B_{12} & B_{22} & B_{26} & D_{12} & D_{22} & D_{26} \\ B_{16} & B_{26} & B_{66} & D_{16} & D_{26} & D_{66} \end{bmatrix} \begin{Bmatrix} 0 \\ w/R \\ 0 \\ -\partial^2 w / \partial x^2 \\ -w/R^2 \\ 0 \end{Bmatrix} \quad (3.22)$$

The two equations required from the set of equations (3.22) may be written as:

$$N_y = A_{22} \frac{w}{R} - B_{12} \frac{\partial^2 w}{\partial x^2} - B_{22} \frac{w}{R^2} \quad (3.23)$$

$$M_x = B_{12} \frac{w}{R} - D_{11} \frac{\partial^2 w}{\partial x^2} - D_{12} \frac{w}{R^2} \quad (3.24)$$

The relationships which are needed to make equation (3.11) solvable have now been found.

3.3 The governing equation of motion

Equations (3.23) and (3.24) are rearranged for convenience:

$$N_y = -B_{12} \frac{\partial^2 w}{\partial x^2} + \left(\frac{A_{22}}{R} - \frac{B_{22}}{R^2} \right) w \quad (3.25)$$

$$M_x = -D_{11} \frac{\partial^2 w}{\partial x^2} + \left(\frac{B_{12}}{R} - \frac{D_{12}}{R^2} \right) w \quad (3.26)$$

In equation (3.11), $\partial^2 M_x / \partial x^2$ occurs. Equation (3.26) therefore needs to be differentiated twice:

$$\frac{\partial M_x}{\partial x} = -D_{11} \frac{\partial^3 w}{\partial x^3} + \left(\frac{B_{12}}{R} - \frac{D_{12}}{R^2} \right) \frac{\partial w}{\partial x} \quad (3.27)$$

$$\frac{\partial^2 M_x}{\partial x^2} = -D_{11} \frac{\partial^4 w}{\partial x^4} + \left(\frac{B_{12}}{R} - \frac{D_{12}}{R^2} \right) \frac{\partial^2 w}{\partial x^2} \quad (3.28)$$

Equations (3.25) and (3.28) are now inserted into equation (3.11), yielding:

$$-\frac{1}{R} B_{12} \frac{\partial^2 w}{\partial x^2} + \frac{1}{R} \left(\frac{A_{22}}{R} - \frac{B_{22}}{R^2} \right) w + D_{11} \frac{\partial^4 w}{\partial x^4} - \left(\frac{B_{12}}{R} - \frac{D_{12}}{R^2} \right) \frac{\partial^2 w}{\partial x^2} + \rho_m h \frac{\partial^2 w}{\partial t^2} = p(x, t) \quad (3.29)$$

This expression is rearranged:

$$D_{11} \frac{\partial^4 w}{\partial x^4} + \left(\frac{D_{12}}{R^2} - 2 \frac{B_{12}}{R} \right) \frac{\partial^2 w}{\partial x^2} + \left(\frac{A_{22}}{R^2} - \frac{B_{22}}{R^3} \right) w + \rho_m h \frac{\partial^2 w}{\partial t^2} = p(x, t) \quad (3.30)$$

The constant coefficients may be given their own symbols:

$$\lambda_1 = D_{11} \quad (3.31)$$

$$\lambda_2 = \frac{D_{12}}{R^2} - 2 \frac{B_{12}}{R} \quad (3.32)$$

$$\lambda_3 = \frac{A_{22}}{R^2} - \frac{B_{22}}{R^3} \quad (3.33)$$

Equation (3.30) may then be written as:

$$\lambda_1 \frac{\partial^4 w}{\partial x^4} + \lambda_2 \frac{\partial^2 w}{\partial x^2} + \lambda_3 w + \rho_m h \frac{\partial^2 w}{\partial t^2} = p(x, t) \quad (3.34)$$

This is the governing equation of motion for the pipe wall, which may be solved for the radial displacement $w(x, t)$. However, we still need expressions for ρ_m and $p(x, t)$ in order to solve this equation.

3.3.1 The mean density of the pipe wall

As the pipe wall consists of two materials (the old steel pipe and the FRP overwrap), ρ_m in equation (3.34) should be the mean density of the small element of the pipe wall shown in figure 3. Let IR be the inner radius of the steel pipe, MR is the outer radius of the steel pipe, and OR is the outer radius of the FRP overwrap. Furthermore, let h_{st} be the thickness of the steel pipe, and let h_{la} be the thickness of each of the N FRP laminae. The relationships between the different radii are found from the following expressions:

$$IR = MR - h_{st} \quad (3.35)$$

$$OR = MR + Nh_{la} \quad (3.36)$$

$$R = \frac{OR + IR}{2} \quad (3.37)$$

The average density of the composite pipe may be defined as:

$$\rho_m = \frac{V_{st}\rho_{st} + V_{FRP}\rho_{FRP}}{V} \quad (3.38)$$

where V_{st} and ρ_{st} are the volume and density of the steel pipe, respectively, V_{FRP} and ρ_{FRP} are the volume and density of the FRP material, and V is the volume of the entire pipe. Expressions for each of the cylinder volumes are inserted:

$$\rho_m = \frac{L\pi(MR^2 - IR^2)\rho_{st} + L\pi(OR^2 - MR^2)\rho_{FRP}}{L\pi(OR^2 - IR^2)} \quad (3.39)$$

$L\pi$ may be removed from all terms, yielding the following expression for the mean density of the pipe wall:

$$\rho_m = \frac{(MR^2 - IR^2)\rho_{st} + (OR^2 - MR^2)\rho_{FRP}}{OR^2 - IR^2} \quad (3.40)$$

3.3.2 The velocity of the pressure wave in a steel pipe with FRP overwrap

In order to mathematically formulate the pressure wave due to water hammer conditions, the pressure wave speed α is needed. For a pipe made of symmetric balanced FRP laminate, this speed is given by equation (2.34):

$$\alpha = \sqrt{\frac{1}{\rho_f \left(\frac{1}{K} + \frac{2R}{A_{22}} \right)}} \quad (2.34)$$

The difference in the laminate stiffness matrix (3.22) between a pipe made of symmetric balanced FRP laminate, and a steel pipe repaired with a balanced FRP overwrap, is that $B_{ij}=0$ for the former. In the derivation of equation (2.34), $N_y = A_{22}w/R$ is used [1]. For a steel pipe with a FRP overwrap, N_y is given by equation (3.23):

$$N_y = A_{22} \frac{w}{R} - B_{12} \frac{\partial^2 w}{\partial x^2} - B_{22} \frac{w}{R^2} \quad (3.23)$$

However, according to the Korteweg approximation, the bending stiffness of the pipe should be neglected in the derivation of the velocity of the pressure wave, α . B_{ij} relates the bending moments in the pipe to its strains, and may therefore be regarded as part of its bending stiffness. In that case, equation (3.23) is reduced to $N_y = A_{22}w/R$, the same as for a pipe made of symmetric balanced FRP laminate. Therefore, equation (2.34) is applicable also for a steel pipe repaired with a FRP overwrap, as long as the stiffness of the steel pipe is taken into account in the calculation of A_{22} .

3.3.3 Mathematical formulation of the pressure wave

As mentioned in the beginning of this chapter, the developed model will be uncoupled. When fluid friction, pipe material damping and fluid-structure interaction all are neglected, the internal fluid pressure will vary as indicated in figure 2, subsection 2.3.1, after an instantaneous valve closure. This pressure variation may be described by the Heaviside step function [29]. The Heaviside step (or unit step) function $H(x-a)$ is equal to 0 when $x < a$, and is equal to 1 when $x \geq a$ [37]. When the pressure wave is travelling from the valve, the pressure is equal to $p_0 + \Delta p$ behind the pressure wave, and equal to p_0 in front of the pressure wave. This behaviour may be represented by the following function:

$$p_{tot}(x,t) = p_0 + \Delta p [1 - H(x - \alpha t)] \quad \text{for } 0 \leq t \leq T_r/2 \quad (3.41)$$

Here, x is distance from the valve, and t is the time from valve closure. Δp is the magnitude of the pressure wave, found from equation (2.28):

$$\Delta p = \pm \rho_f \alpha \Delta V \quad (2.28)$$

α is the velocity of the pressure wave, found by equation (2.34).

Equation (3.41) is only applicable from the flow is suddenly stopped, until the pressure wave has reached the other end of the pipe, i.e. for $0 \leq t \leq T_r/2$. At this instant, a wave of pressure unloading will begin to travel through the pipe in the

opposite direction. For $T_r/2 \leq t \leq T_r$, the pressure will be represented by the following function:

$$p_{tot}(x,t) = p_0 + \Delta p \left[1 - H(x - (2L - \alpha t)) \right] \text{ for } T_r/2 \leq t \leq T_r \quad (3.42)$$

A wave of low pressure will then travel from the valve, which may be formulated as:

$$p_{tot}(x,t) = p_0 - \Delta p \left[1 - H(x - \alpha t + 2L) \right] \text{ for } T_r \leq t \leq 3T_r/2 \quad (3.43)$$

This wave will also be reflected:

$$p_{tot}(x,t) = p_0 - \Delta p \left[1 - H(x - (4L - \alpha t)) \right] \text{ for } 3T_r/2 \leq t \leq 2T_r \quad (3.44)$$

At $t = 2T_r$, a new pressure wave will start, which may be described by equation (3.41) if t is replaced by $t - 2T_r$ in this expression.

In the solution for the dynamic response due to the water hammer, only the dynamic term of the pressure can be taken into account:

$$p(x,t) = \Delta p \left[1 - H(x - \alpha t) \right] \text{ for } 0 \leq t \leq T_r/2 \quad (3.45)$$

The structural response of the pipe due to the static pressure p_0 must be found by solution of the static governing differential equation, without the terms due to inertia, and superposed to the dynamic response. For now, we will only consider the first half round trip of the wave. The proceeding motions are considered in section 3.7.

3.4 Analytical solution of the governing equation of motion

By implementing equation (3.45) into equation (3.34), the governing equation of motion for the pipe wall may be expressed as:

$$\lambda_1 \frac{\partial^4 w}{\partial x^4} + \lambda_2 \frac{\partial^2 w}{\partial x^2} + \lambda_3 w + \rho_m h \frac{\partial^2 w}{\partial t^2} = \Delta p \left[1 - H(x - \alpha t) \right] \quad (3.46)$$

The ends of the pipe are assumed to be simply supported along their perimeters, yielding the following boundary conditions to the differential equation:

$$w(0,t) = w(L,t) = 0 \quad (3.47)$$

$$\left. \frac{\partial^2 w(x,t)}{\partial x^2} \right|_{x=0} = \left. \frac{\partial^2 w(x,t)}{\partial x^2} \right|_{x=L} = 0 \quad (3.48)$$

When only the dynamic pressure is considered, the pipe will not be deformed at $t = 0$ (the static response will be superposed to the dynamic response later). The following initial conditions may therefore be applied:

$$w(x,0) = 0 \text{ and } \left. \frac{\partial w(x,t)}{\partial t} \right|_{t=0} = 0 \quad (3.49)$$

Equation (3.46) is a partial differential equation with two variables. It is chosen to solve it by utilizing a Fourier series solution, as has previously been done by Pavlou [1,13] and Simkins [28]. This way, it may be transformed into an ordinary differential equation with respect to time. All the mathematical details are not included in these

works, and a complete derivation from known mathematics is therefore conducted in this section, for clarification.

The boundary conditions (3.47) and (3.48) are automatically satisfied by a Fourier sine series [38]. A Fourier sine series for $w(x, t)$ may be given as [38:p573]:

$$w(x, t) = \frac{2}{L} \sum_{n=1}^{\infty} W_n(t) \sin \frac{n\pi x}{L} \quad (3.50)$$

where $W_n(t)$ is n coefficients which are functions of time, and given as:

$$W_n(t) = \int_0^L w(x, t) \sin \frac{n\pi x}{L} dx \quad (3.51)$$

If $W_n(t)$ can be expressed in terms of known variables, the radial deflection may be calculated by equation (3.50). This will be done by applying equation (3.50) to equation (3.46).

The derivatives of equation (3.50) are needed to reach the solution:

$$\frac{\partial w}{\partial x} = \frac{2}{L} \sum_{n=1}^{\infty} W_n(t) \frac{n\pi}{L} \cos \frac{n\pi x}{L} \quad (3.52)$$

$$\frac{\partial^2 w}{\partial x^2} = -\frac{2}{L} \sum_{n=1}^{\infty} W_n(t) \frac{n^2 \pi^2}{L^2} \sin \frac{n\pi x}{L} \quad (3.53)$$

$$\frac{\partial^3 w}{\partial x^3} = -\frac{2}{L} \sum_{n=1}^{\infty} W_n(t) \frac{n^3 \pi^3}{L^3} \cos \frac{n\pi x}{L} \quad (3.54)$$

$$\frac{\partial^4 w}{\partial x^4} = \frac{2}{L} \sum_{n=1}^{\infty} W_n(t) \frac{n^4 \pi^4}{L^4} \sin \frac{n\pi x}{L} \quad (3.55)$$

The right-side term of equation (3.46) must also be expressed in terms of a Fourier sine series, in order to reach the solution:

$$p(x, t) = \Delta p [1 - H(x - \alpha t)] = \frac{2}{L} \sum_{n=1}^{\infty} b_n(t) \sin \frac{n\pi x}{L} \quad (3.56)$$

The coefficient $b_n(t)$ may be found using the definition found in [38:p573]:

$$b_n(t) = \int_0^L p(x, t) \sin \frac{n\pi x}{L} dx \quad (3.57)$$

The pressure should be equal to Δp when $0 \leq x \leq \alpha t$, and equal to 0 when $\alpha t \leq x \leq L$:

$$b_n(t) = \int_0^{\alpha t} \Delta p \sin \frac{n\pi x}{L} dx + \int_{\alpha t}^L 0 \cdot \sin \frac{n\pi x}{L} dx \quad (3.58)$$

Executing the integration:

$$b_n(t) = \Delta p \left[-\frac{L}{n\pi} \cos \frac{n\pi x}{L} \right]_0^{\alpha t} \quad (3.59)$$

Introducing the integration limits:

$$b_n(t) = \Delta p \left(-\frac{L}{n\pi} \right) \left(\cos \frac{n\pi \alpha t}{L} - \cos 0 \right) \quad (3.60)$$

The expression for $b_n(t)$ has been found:

$$b_n(t) = \frac{L}{n\pi} \Delta p \left(1 - \cos \frac{n\pi\alpha t}{L} \right) \quad (3.61)$$

The Fourier sine series for the dynamic pressure term is therefore:

$$\Delta p [1 - H(x - \alpha t)] = \frac{2}{L} \sum_{n=1}^{\infty} \frac{L}{n\pi} \Delta p \left(1 - \cos \frac{n\pi\alpha t}{L} \right) \sin \frac{n\pi x}{L} \quad (3.62)$$

This series will converge to 0 at $x=0$ because Fourier sine series represent an odd extension outside the interval $0 \leq x \leq L$ [38]. However, the series will rapidly rise to Δp for higher values of x . At $x=0$ the pipe is supported against radial deflection, and it is therefore unproblematic that the series equals zero instead of Δp here, as the pressure at $x=0$ would be fully resisted by the support anyway, and not cause any deflection.

Expressions (3.50), (3.53), (3.55) and (3.62) may now be implemented into equation (3.46):

$$\begin{aligned} \lambda_1 \frac{2}{L} \sum_{n=1}^{\infty} W_n(t) \frac{n^4 \pi^4}{L^4} \sin \frac{n\pi x}{L} - \lambda_2 \frac{2}{L} \sum_{n=1}^{\infty} W_n(t) \frac{n^2 \pi^2}{L^2} \sin \frac{n\pi x}{L} + \lambda_3 \frac{2}{L} \sum_{n=1}^{\infty} W_n(t) \sin \frac{n\pi x}{L} \\ + \rho_m h \frac{2}{L} \sum_{n=1}^{\infty} \ddot{W}_n(t) \sin \frac{n\pi x}{L} = \frac{2}{L} \sum_{n=1}^{\infty} \frac{L}{n\pi} \Delta p \left(1 - \cos \frac{n\pi\alpha t}{L} \right) \sin \frac{n\pi x}{L} \end{aligned} \quad (3.63)$$

Please note that $\ddot{W}_n(t) = d^2 W_n(t) / dt^2$. All the terms are sums, and the coefficient $\sin(n\pi x/L)$ is common for all the terms:

$$\sum_{n=1}^{\infty} \left[\rho_m h \ddot{W}_n(t) + \lambda_1 W_n(t) \frac{n^4 \pi^4}{L^4} - \lambda_2 W_n(t) \frac{n^2 \pi^2}{L^2} + \lambda_3 W_n(t) - \frac{L}{n\pi} \Delta p \left(1 - \cos \frac{n\pi\alpha t}{L} \right) \right] \sin \frac{n\pi x}{L} = 0 \quad (3.64)$$

In order for a sum of infinitely many terms to be precisely equal to zero, each term of the sum should be equal to zero:

$$\rho_m h \ddot{W}_n(t) + \lambda_1 W_n(t) \frac{n^4 \pi^4}{L^4} - \lambda_2 W_n(t) \frac{n^2 \pi^2}{L^2} + \lambda_3 W_n(t) = \frac{L}{n\pi} \Delta p \left(1 - \cos \frac{n\pi\alpha t}{L} \right) \quad (3.65)$$

The following notation is introduced:

$$\omega_n = \frac{n\pi}{L} \quad (3.66)$$

$$\Omega_n^2 = \frac{1}{\rho_m h} (\omega_n^4 \lambda_1 - \omega_n^2 \lambda_2 + \lambda_3) \quad (3.67)$$

$$\omega = \frac{\pi\alpha}{L} \quad (3.68)$$

$$p_n^* = \frac{\Delta p}{\rho_m h} \frac{L}{n\pi} \quad (3.69)$$

This allows equation (3.65) to be rewritten into:

$$\ddot{W}_n(t) + \Omega_n^2 W_n(t) = p_n^* (1 - \cos n\omega t) \quad (3.70)$$

The partial differential equation (3.46) has been transformed into an ordinary differential equation, which can easily be solved.

The particular solution of the differential equation (3.70) is similar to its right-side term:

$$W_{n,p}(t) = F - E \cos n\omega t \quad (3.71)$$

where F and E are constants. Its second derivative is:

$$\ddot{W}_{n,p}(t) = En^2\omega^2 \cos n\omega t \quad (3.72)$$

Expressions (3.71) and (3.72) are inserted into equation (3.65):

$$En^2\omega^2 \cos n\omega t + \Omega_n^2 F - \Omega_n^2 E \cos n\omega t = p_n^* - p_n^* \cos n\omega t \quad (3.73)$$

F is found from the two constant (with respect to time) terms to be:

$$\Omega_n^2 F = p_n^* \Rightarrow F = \frac{p_n^*}{\Omega_n^2} \quad (3.74)$$

E is found from the coefficients in front of the cosine terms:

$$En^2\omega^2 - \Omega_n^2 E = -p_n^* \Rightarrow E = \frac{p_n^*}{\Omega_n^2 - n^2\omega^2} \quad (3.75)$$

The particular solution is therefore:

$$W_{n,p}(t) = p_n^* \left(\frac{1}{\Omega_n^2} - \frac{1}{\Omega_n^2 - n^2\omega^2} \cos n\omega t \right) \quad (3.76)$$

The homogeneous solution of equation (3.70) is given by its characteristic equation:

$$r^2 + \Omega_n^2 = 0 \Rightarrow r = \pm \Omega_n i \quad (3.77)$$

These roots yield the following general solution of the differential equation [38]:

$$W_{n,h}(t) = C \cos \Omega_n t + D \sin \Omega_n t \quad (3.78)$$

where C and D are constants which depend on the initial conditions. The full solution is the sum of the homogeneous and the particular solution:

$$W_n(t) = W_{n,h}(t) + W_{n,p}(t) = C \cos \Omega_n t + D \sin \Omega_n t + p_n^* \left(\frac{1}{\Omega_n^2} - \frac{1}{\Omega_n^2 - n^2\omega^2} \cos n\omega t \right) \quad (3.79)$$

The initial conditions (3.49) are transformed using equation (3.51):

$$w(x,0) = 0 \Rightarrow W_n(0) = 0 \quad (3.80)$$

$$\left. \frac{\partial w(x,t)}{\partial t} \right|_{t=0} = 0 \Rightarrow \dot{W}_n(0) = 0 \quad (3.81)$$

Taking initial condition (3.81) into account first:

$$\dot{W}_n(t) = -\Omega_n C \sin(\Omega_n t) + \Omega_n D \cos(\Omega_n t) + \frac{p_n^* \cdot n\omega}{\Omega_n^2 - n^2\omega^2} \sin n\omega t \quad (3.82)$$

$$\dot{W}_n(0) = \Omega_n D = 0 \Rightarrow D = 0 \quad (3.83)$$

Initial condition (3.80):

$$W_n(0) = C + p_n^* \left(\frac{1}{\Omega_n^2} - \frac{1}{\Omega_n^2 - n^2\omega^2} \right) = 0 \Rightarrow C = -p_n^* \left(\frac{1}{\Omega_n^2} - \frac{1}{\Omega_n^2 - n^2\omega^2} \right) \quad (3.84)$$

The solution of equation (3.70) with the given initial conditions has been found:

$$W_n(t) = p_n^* \left[\frac{1}{\Omega_n^2 - n^2 \omega^2} (\cos \Omega_n t - \cos n \omega t) + \frac{1}{\Omega_n^2} (1 - \cos \Omega_n t) \right] \quad (3.85)$$

Combining expressions (3.50) and (3.85), an analytical solution for the radial deflection has been found:

$$w(x, t) = \frac{2}{L} \sum_{n=1}^{\infty} p_n^* \left[\frac{\cos \Omega_n t - \cos n \omega t}{\Omega_n^2 - n^2 \omega^2} + \frac{1 - \cos \Omega_n t}{\Omega_n^2} \right] \sin \frac{n \pi x}{L} \quad (3.86)$$

This radial deflection is related to pipe wall stresses in section 3.8. The expression may also be used in the special cases where the pipe consists only of steel ($N = 0$), or only of FRP material ($h_{st} = 0$). Several MATLAB-scripts which can be used to calculate $w(x, t)$ using this expression can be found in appendix A.

3.4.1 Convergence of the sum

Most common Fourier series converge [39:p695]. From expressions (3.66), (3.67), (3.69) and (3.86), it is observed that all the terms in the series are divided by a fifth degree polynomial of n . The coefficient in front of the sine expression will therefore become smaller and smaller. This fact does not prove that the series necessarily do converge [40:p344], but indicates that it is plausible.

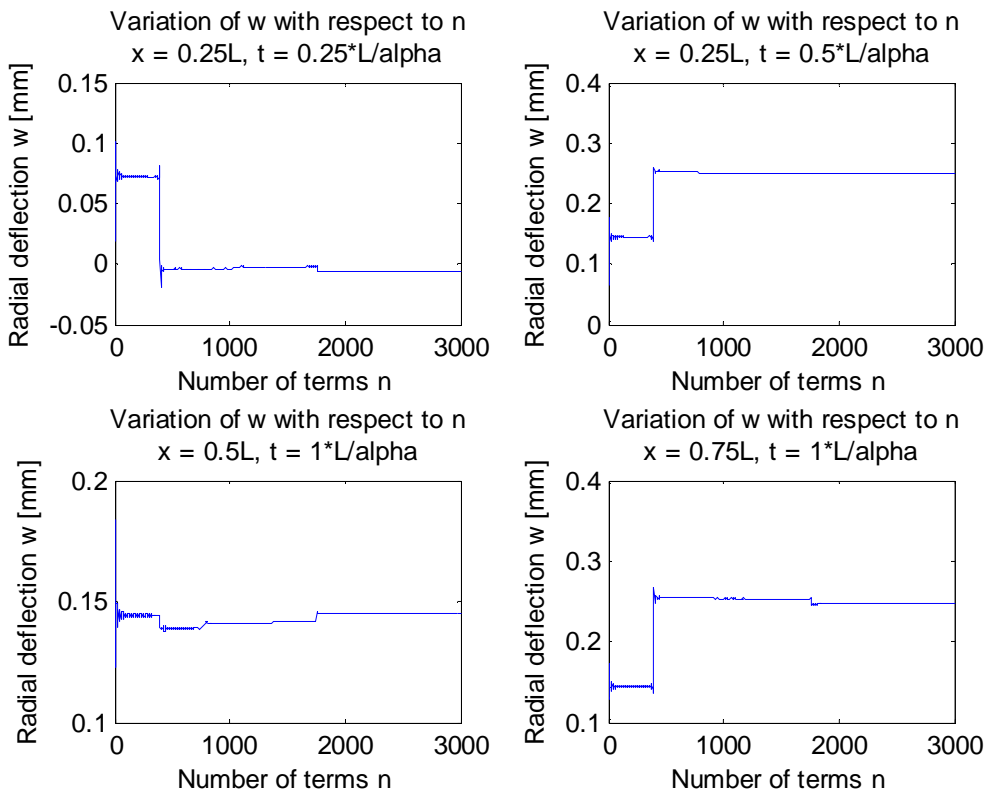


Figure 6: Variation of the radial deflection w with respect to the number of terms included in expression (3.86).

In figure 6, the radial deflection, w , given by expression (3.86), has been plotted in MATLAB as a function of the number of terms included, at four different combinations of position and time, for a representative example. In all 4 cases, there is a large jump in w for $n < 1000$, while it remains constant for $2000 < n < 3000$. As convergence is assumed in the other works utilizing a Fourier series solution [1,13,28], it should therefore be safe to assume that the Fourier series (3.86) actually does converge towards the true solution of the differential equation (3.46) when $n \rightarrow \infty$.

In practice, it is impossible to calculate infinitely many terms, and the sum must therefore be truncated. In order to reduce the computation time, the number of terms calculated should be minimized. However, the truncation error should also be limited. It is therefore required to establish some kind of guideline about how many terms which need to be included. None of the three previous works considered [1,13,28] has given such a guideline, or mentioned the need for it.

In figure 6, it is clearly visible that a change happens after about 1750 terms. If less than 1750 terms are included in this sum, the truncation error may be significant to the calculated dynamic behaviour of the pipe, as vibrations may be flattened out due to this error, etc. The reason behind the sudden change is that the denominator $\Omega_n^2 - n^2\omega^2$ is not monotonically increasing, but rather has a minimum for some $n \in [0, \infty]$. When this denominator is low, its influence on the sum is high. Therefore, the sum must not be truncated before the minimum of this denominator (for the highest value of n) has been passed by a sufficient margin. Trials have shown that if the denominator passes zero, it is sufficient to exceed this value of n by 10 %. The denominator passes zero when:

$$\Omega_n^2 - n^2\omega^2 = \frac{1}{\rho_m h} \left(\frac{n^4 \pi^4}{L^4} \lambda_1 - \frac{n^2 \pi^2}{L^2} \lambda_2 + \lambda_3 \right) - \frac{n^2 \pi^2 \alpha^2}{L^2} = 0 \quad (3.87)$$

This equation may be solved for its largest value for n :

$$n_0 = \frac{L}{\pi} \sqrt{\frac{\lambda_2 + \alpha^2 \rho_m h + \sqrt{(\lambda_2 + \alpha^2 \rho_m h)^2 - 4\lambda_1 \lambda_3}}{2\lambda_1}} \quad (3.88)$$

The sum should be truncated when this value has been exceeded by 10 %:

$$N_F = 1.1 \cdot \frac{L}{\pi} \sqrt{\frac{\lambda_2 + \alpha^2 \rho_m h + \sqrt{(\lambda_2 + \alpha^2 \rho_m h)^2 - 4\lambda_1 \lambda_3}}{2\lambda_1}} \quad (3.89)$$

If $(\lambda_2 + \alpha^2 \rho_m h)^2 < 4\lambda_1 \lambda_3$, the denominator $\Omega_n^2 - n^2\omega^2$ will never reach zero. Then, its minimum value must be exceeded, instead. The minimum value is found by setting its derivative equal to zero:

$$\frac{\partial}{\partial n} (\Omega_n^2 - n^2\omega^2) = 4 \frac{\pi^4}{L^4} \lambda_1 n^3 - 2 \frac{\pi^2}{L^2} (\lambda_2 + \alpha^2 \rho_m h) n = 0 \quad (3.90)$$

Solving this equation for its largest value of n yields:

$$n_{\min} = \frac{L}{\pi} \sqrt{\frac{\lambda_2 + \alpha^2 \rho_m h}{2\lambda_1}} \quad (3.91)$$

Trials have shown that this value should be exceeded by 50 % to properly reach convergence:

$$N_F = 1.5 \cdot \frac{L}{\pi} \sqrt{\frac{\lambda_2 + \alpha^2 \rho_m h}{2\lambda_1}} \quad (3.92)$$

These two limits are implemented into the MATLAB program provided in appendix A, and are used in all evaluations of expression (3.86) shown in this thesis.

3.5 Static pipe deformation

Often, the pipe will be subjected to a static steady-state pressure, p_0 , before the valve is closed and water hammer conditions occur. The radial deflection due to this static pressure should also be taken into account, in order to find the total radial deflection. The equilibrium equation for the pipe is equation (3.34) with the inertia term removed:

$$\lambda_1 \frac{d^4 w_0}{dx^4} + \lambda_2 \frac{d^2 w_0}{dx^2} + \lambda_3 w_0 = p_0 \quad (3.93)$$

Apart from in a narrow boundary zone at the ends of the pipe, the radial deflection due to a static pressure will be:

$$w_0 \approx \frac{P_0}{\lambda_3} \quad (3.94)$$

At the ends however, the radial deflection will be higher, and influenced by the bending stiffness of the pipe.

For a steel pipe, the radial deflection as a function of x is given in [24] and [34:p468]. However, these solutions contain the coefficients $e^{\beta x}$ and $e^{-\beta x}$, where $\beta^4 = 3(1-\nu^2)/R^2 h^2$. When the pipe is very long (say, more than 100 times the diameter), these coefficients approach infinity and zero, respectively, and can therefore not be used. For longer pipes, it should be possible to solve equation (3.93) using Fourier series, similarly to what was done in section 3.4. Once more the pipe is assumed to be simply supported in its ends, a support condition which is automatically fulfilled by Fourier sine series. Let the Fourier sine series for the static deflection and its coefficients be given as:

$$w_0(x) = \frac{2}{L} \sum_{n=1}^{\infty} W_{0,n} \sin \frac{n\pi x}{L} \quad (3.95)$$

where

$$W_{0,n} = \int_0^L w_0(x) \sin \frac{n\pi x}{L} dx \quad (3.96)$$

The Fourier sine series of the static pressure may be found to be:

$$p_0 = \frac{2}{L} \sum_{n=1}^{\infty} \frac{p_0 L}{n\pi} (1 - \cos n\pi) \sin \frac{n\pi x}{L} \quad (3.97)$$

The differential equation (3.93) may now be written as:

$$\lambda_1 W_{0,n} \frac{n^4 \pi^4}{L^4} - \lambda_2 W_{0,n} \frac{n^2 \pi^2}{L^2} + \lambda_3 W_{0,n} = \frac{p_0 L}{n\pi} (1 - \cos n\pi) \quad (3.98)$$

This is a simple equation, with the following solution:

$$W_{0,n} = \frac{p_0 L}{n\pi} \cdot \frac{1 - \cos n\pi}{\lambda_1 \omega_n^4 - \lambda_2 \omega_n^2 + \lambda_3} \quad (3.99)$$

The radial deflection of a pipe, subjected to a static pressure may therefore be expressed as:

$$w_0(x) = \frac{2p_0}{\pi} \sum_{n=1}^{\infty} \frac{1}{n} \cdot \frac{1 - \cos n\pi}{\lambda_1 \omega_n^4 - \lambda_2 \omega_n^2 + \lambda_3} \sin \frac{n\pi x}{L} \quad (3.100)$$

where ω_n is defined by expression (3.66).

We have now reached one expression which relates a static pressure to static radial deflection, and one which relates a pressure wave to dynamic radial pipe wall deflection. If the superposition principle can be applied to this problem, the two different deflections may be summed for all $x \in [0, L]$, in order to obtain the radial deflection of a pipe subjected to water hammer conditions, in addition to a steady-state pressure. Two conditions must be satisfied if the principle of superposition is to be applied [41:p136]: First, there must be a linear relationship between the pressure and the displacement. Equations (3.86) and (3.100) show that this condition is satisfied. Secondly, the loading must not significantly change the original geometry or configuration of the pipe. The model derived in this thesis is intended to be used below the yield strength of the pipeline material. Within this limit the deformations are quite small, and the second condition may also be considered to be satisfied. Hence, the principle of superposition may be applied, and the total radial deflection may be found by summing the two contributions.

3.6 The critical velocity

When evaluated with numbers, expression (3.86) shows that the pipe will vibrate when subjected to water hammer conditions. See section 4.3. If the maximum radial deflection obtained by this expression is divided by the equivalent static deflection, $w_{st} \approx \Delta p / \lambda_3$, where the pressure $\Delta p = \rho_f \alpha \Delta V$ is regarded as a static pressure, we obtain a factor which is called the dynamic load factor (DLF) [29]. According to Simkins [28] and Leishear [29], there is a critical velocity for the pressure wave at which the DLF will have its maximum value, i.e. where the pressure wave will cause resonance. It will be convenient to be able to calculate this critical velocity for a steel pipe repaired with a FRP overwrap. The critical velocity depends on the stiffness and mass of the pipe, i.e. its natural frequency.

Leishear [29] has solved the equation of motion for a steel pipe subjected to water hammer analytically, but his solution is strange, as it predicts dynamic radial deflection $w \neq 0$ at $t = 0$, i.e. at the same instant that the valve is closed. This does not seem realistic, as the pressure wave has a finite velocity, and therefore cannot cause an instant response. However, his derivation of the critical velocity of a pressure wave through a steel pipe fits the model developed in this thesis (when the number of FRP lamina, N , is set equal to zero). His derivation will therefore be used as a basis to calculate an expression for the critical velocity in a steel pipe repaired with a FRP overwrap.

Consider equation (3.46):

$$\lambda_1 \frac{\partial^4 w}{\partial x^4} + \lambda_2 \frac{\partial^2 w}{\partial x^2} + \lambda_3 w + \rho_m h \frac{\partial^2 w}{\partial t^2} = \Delta p [1 - H(x - \alpha t)] \quad (3.46)$$

A change in variables is performed, by introducing a new variable:

$$X = x - \alpha t \quad (3.101)$$

Using this new variable, the following relationships are applicable [42]:

$$\frac{\partial^4 w}{\partial x^4} = \frac{d^4 w}{dX^4}, \quad \frac{\partial^2 w}{\partial x^2} = \frac{d^2 w}{dX^2}, \quad \frac{\partial^2 w}{\partial t^2} = \alpha^2 \frac{d^2 w}{dX^2} \quad (3.102)$$

Equation (3.46) may be rewritten, using relationships (3.101) and (3.102):

$$\lambda_1 \frac{d^4 w}{dX^4} + \lambda_3 w + (\lambda_2 + \rho_m h \alpha^2) \frac{d^2 w}{dX^2} = \Delta p (1 - H(X)) \quad (3.103)$$

$$\frac{\lambda_1}{\lambda_3} \frac{d^4 w}{dX^4} + w + \frac{\lambda_2 + \rho_m h \alpha^2}{\lambda_3} \frac{d^2 w}{dX^2} = \frac{\Delta p}{\lambda_3} (1 - H(X))$$

Two new variables are introduced:

$$\gamma = \sqrt[4]{\frac{\lambda_3}{\lambda_1}} \quad \text{and} \quad \xi = \gamma X \quad (3.104)$$

In this case, the following relationships may be derived:

$$\frac{d^4 w}{dX^4} = \gamma^4 \frac{d^4 w}{d\xi^4}, \quad \frac{d^2 w}{dX^2} = \gamma^2 \frac{d^2 w}{d\xi^2}, \quad \lambda_3 = \lambda_1 \gamma^2 \sqrt{\frac{\lambda_3}{\lambda_1}} \quad (3.105)$$

Expressions (3.104) and (3.105) are introduced to equation (3.103):

$$\frac{1}{\gamma^4} \cdot \gamma^4 \frac{d^4 w}{d\xi^4} + w + \frac{\lambda_2 + \rho_m h \alpha^2}{\lambda_1 \gamma^2 \sqrt{\frac{\lambda_3}{\lambda_1}}} \cdot \gamma^2 \frac{d^2 w}{d\xi^2} = \frac{\Delta p}{\lambda_3} (1 - H(X)) \quad (3.106)$$

$$\frac{d^4 w}{d\xi^4} + w + \frac{\lambda_2 + \rho_m h \alpha^2}{\sqrt{\lambda_1^2 \cdot \frac{\lambda_3}{\lambda_1}}} \frac{d^2 w}{d\xi^2} = \frac{\Delta p}{\lambda_3} (1 - H(X))$$

Yet another coefficient is introduced:

$$2\Lambda = \frac{\lambda_2 + \rho_m h \alpha^2}{\sqrt{\lambda_1 \lambda_3}} \quad (3.107)$$

According to Leishear [29], $\Lambda=1$ when the pressure wave travels at the critical velocity. Solving equation (3.107), with respect to α , where $\Lambda=1$, yields the expression for the critical velocity of a pressure wave through a steel pipe repaired with a FRP overwrap:

$$\alpha_{cr} = \sqrt{\frac{2\sqrt{\lambda_1\lambda_3} - \lambda_2}{\rho_m h}} \quad (3.108)$$

This expression is in agreement to the results provided by the Fourier solution expression (3.86).

3.7 The radial deflection during the wave of pressure unloading

As previously mentioned, expression (3.86) is only applicable for the first half round trip of the pressure wave, i.e. for $0 \leq t \leq T_r/2$. Previous uncoupled models [1,13,29,30] have only considered this first half round trip. However, as the pipe wall already is in motion when the pressure is unloaded, there is no guarantee that the maximum radial deflection (and thereby the maximum stresses) will occur during the first half round trip. Therefore, an expression for the dynamic radial deflection during the second half of the round trip should also be derived.

The same procedure as in section 3.4 may be used, with the dynamic pressure from expression (3.42). The initial condition should be that W_n for the new expression should be equal to W_n for the old one when $t = T_r/2$, however. It can be shown that the solution for the second half of the round trip then will be:

$$w(x,t) = \frac{2}{L} \sum_{n=1}^{\infty} p_n^* \left[\frac{\cos \Omega_n t - \cos n(2\pi - \omega t)}{\Omega_n^2 - n^2 \omega^2} + \frac{1 - \cos \Omega_n t}{\Omega_n^2} \right] \sin \frac{n\pi x}{L} \quad (3.109)$$

for $T_r/2 \leq t \leq T_r$, where the symbols have the same definitions as in expression (3.86).

In a similar way, the governing differential equation may be solved for the third half round, i.e. for $T_r \leq t \leq 3T_r/2$. The solution would be:

$$w(x,t) = \frac{2}{L} \sum_{n=1}^{\infty} p_n^* \left[\left(\cos \Omega_n t - 2 \frac{\sin \Omega_n t}{\sin(2\Omega_n L / \alpha)} \right) \left(\frac{1}{\Omega_n^2 - n^2 \omega^2} - \frac{1}{\Omega_n^2} \right) + \frac{\cos n(\omega t - 2\pi)}{\Omega_n^2 - n^2 \omega^2} - \frac{1}{\Omega_n^2} \right] \sin \frac{n\pi x}{L} \quad (3.110)$$

This solution will be discussed in subsection 4.3.2.

3.8 Pipeline stresses

In order to check whether the calculated dynamic radial deflections are acceptable, they need to be related to the pipeline stresses and failure criteria. The pipe is still considered to be a thin-walled axisymmetric cylinder. The non-zero mid-surface strains and curvatures will be:

$$\varepsilon_y^0 = \frac{w}{R} \quad (3.17)$$

$$k_x^0 = -\frac{\partial^2 w}{\partial x^2} \quad (3.19)$$

$$k_y^0 = -\frac{w}{R^2} \quad (3.20)$$

The corresponding strains in each lamina are given by [15:p29]:

$$\varepsilon_x = \varepsilon_x^0 + zk_x^0 = -z \frac{\partial^2 w}{\partial x^2} \quad (3.111)$$

$$\varepsilon_y = \varepsilon_y^0 + zk_y^0 = \frac{w}{R} - z \frac{w}{R^2} = \frac{w}{R} \left(1 - \frac{z}{R}\right) \quad (3.112)$$

where z is the radial distance, as shown in figure 5, page 27. As the curvature k_y^0 has negative sign, the inner layers will be subjected to the highest hoop stresses. As the pipe wall is thin, ε_y^0 will likely be the largest contribution to the stress. Additionally, expressions (3.50) and (3.53) indicate that $\partial^2 w / \partial x^2$ has a minimum value when w is at its maximum. There is therefore great reason to believe that the maximum stress will occur when the radial deflection is at its maximum. When the position x and time t for the maximum radial deflection have been found, $\partial^2 w / \partial x^2$ may be calculated using expressions (3.53) and (3.85).

For the steel pipe, the stresses with largest magnitudes occur at $z = -h/2$, and the stiffnesses are given in expressions (3.12)-(3.13). The stress components will therefore be:

$$\sigma_{x,st} = \frac{E_{st}}{1-\nu_{st}^2} \left(\frac{h}{2} \frac{\partial^2 w}{\partial x^2} + \nu_{st} \frac{w}{R} \left(1 + \frac{h}{2R}\right) \right) \quad (3.113)$$

$$\sigma_{y,st} = \frac{E_{st}}{1-\nu_{st}^2} \left(\frac{w}{R} \left(1 + \frac{h}{2R}\right) + \nu_{st} \frac{h}{2} \frac{\partial^2 w}{\partial x^2} \right) \quad (3.114)$$

A common failure criterion for steel is the von Mises criterion. The von Mises equivalent stress is given as [35:p121]:

$$\sigma_e = \sqrt{\frac{1}{2} \left[(\sigma_x - \sigma_y)^2 + (\sigma_y - \sigma_z)^2 + (\sigma_z - \sigma_x)^2 \right] + 3(\tau_{xy}^2 + \tau_{yz}^2 + \tau_{xz}^2)} \quad (3.115)$$

Under plane stress conditions, this expression may be shortened to:

$$\sigma_e = \sqrt{\sigma_x^2 - \sigma_x \sigma_y + \sigma_y^2 + 3\tau_{xy}^2} \quad (3.116)$$

This equivalent stress may then be compared to the yield strength of the steel. Yielding occurs if the equivalent stress is equal to or higher than the yield strength.

For the FRP overwrap, the maximum hoop strain occurs at $z = -h/2 + h_{st}$, while the axial strain has its largest magnitude at $z = h/2$. The strains must be calculated at both places by expressions (3.111)-(3.112), and may be related to stresses in the xy coordinate system using equation (2.7). These stresses must then be related to stresses in the principal directions of the lamina, using the following relationship [15:p14]:

$$\begin{Bmatrix} \sigma_1 \\ \sigma_2 \\ \tau_{12} \end{Bmatrix} = \begin{bmatrix} m^2 & n^2 & 2mn \\ n^2 & m^2 & -2mn \\ -mn & mn & m^2 - n^2 \end{bmatrix} \begin{Bmatrix} \sigma_x \\ \sigma_y \\ \tau_{xy} \end{Bmatrix} \quad (3.117)$$

Like before, $m = \cos \theta$, $n = \sin \theta$, and θ is the angle between the x-axis and principal direction 1. These stresses may now be inserted into the Tsai-Wu failure criterion for FRP laminae, expression (2.18). MATLAB scripts for the evaluation of pipe failure are given in appendix A.

4. Results and Discussion

In chapter 3, a mathematical model for the vibration of a steel pipeline repaired with a FRP overwrap, subjected to water hammer conditions, was developed. In this chapter, the model will be applied to relevant examples, and discussed.

4.1 *Immediate comments to the derived model*

When the result of the derivation, expression (3.86), is calculated for a pure steel pipe, its solution coincides with the solution by Simkins [28] to a similar problem, as long as the same axial support conditions are used in both models. This indicates that expression (3.86) is a correct mathematical solution of the governing equation of motion (3.34). The static solution derived, expression (3.100), does also coincide with previous solutions [24,34], when it is calculated for a pure steel pipe. The derived model is therefore considered to be correct, under the assumptions and approximations stated in chapter 3.

The derived model is an analytical model. Yet, as it consists of an infinite sum, in practice its result has to be calculated by a computer. Its values must therefore be calculated at finite values of x and t . As the sum also consists of sine functions with varying angular frequency, it is not practical to find its maxima and minima analytically. In order to find the maxima of the function, which is needed to find the maximum stresses, it needs to be evaluated at multiple combinations of x and t , and compared to previous values. The intervals between each sampling point will be called dx and dt . When these intervals are reduced, the probability of hitting the actual maximum is increased, at the cost of increased computational effort/time. It is possible to implement numerical analysis algorithms to find the maximum more exactly and efficiently, but this is beyond the scope of this thesis.

Another important factor for the computation time is the number of terms of the sum (3.86) which is included, N_F . Two different truncation limits have been given, expression (3.89) and (3.92). Both are proportional to the length of the pipe, L . This means that if L is doubled, the number of calculations required to evaluate w in each sampling point must be doubled, in order to ensure that the truncation error is sufficiently small. Furthermore, the pressure wave will use twice as long time to travel through the longer pipe. If dx and dt are kept constant, the total computation time will therefore be proportional to L^3 . The computation time will therefore increase significantly for longer pipes. This is a weakness to the derived model.

4.2 Implementation of the model

The model derived in chapter 3 will now be implemented to different relevant examples, in order to illustrate, verify and discuss the model. All the examples are variations of one base example, with changes in one or more of the variables, in order to illustrate how the model responds to these changes. The variations are shown in table 2. The variables which are equal for all the examples are given in the text below. Material properties for the FRP laminae are given in table 1, section 2.1.1.

Table 2. Definition of the examples.

ID	FRP material	Stacking sequence	Length of pipe, L	Diameter of steel pipe, $2MR$	Steady-state pressure, p_0
1a	E-Glass/ Epoxy	+/-45°	10 m	400 mm	0
1b		+/-45°	50 m	400 mm	0
2a		+/-45°	10 m	400 mm	800 kPa
2b		+/-45°	10 m	1215 mm *	800 kPa
3		90/90/0°	10 m	400 mm	800 kPa
4	T300/5208	+/-45°	10 m	400 mm	800 kPa

* Example 2b also has $V = 2.3\text{ m/s}$ and $h_{st} = 10\text{ mm}$, in order to balance the increased diameter.

Consider a 16" steel pipeline with length L . The pipeline has been subjected to general corrosion, so that its effective, load carrying cross-sectional area has been reduced. The behaviour of the corroded steel pipe is modelled by its effective thickness after corrosion (see subsection 2.2.4), $h_{st} = 3.5\text{ mm}$, while its "effective" outer diameter is $2MR = 400\text{ mm}$. The pipe material is API 5L X52N, which is a carbon steel pipe material with density $\rho_{st} = 7850\text{ kg/m}^3$, yield strength $f_y = 360\text{ MPa}$ [43], elastic modulus $E_{st} = 210\text{ GPa}$ and Poisson's ratio $\nu_{st} = 0.3$. The pipe is considered to be simply supported against radial deflection in each end, and supported against axial motion throughout.

This pipe has been repaired by an overwrap composed by $N = 20$ FRP laminae, with the material and stacking sequence given in table 2. Each lamina has thickness $h_{la} = 0.15\text{ mm}$ (reparation laminates with total thickness as low as 0.18 mm exist [44], while one of the most trusted commercial systems [19] contains laminae with thickness 1.6 mm each [21]). The lamina thickness has been chosen to be low, so that the effect of adding more laminae may be illustrated, while still staying inside the thin-walled shell theory. The stacking sequence of the laminate is balanced, as shown in table 2, but not symmetric.

The above pipeline conveys water at 20 °C, which has density $\rho_f = 998.2 \text{ kg/m}^3$ and bulk modulus of elasticity $K = 2.18 \cdot 10^6 \text{ kN/m}^2$ [8:p732], at a steady-state velocity $V = 2.5 \text{ m/s}$. The steady-state pressure, relative to the exterior of the pipe, is p_0 . A sudden stop of the flow happens, and water hammer conditions occur.

For example 1a, the following components of the stiffness matrix are calculated, using equations (2.2)-(2.17), in addition to (3.12)-(3.15): $A_{12} = 2.7091 \cdot 10^8$, $A_{22} = 8.5910 \cdot 10^8$, $B_{12} = -3.1341 \cdot 10^5$, $B_{22} = -1.1216 \cdot 10^6$, $D_{11} = 2837.8$ and $D_{12} = 901.60$. By using expressions (3.31-3.33), the governing differential equation (3.34) does then get the following coefficients: $\lambda_1 = 2837.8$, $\lambda_2 = 3.1606 \cdot 10^6$ and $\lambda_3 = 2.1672 \cdot 10^{10}$. The mean density of the pipe wall, given by expression (3.40), is found to be $\rho_m = 5172.9 \text{ kg/m}^3$ when $N = 20$, while $h = 6.5 \text{ mm}$. The velocity of the pressure wave may be found by expression (2.34) to be $\alpha = 1041.4 \text{ m/s}$, while the pressure rise in its wake is found from equation (2.28) to be $\Delta p = 2.5988 \text{ MPa}$. Expression (2.27) states the time required for the pressure wave to travel a full round trip to be $T_r = 19.2 \text{ ms}$. Using equation (3.89), $N_F = 405$ terms are found to be needed, in order to reach convergence. The resulting dynamic radial deflection for $0 \leq t \leq T_r$ may now be found by applying expressions (3.66)-(3.68) and (3.86).

4.3 The behaviour of the pipeline under water hammer conditions

In this section, the general behaviour of the pipeline under water hammer conditions, predicted by the derived model, will be illustrated and discussed. Certain interesting observations which are not (or just briefly) mentioned in the examined literature are discussed, and explanations are proposed. This understanding is important to evaluate the influence of the fibre-reinforced polymer overwrap, which will be discussed in the next section.

4.3.1 The deformed shape

In figure 7, the radial deflection of the pipe in case 1a (ref. table 2), subjected to a dead pressure with magnitude 2.5988 MPa , is shown. The figure has been generated in MATLAB by plotting expression (3.100). This figure will be a good reference for the discussion of the radial deflection due to the dynamic pressure. It is observed that apart from in the ends, the pipe is radially deflected 0.12 mm, as predicted by expression (3.94). In both ends the radial deflection is a bit higher, as expected according to thin-walled shell theory.

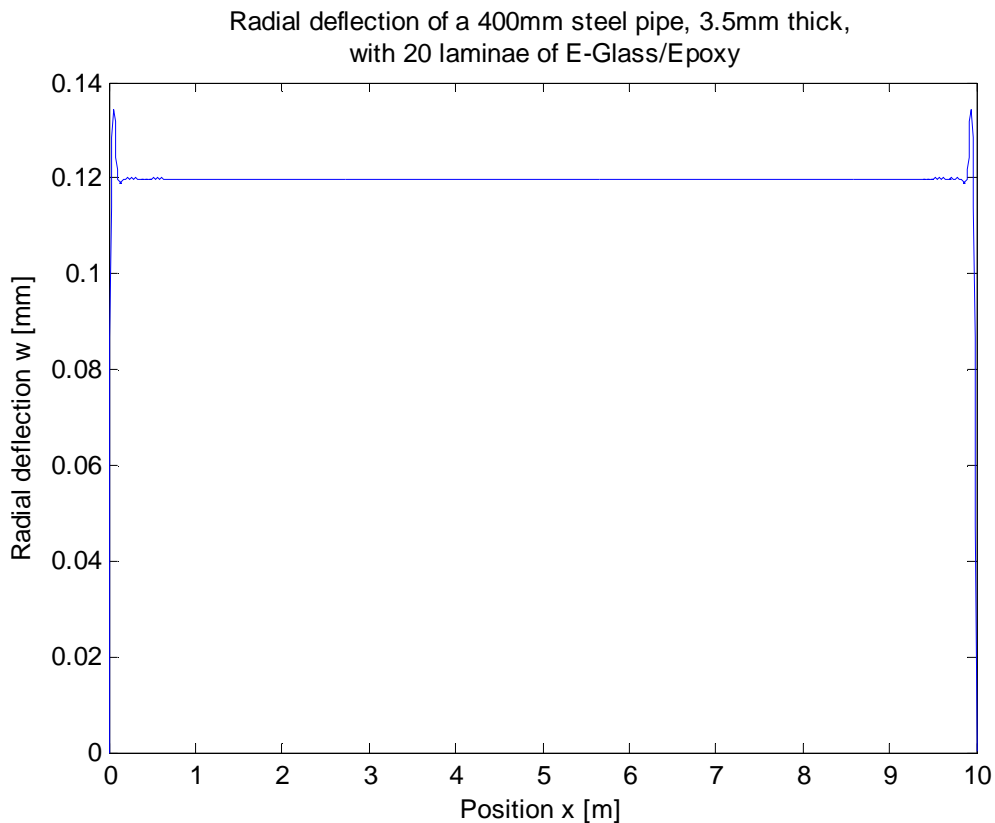


Figure 7: Radial deflection of pipe 1a, only due to a dead pressure of 2.5988 MPa.

The dynamic deflection due to a pressure wave, predicted by expression (3.86) is difficult to properly visualize with figures, because it is heavily oscillating with respect to time. An attempt is made with figures generated with MATLAB, but the best option is to use a software package to generate animated plots of the radial deflection with respect to position along the pipe. The MATLAB script "WHmovie.m" in appendix A may be used to generate such animations.

Figure 8 shows the radial deflection of the pipe in case 1a when the pressure wave is midway through the pipe; $t = T_r/4$. A similar plot for case 1b is shown in figure 9. The only difference between case 1a and case 1b is the length of the pipe. Please note that the sudden stop of flow happens at $x = 0$ (i.e. the valve is placed at $x = 0$, while the pipe is connected to a reservoir at $x = L$).

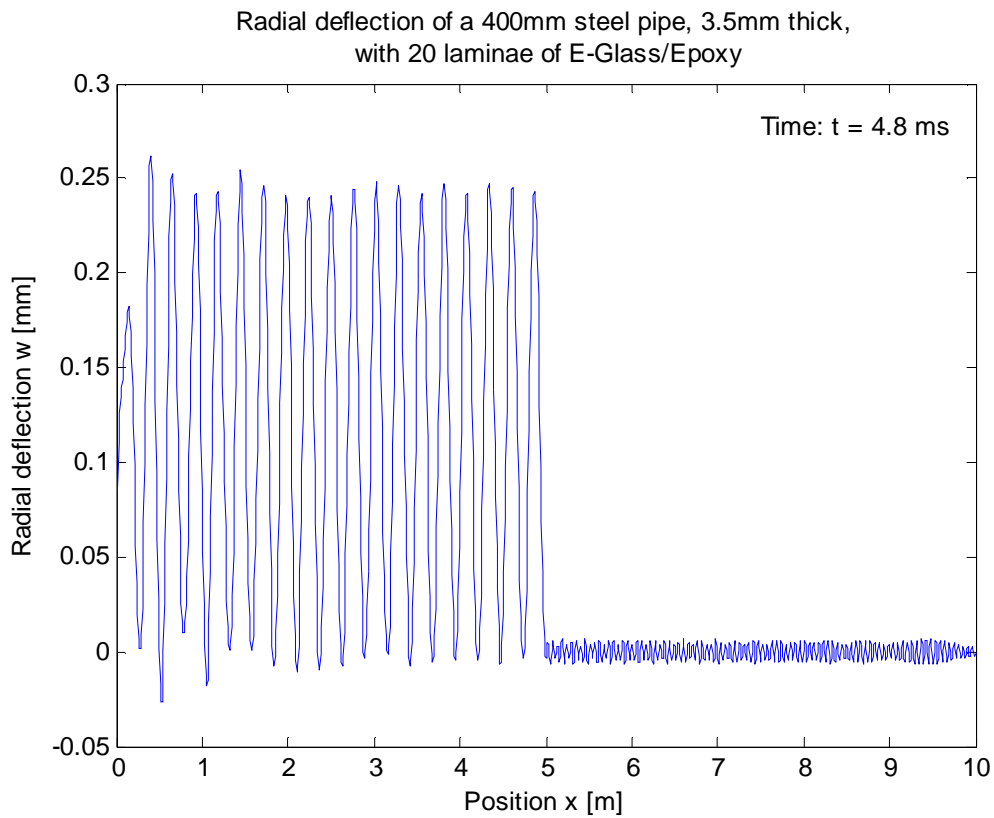


Figure 8: Radial deflection of pipe 1a, when the pressure wave has travelled halfway through the pipe. The pressure wave travels to the right.

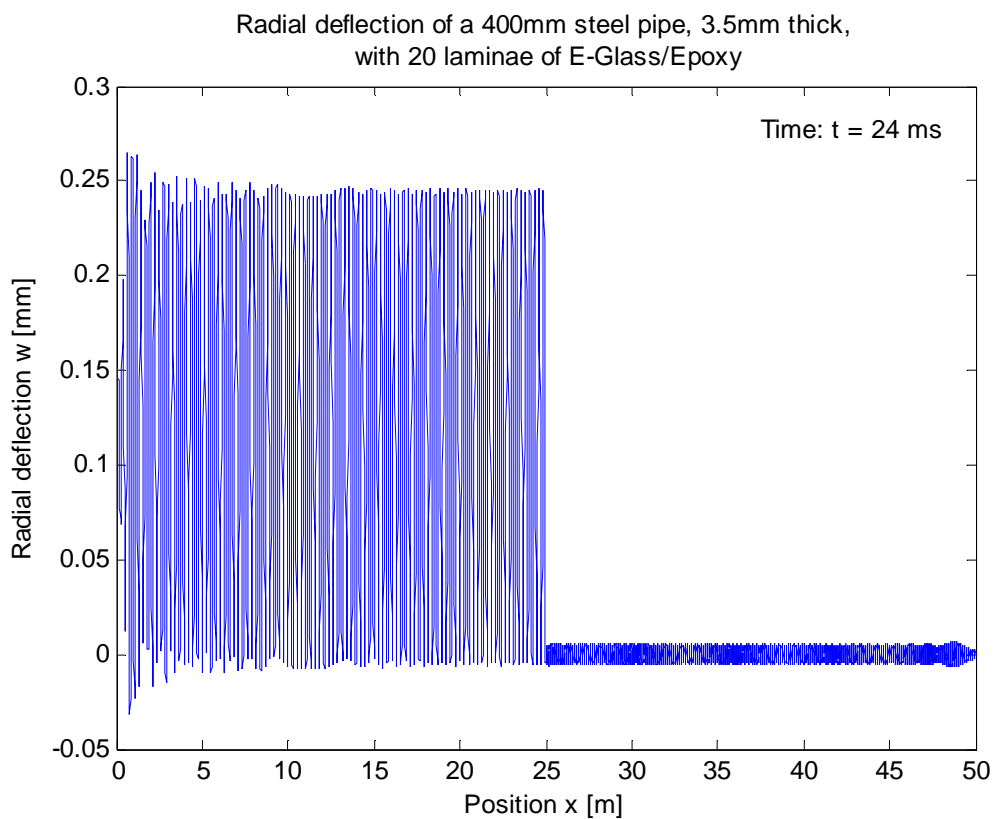


Figure 9: Radial deflection of pipe 1b, when the pressure wave has travelled halfway through the pipe. The pressure wave travels to the right.

The radial deflection due to the water hammer-induced pressure wave is observed to oscillate heavily about the static deflection of 0.12 mm, seen in figure 7, which would have been the deflection if the pressure had been static. At the current instant, the maximum radial deflection is 2.2 times higher than this static deflection. In the interval $t \in [0, T_r]$, the maximum of this factor is 2.35, which means that the dynamic load factor (DLF) is equal to 2.35 for this case.

Figure 8 and 9 also indicate a small precursor vibration in front of the pressure wave, which has earlier also been calculated for steel pipes [29].

It is observed that the displacement goes from its maximum to its minimum value over a length of ca. 130 mm both for the 10 m pipe and the 50 m pipe. In the figures, this may seem like a very short length between each maximum and minimum, but it actually corresponds to a slope of just 0.2%. The static solution, as shown in figure 7, shows that this slope actually is realistic. Another interesting question is why the deflection curve behind the pressure wave is not more flat. Intuitively, one would perhaps guess that the deformed shape behind the pressure wave (for $x < 5m$ in figure 8) would be more similar to the shape shown in figure 7, with all points vibrating in phase between their maximum and minimum value. The reason why all the points do not vibrate in phase is thought to be that when the pressure wave reaches the pipe wall at $x = 5.13m$, pushing it outwards, the pipe wall at $x = 5.00m$ is already at its maximum radial deflection, and therefore on its way inwards again. The pipe wall at $x = 5.13m$ does therefore travel outwards simultaneously as it travels inwards at $x = 5.00m$, resulting in the oscillating pattern observed in figure 8 and 9. Anyway, the length of the pipe does not seem to considerably influence the deformed shape of the pipe. Therefore, the rest of the examples have been calculated only for a 10 m long pipe.

4.3.2 The wave of pressure unloading

When the pressure wave has reached the far end of the pipeline, $x = L$, a wave of pressure unloading begins travelling in the other direction, as indicated in subsection 2.3.1. The radial deflection due to this wave of pressure unloading is modelled by expression (3.109). The pipe wall will continue to vibrate also after it has been unloaded, because it already is in motion. In real life, the vibrations will decrease over time, because of damping and friction (i.e. energy dissipation), but this is not taken into account in the current model. The vibrations predicted by the current model are quite different before and after the wave of pressure unloading, as illustrated in figures 10 and 11.

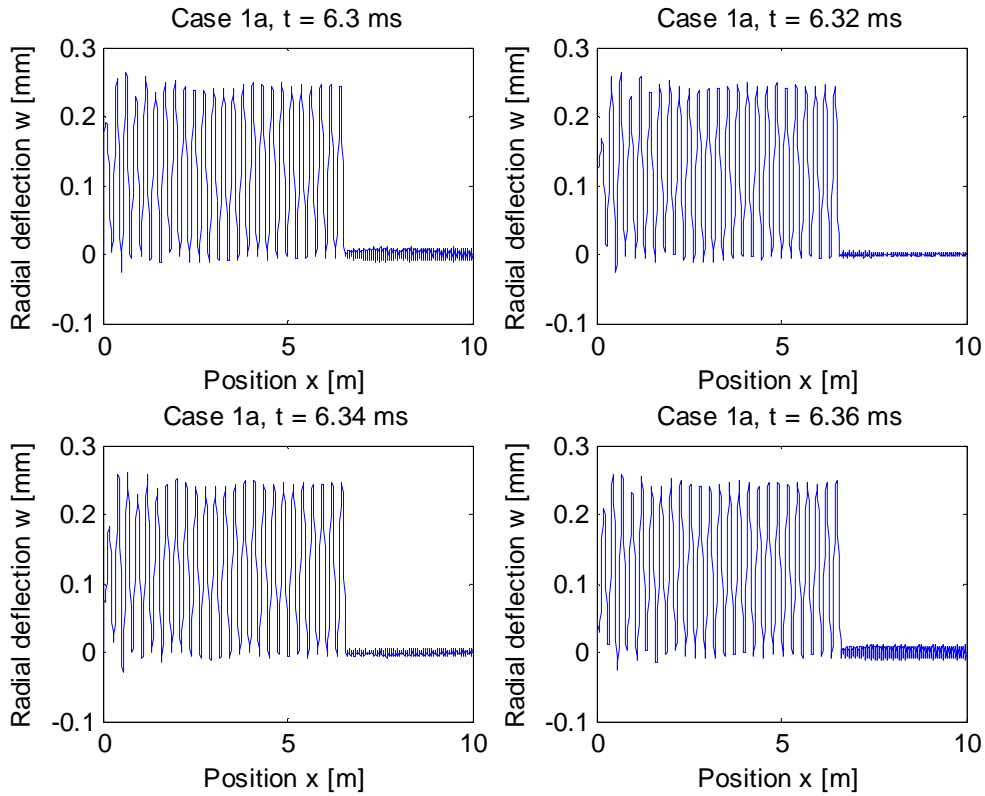


Figure 10: Radial deflection of pipe 1a. The pressure wave travels to the right.

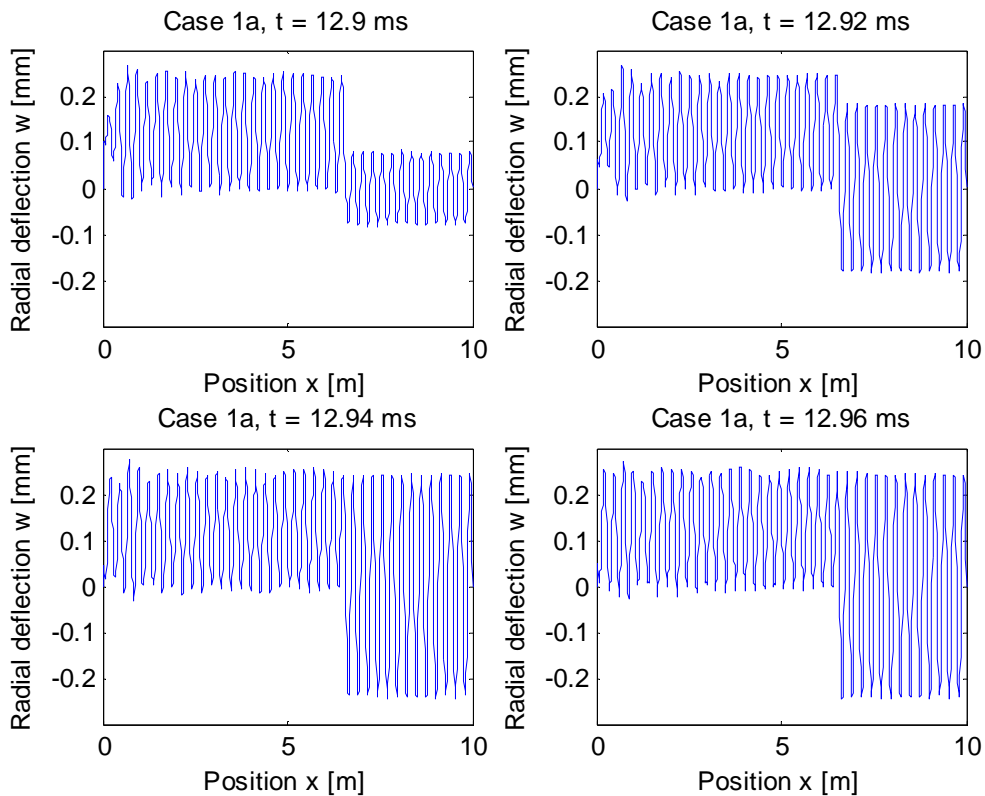


Figure 11: Radial deflection of pipe 1a. The wave of pressure unloading travels to the left.

Figure 10 shows four stills of the radial vibration at intervals of 0.02 ms when the pressure wave is travelling to the right, while figure 11 shows similar stills when the wave of pressure unloading is travelling to the left. When the pressure wave is travelling to the right (figure 10), a wave of radial deflection is travelling along the pressure wave. In the wake of the pressure wave, there are new waves of radial deflection, so that every point in the wake vibrates between 0 and 0.27 mm, approximately.

When the wave of pressure unloading has passed on its way to the left, however, there is another vibration pattern. The pipe wall does then vibrate about its initial radial deflection (here, $w = 0$), because the dynamic pressure has been reduced to zero. However, as shown in figure 11, some points vibrate between -0.27 mm and +0.27 mm, approximately, while other points almost do not vibrate at all. The results show that the vibration after the wave of pressure unloading depends on what the radial deflection at x was at the instant when the pipe wall at x was unloaded. The explanation is that a short section of the pipe wall obtains additional mechanical energy when it is pushed outwards by the pressure (the pressure performs a positive work), whereas it loses energy when it retracts, travelling in the opposite direction of the pressure. If a short section of the wall is deflected +0.27 mm when the pressure decreases at this section, it will not lose this energy during its retraction, and it will therefore retract all the way down to approximately -0.27 mm, and continue vibrating between +0.27 mm and -0.27 mm. On the other hand, if the section already has retracted a bit, it has lost some of its mechanical energy, and it will therefore not be able to reach the extrema +/-0.27 mm anymore, because no new energy is supplied to the pipe wall when the wave of pressure unloading has passed. Therefore, the amplitude of this vibration will vary along the length of the pipe.

It should be noted that in most cases, the maximum radial deflection of the pipe wall occurs during the wave of pressure unloading. Presumably, this is caused by the effect of the pipe wall bending stiffness and inertia on the pipe wall vibration.

4.3.3 The wave of low pressure

The governing differential equation has also been solved for the wave of low pressure (see sections 2.3.1 and 3.7), giving the expression (3.110). The vibrations predicted by this expression seemed unrealistically high, compared with the vibrations predicted for the first pressure wave, and the wave of pressure unloading. The reason for this is possibly the neglect of pipe material damping, friction between the liquid and the pipe wall, and fluid-structure interaction. The previous, similar water hammer models [1,13,29,30] have not considered the vibration due to the wave of low pressure, possibly because of the same reason. Therefore, this vibration, i.e. for $t > T_r$, will not be considered in the rest of this thesis.

4.3.4 The frequency of the vibration, and possibility for fatigue

Figure 12 shows how the radial deflection at the middle of the pipe in case 1a varies as a function of the time from valve closure. For the first 2 ms, this section of the pipe does not "feel" that the valve has been closed, and remains stationary. After 2 ms, the precursor vibration reaches this section, causing some minor vibration. The real pressure wave does not reach this section before 4.8 ms has passed, at which time the real vibration starts. The amplitude and frequency of the vibration remain relatively constant (the deviations in the amplitude are quite small compared to the magnitude of the amplitude), until the wave of pressure unloading reaches this point after 14.4 ms. The pipe wall continues to vibrate after this moment, but the amplitude at this point is very small.

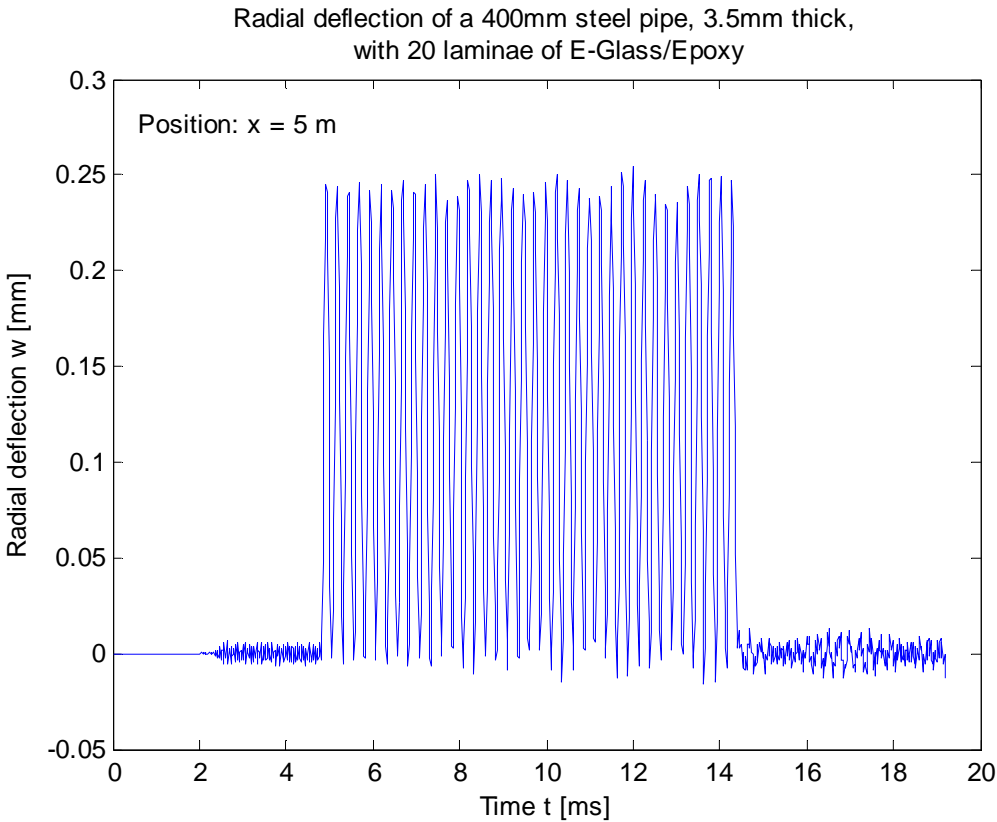


Figure 12: Radial deflection at the middle of pipe 1a, as a function of time.

During the 9.6 ms that this section vibrates at full amplitude, it undergoes 37 oscillations. This means that it vibrates at a frequency around 3850 Hz. The vibrations due to pressure waves through gas-filled aluminium pipes have been measured to have even higher frequencies [14]. Similar reasonable and clear measurements for water hammer-induced vibrations have not been found. Therefore, the frequency of 3850 Hz does not seem entirely unrealistic, even though it is very high. The high frequency implies that fatigue damage is likely to happen if the pipeline is subjected to water hammer conditions multiple times, even though the stresses do not exceed the yield strength of the steel/failure stress of the FRP. This needs to be taken into account during the design of FRP overwraps for susceptible

pipelines. It should be noted that fatigue damage is most likely occur at the end of the pipe where it is connected to the valve, as the pipe wall there will vibrate for the full round trip of the pressure wave, thereby being subjected to the largest number of oscillations.

If the steel pipe already has survived a couple of water hammers, it may be better to replace the whole pipe, instead of repairing it, because of the accumulated fatigue damage which still is in the steel. This must be evaluated at the time of repair, by taking the number of previous water hammer occurrences into account when calculating the new fatigue life after reparation.

4.4 The influence of the FRP overwrap

When designing the FRP overwrap for a damaged steel pipe subjected to water hammer conditions, it will be important that the repaired pipe will be able to survive the pressure wave. This means that the maximum stress experienced by the FRP overwrap must be less than its failure stress, and that the steel pipe must not be catastrophically loaded. If water hammer is very unlikely to occur, it should be sufficient that the maximum stresses in the steel pipe remain well below its ultimate tensile strength, as the pressure wave then would be regarded as an accidental load. On the other hand, if water hammer conditions are more likely to occur multiple times during the extended life of the pipeline, the maximum stresses should at least stay below the yield strength of the pipe, in order to avoid rapid fatigue failure. In the current discussion we will regard yielding of the steel pipe as a failure criterion. The fatigue life of the pipe and its overwrap should also have been calculated, but the current model does not predict the total number of oscillations experienced because of one water hammer occurrence. Damping needs to be implemented to the model, in order to obtain this information, but implementation of damping is beyond the scope of this thesis.

In the next four subsections, the influence of the number of FRP laminae (in the overwrap), N , on the dynamic response of the pipe will be investigated for three different laminates. It is assumed (refer to section 3.8) that the maximum stress will occur where the radial deflection has its maximum. The maximum dynamic radial deflection has been estimated by calculating the radial deflection at every $dx = 10\text{mm}$ along the pipe for every $dt = 20\mu\text{s}$ numerically, for the first round trip of the pressure wave, $0 \leq t \leq T_r$. As the maxima for all N were found to lie in the interval $T_r/2 \leq t \leq T_r$, the deflections in this interval were calculated once more for every $dt = 5\mu\text{s}$, in order to get better results. It is assumed that any trend observed for this interval will be valid for the full duration of the vibration. Better estimates may be found by using smaller length steps or time steps, at the cost of increased computation time, but the difference when doing so has been found to be small. The calculated values can only

be seen as approximate, because of the assumptions and approximations on which the current model has been based.

For reference, the mean radial deflection for each case has also been calculated, using the following formula:

$$w_{mean} = \frac{p_0 + \Delta p}{\lambda_3} \quad (4.1)$$

The stresses will be evaluated by calculating the usage factor, which is the inverse of the safety factor. This means that failure occurs if the usage factor is higher than or equal to 1.0. For the FRP laminae, the usage factor is equal to the left hand side of the Tsai-Wu failure criterion, expression (2.18). For the steel pipe, the usage factor with respect to yielding is equal to the von Mises equivalent stress σ_e divided by the yield strength f_y .

4.4.1 E-Glass/Epoxy laminate with fibre directions +/- 45°

The variation of the maximum dynamic and mean radial deflection, with respect to the number of FRP laminae applied to the pipe, for case 2a, is shown in figure 13. When more than 44 laminae, each 0.15 mm thick, are applied, the limit of the thin-walled shell theory is exceeded. The fibre direction alternates between +45° and -45°, which should strengthen the pipe both in the axial and radial directions. Equally many laminae in both directions need to be applied, so that the resulting overwrap is balanced. The laminae consist of a matrix of epoxy and fibres of E-Glass, which is quite common for pipeline reinforcement, because it is less expensive than other FRP materials.

As expected, the mean radial deflection is steadily decreasing when the number of FRP laminae is increased, as each lamina increases the static strength of the pipe. The maximum dynamic displacement, on the other hand, does not follow a monotonic trend. Instead, it decreases for the first ten laminae, before it flattens out, and later starts to increase. When 44 laminae are applied, the maximum dynamic displacement is 3 % higher than when no laminae are applied. This is not a very large increase, but as shown in figure 14, it results in a considerably higher usage factor. When less than 24 laminae are applied to the pipe, the steel pipe does not yield, but no more laminae can be added if yielding should be avoided. This shows that a laminate consisting of many FRP laminae increases the pipeline's strength against static pressures, but actually decreases its strength against water hammer-induced damage.

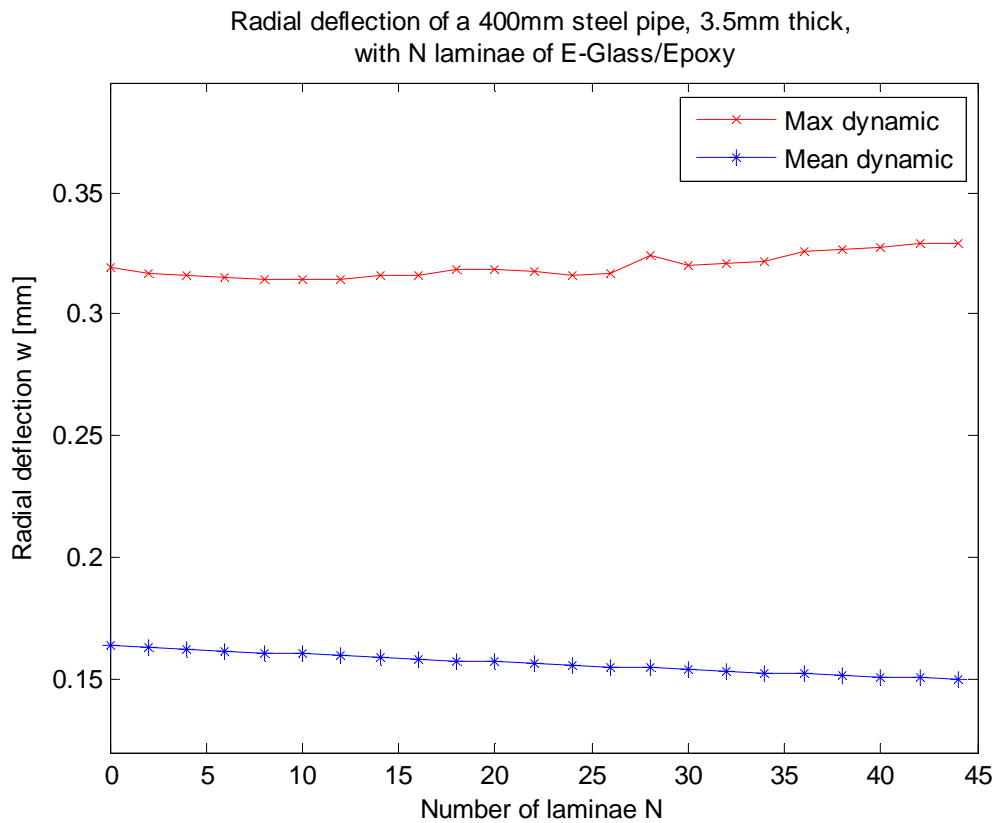


Figure 13: Influence of the number of FRP laminae on the radial deflection of pipe 2a.

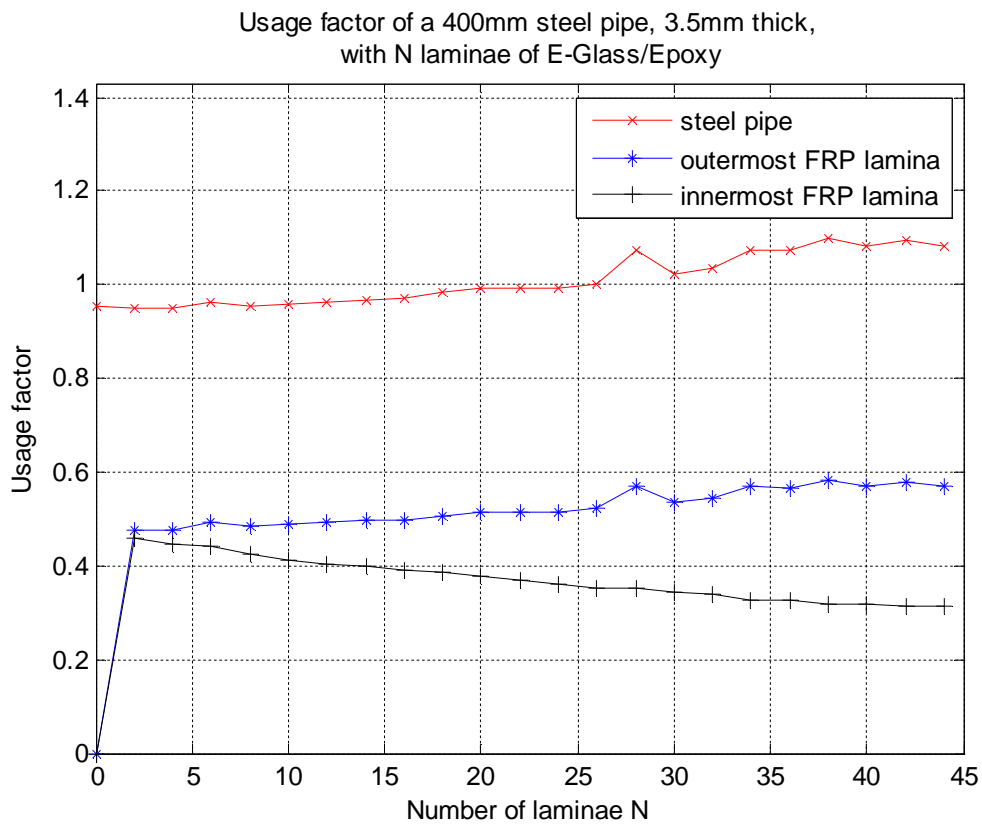


Figure 14: Influence of the number of FRP laminae on the usage factors of pipe 2a.

The reason for the increasing dynamic displacements and stresses is assumed to be that the natural frequency of the pipe changes. E-Glass/Epoxy is approximately 4 times lighter than steel, which makes the average pipe wall density decrease when more laminae are applied. Because of this, the stiffness of the pipe increases faster than its inertia, causing its natural frequency to change. This means that a steel pipe repaired with a FRP overwrap may be closer to a state of resonance than the steel pipe alone, leading to increased amplitudes of its vibration due to water hammer. The occurrence of resonance in a pipeline due to water hammer has earlier been described by Leishear [29], and also mentioned by Shepherd et.al. [14]. Resonance occurs if the pressure wave travels at, or near, the critical velocity, determined in section 3.6.

When no laminate has been applied to the pipe, the water hammer-induced pressure wave travels through the pipe at velocity $\alpha = 1027 \text{ m/s}$, while the critical velocity through the pipe is $\alpha_{cr} = 547 \text{ m/s}$. On the other hand, when 44 laminae are applied, the pressure wave travels at velocity $\alpha = 1057 \text{ m/s}$, while the critical velocity is $\alpha_{cr} = 764 \text{ m/s}$. The difference between the two velocities is now smaller, in which case the DLF, i.e. the amplitude of the vibrations, becomes larger [29]. A larger vibration leads to higher strains, and thereby higher stresses, just like what is observed from figure 14.

It is noted that the usage factor for the steel pipe increases faster (with respect to N) than the maximum radial deflection. The reason is that when more laminae are applied, the stiffness of the pipe increases, so that a larger stress is needed in order to get the same radial deflection. Figure 14 also shows that the steel pipe is loaded more critically than the FRP overwrap, even though E-Glass/Epoxy is a relatively weak FRP material. If the pipe was subjected to a little higher pressure, so that the steel would yield due to the water hammer, figure 14 shows that the E-Glass/Epoxy laminate is unable to prevent yielding, no matter how many laminae one adds (below 45). The usage factor for the steel pipe decreases only when 2 or 4 laminae are applied, but the decrease is so small that it is negligible. As such, this E-Glass/Epoxy overwrap is not able to strengthen the pipe's resistance to water hammer conditions.

In figure 14, it is observed that while the usage factors for the steel pipe and for the outermost FRP lamina increase, the usage factor for the innermost FRP lamina decreases. This indicates that the strain caused by the pipe wall curvature is significant. When the radial deflection increases, the magnitude of the pipe wall curvature $\partial^2 w / \partial x^2$ also increases, causing the tensile axial strain at the outer surface of the laminate to increase. The usage factor for the outermost FRP lamina is therefore increasing. The innermost lamina, on the other hand, is gradually subjected to a smaller tensile axial strain, which later becomes increasingly compressive, as the innermost lamina is positioned deeper in the laminate. Even though the hoop strain is higher deep in the laminate, the decreasing axial strain leads to a lower usage factor

for the innermost lamina, as the total number of laminae is increased. This means that not only the radial deflection, but also the pipe wall curvature, is an important property for the evaluation of stresses in FRP repaired pipes subjected to water hammer conditions. Therefore, it would have been better to implement an algorithm which finds the maximum usage factor for $0 \leq t \leq T_r$, instead of just finding the usage factor where the radial deflection has its maximum, when plots like figure 14 should be made.

4.4.2 E-Glass/Epoxy laminate, fibre directions +/- 45°, for a larger pipe

The variation of the stresses with respect to the number of laminae has also been calculated for a larger pipe in case 2b. This pipe has outer diameter $2MR = 1215mm$ and effective thickness $h_{st} = 10mm$. The steady-state flow velocity was set to $V = 2.3m/s$. As the pipe diameter is larger, the thin-walled shell theory may be used for a thicker pipe. The result is shown in figure 15.

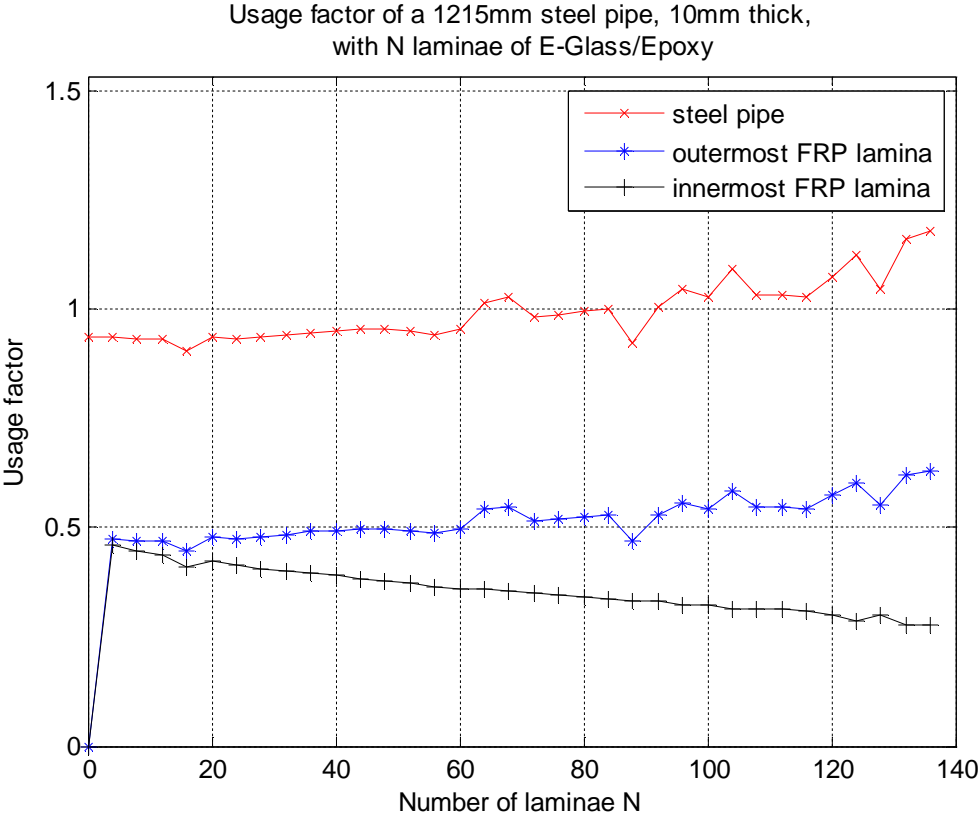


Figure 15: Influence of the number of FRP laminae on the usage factors of pipe 2b.

The same trend is observed, where the usage factor is increasing when many FRP laminae are applied. As this steel pipe has higher thickness, more laminae may be applied before the natural frequency is changed so much that the stresses become unacceptable, but it still happens. Thus, we can conclude that the increasing amplitude of the vibration is experienced for pipes of both small and large diameters.

It is observed that figure 15, and to some extent figure 14, contain some "spikes", where the usage factors for some N are significantly different from those to both sides of this value of N . This may have multiple explanations; the length step dx and time step dt may be too large, larger deflections could maybe occur when $t > T_r$, or a specific value for N may simply give a particular combination of bending stiffness and pipe inertia which produces an extreme radial deflection compared to surrounding values of N . The maximum radial deflection occurs at different values of x and t each time N is changed, so there is no guarantee for the variation of the maximum deflection with respect to N to be monotonic. If the "spikes" are realistic, figure 15 shows that 16 or 88 E-Glass/Epoxy laminae would strengthen this pipe's resistance to water hammer conditions a bit.

4.4.3 E-Glass/Epoxy laminate with fibre directions 90/90/0°

When preparing the FRP overwrap, it will often be easier to align all the fibres in one lamina either along the pipe, or around the pipe, instead of at an angle from the axial direction. Such an overwrap will now be considered, as specified in section 4.2 as case 3. The overwrap has two laminae where the fibres run around the pipe (fibre direction 90°), for every lamina where the fibres run along the pipe (0°). This strengthens the pipe considerably in the hoop direction, which is important to withstand a static pressure. This overwrap also makes the pipe completely axisymmetric. The variation of the radial deflection with respect to the number of

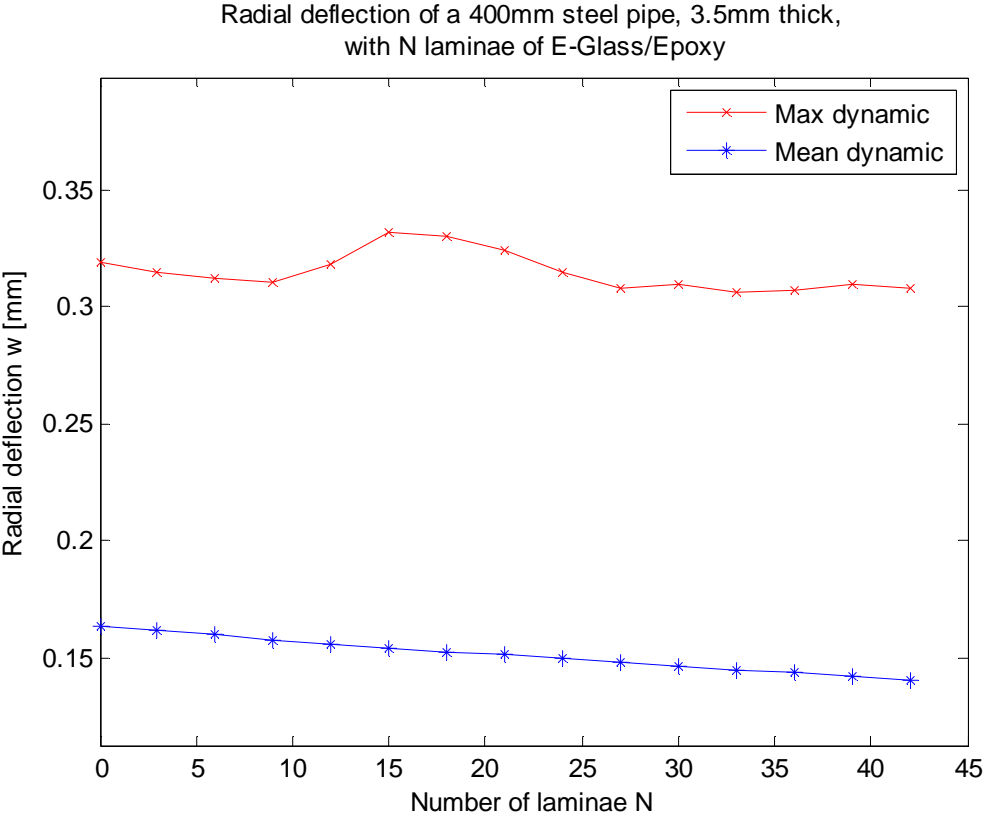


Figure 16: Influence of the number of FRP laminae on the radial deflection of pipe 3.

laminae is shown in figure 16, while the variation of the usage factors is shown in figure 17.

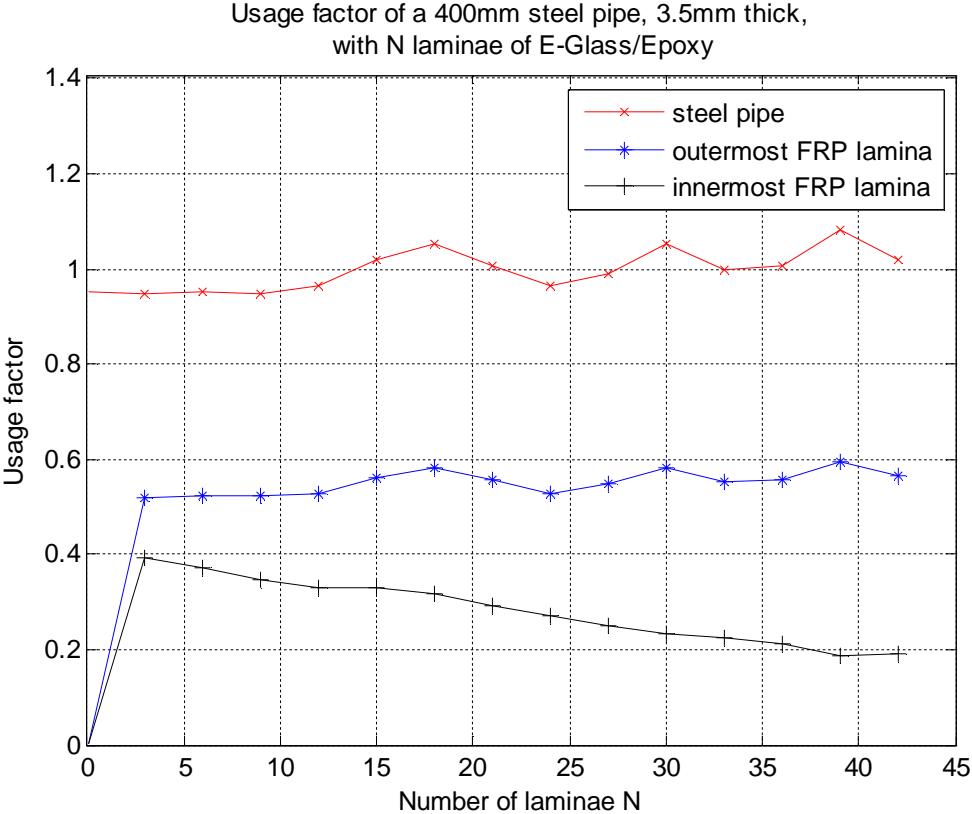


Figure 17: Influence of the number of FRP laminae on the usage factors of pipe 3.

As expected, the mean dynamic radial deflection decreases more by using this fibre configuration, than when $\pm 45^\circ$ was used. The maximum radial deflection, on the other hand, becomes considerably higher for values of N between 12 and 24, even though the velocity of the pressure wave, α , still is far away from the critical velocity α_{cr} . It has not been possible to find a proper explanation for this observation, but it shows that it will be important to perform this kind of analysis when designing the FRP overwrap. Figure 17 shows that yielding of the steel pipe will be prevented if N is less than 15, or equal to 24 or 27. Thus, this fibre configuration cannot be said to be considerably better than $\pm 45^\circ$.

4.4.4 T300/5208 Carbon/Epoxy laminate with fibre directions $\pm 45^\circ$

While E-Glass fibres have relatively low stiffness, carbon fibres have higher stiffness, higher strength and lower density. Carbon fibres are more expensive however, but they are still being used in some FRP overwraps for pipeline repair [20], if high strength or stiffness is required. The derived model has also been applied for an overwrap consisting of T300/5208 Carbon/Epoxy (CFRP) laminae, at fibre directions $\pm 45^\circ$ (case 4), in order to see whether carbon fibres are a better alternative also under water hammer conditions. The results are shown in figure 18 and 19.

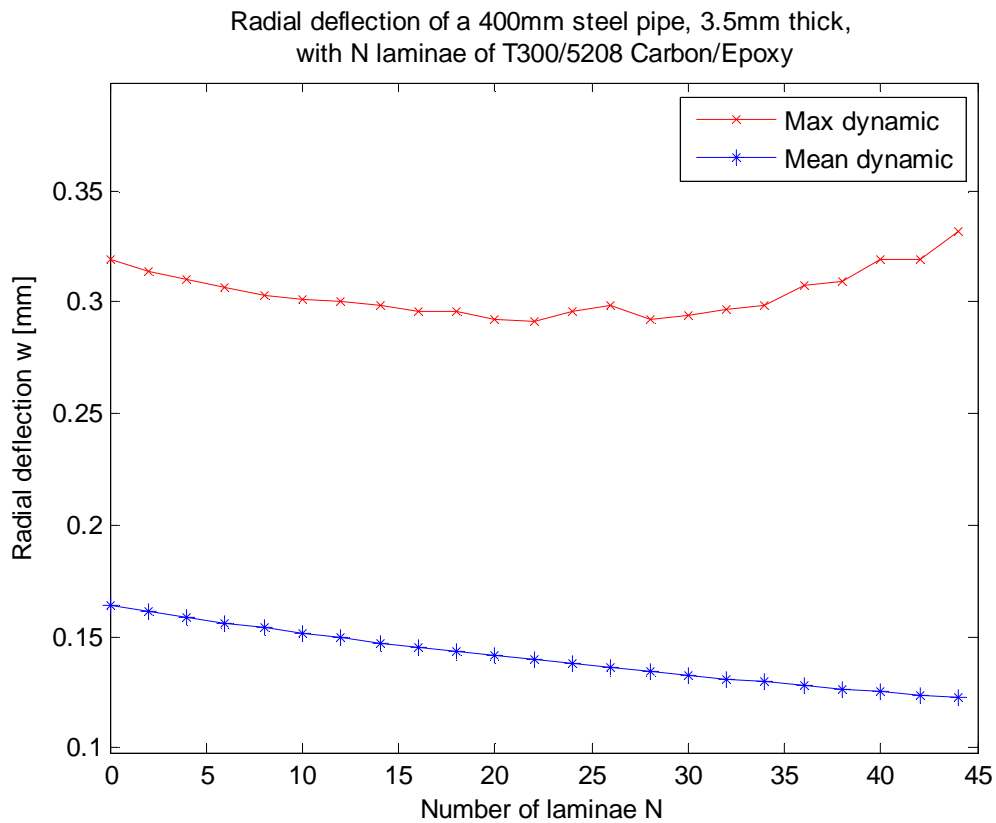


Figure 18: Influence of the number of FRP laminae on the radial deflection of pipe 4.

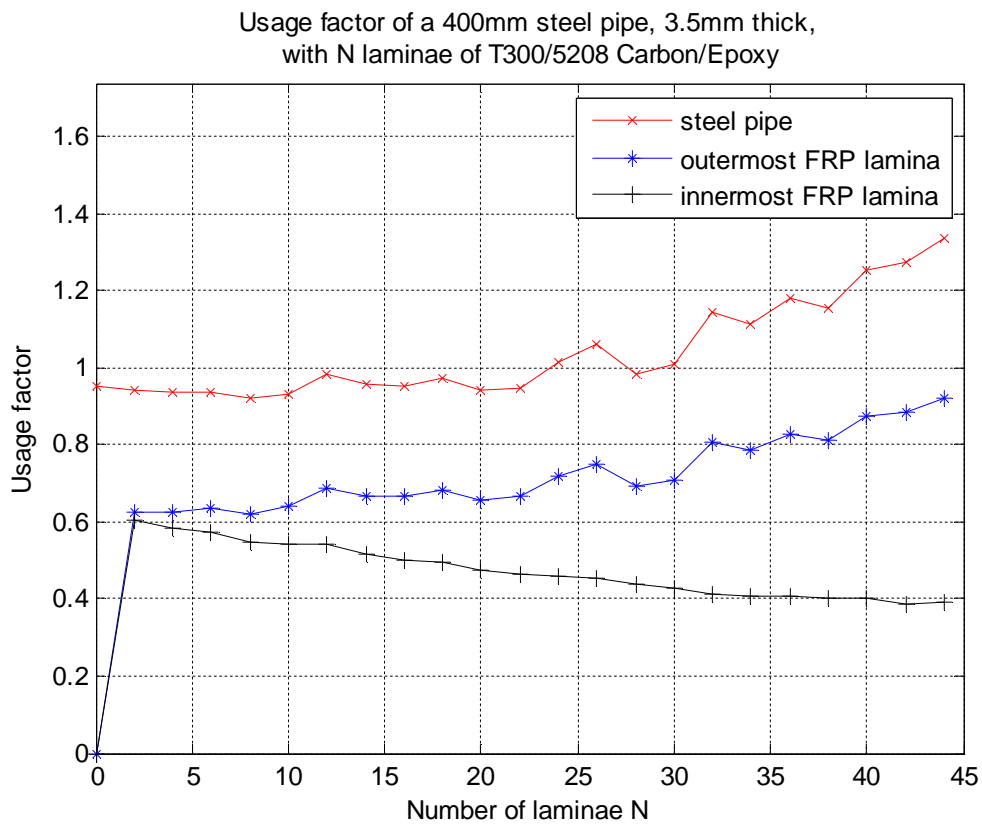


Figure 19: Influence of the number of FRP laminae on the usage factors of pipe 4.

From figure 18, it is observed that applying CFRP laminae decreases the mean radial deflection of the pipe considerably, as expected. The maximum radial deflection is also decreasing for the first 22 CFRP laminae, before it starts to increase. When 44 CFRP laminae are applied, the maximum dynamic displacement is 4 % higher than when no laminae are applied. This is also higher than if 44 E-Glass fibre-reinforced polymer (GFRP) laminae are applied. This means that applying CFRP leads to even larger vibrations than applying GFRP. The reason for this is that the low density and high stiffness of the CFRP causes the critical velocity for the pipe to increase even faster. At $N = 44$, the critical velocity through the pipe is $\alpha_{cr} = 957 \text{ m/s}$, while the water hammer-induced pressure wave travels at $\alpha = 1119 \text{ m/s}$. This means that the pipe is quite close to a state of resonance, hence the large amplitude of the vibration, and a DLF of 3.2.

As shown in figures 19 and 14, the steel pipe starts to yield at approximately 24 laminae, no matter if they are made of E-Glass FRP or CFRP. However, the CFRP is able to reduce the usage factor of the steel pipe by 3 percentage points when 8 laminae are applied. In most cases, this small improvement is hardly worth the cost and trouble, and it would probably be better to replace the steel pipe with a new one, or repair it with a steel sleeve.

4.5 Recommendations for further research

The derived model for the water hammer-induced vibration of steel pipes repaired with a FRP overwrap is an approximate model, where multiple assumptions have been made. It is therefore important that the model is checked, by comparing its theoretical predictions to experimental measurements of pipe strains. According to the author, such data for a FRP repaired pipe does not exist, and experiments should therefore be conducted. A possible experimental apparatus for a steel pipe is described in [45]. In our case, the steel pipe must be fitted with a FRP overwrap. The derived model assumes the pipe to be axially supported throughout, but this boundary condition is rarely seen in practice. The experiment should be conducted both with and without axial supports at each end of the pipe, in order to check the importance of this assumption.

The recommendations regarding how research on the subject should proceed depends on the results from the experiments. Significant differences between the predicted pressure/strain histories and measured pressure/strain histories, i.e. if the hoop strain curve is very different from figure 12 (radial deflection and hoop strain are proportional according to expression (3.112)), indicate that an uncoupled model is too simple to model pipeline behaviour due to water hammer conditions. A coupled fluid-structure interaction model should then be developed, taking Poisson coupling into account.

On the other hand, if the measurements seem to qualitatively match the predicted deflection histories quite well, the current uncoupled model could be further refined. One could then implement pipe material damping, in order to estimate the duration of the vibrations caused by one single valve closure. The measurements could also be used to evaluate the predicted vibrations during the wave of low pressure ($T_r \leq t \leq 1.5T_r$). Furthermore, the assumption of considering the repaired pipe to be entirely axisymmetric should be investigated, and non-axisymmetric shell theory should be implemented if needed. Lastly, the model could be modified to take live internal pressure at the time of laminate application into account, or reformulated for thick-walled pipes.

All these improvements could also be made to a coupled fluid-structure interaction model. Such a model may also be extended to pipes with bends and tees, which is not possible by using a simple uncoupled model. In the long run, it would therefore be best to develop a coupled fluid-structure interaction model.

If the experiments confirm the model, it can be used to investigate whether other FRP laminates are better suited for strengthening pipelines against water hammer conditions.

5. Conclusion

In this thesis, an approximate analytic model for the dynamic radial deflection of a steel pipe, repaired with a fibre-reinforced polymer (FRP) overwrap, subjected to water hammer conditions, has been derived. Because of the assumptions made during the derivation, the model is only applicable for the first round trip of the water hammer pressure wave. Furthermore, the model is limited to straight, thin-walled pipes, which are axially restricted throughout. The result of the model is a Fourier series solution for the radial deflection, as a function of time and distance along the pipe. In order to ensure convergence of the series, it has been shown that the computational effort is proportional to the cube of the length of the pipe, i.e. L^3 . Calculation of long pipelines using this model is therefore time-consuming.

Application of the model to relevant examples showed that the frequency of the imposed vibration is very high. As the amplitude of the vibration also is quite high, there is a great risk for fatigue damage to occur, even if the maximum stress levels are kept below the failure stresses for the steel and the FRP. The examples also indicated that typical steel pipes will yield prior to failure of any FRP lamina, no matter how many laminae one applies. The first couple of laminae reduces the maximum radial deflection and stress in the steel pipe a little bit, but when the laminate becomes as thick, or thicker, than the steel pipe, the amplitude of the vibration increases significantly, causing a higher maximum deflection and higher stress levels. The reason for the increased vibrations is the low density of the FRP material, compared to its stiffness. Application of FRP laminae therefore changes the natural frequency of the pipe considerably, compared to the water hammer pressure wave speed through the pipe, so that the pipe approaches a state of resonance. Carbon fibres, which have the highest strength, cause even more vibration than the cheaper and weaker E-Glass fibres, because carbon fibres are lighter than E-Glass fibres.

While FRP overwraps are able to significantly strengthen a pipe's resistance to a static pressure, the laminates investigated in this thesis were unable to strengthen the pipe's resistance to water hammer conditions significantly. The best laminate considered reduced the usage factor in the steel pipe by just 3 percentage points, which is very little. It is possible that other FRP materials, stacking sequences or a thicker laminate are able to better strengthen the steel pipe. The derived model may be used to explore the effect of other FRP materials or stacking sequences, while the theory of thick-walled cylinders must be applied to evaluate thicker laminates.

As the current model is approximate, and neglects fluid-structure interaction, experiments should be performed, in order to check the validity of the model.

6. References

- [1] D. G. Pavlou, "Undamped Vibration of Laminated Fiber-Reinforced Polymer Pipes in Water Hammer Conditions," *Journal of Offshore Mechanics and Arctic Engineering* vol. 137, no. 6, pp. 061701, 2015.
- [2] M. Geraghty, et al., "Transitioning from Leak Detection to Leak Prevention: Proactive Repair of Steel Pipelines Using Fiber Reinforced Polymer (FRP) Composites," in *Pipelines 2011: A Sound Conduit for Sharing Solutions*, Reston, VA, USA, 2011, pp. 100-107.
- [3] N. Saeed, "Composite Overwrap Repair System for Pipelines – Onshore and Offshore Application." Ph.D. dissertation, The University of Queensland, Queensland, Australia, 2015.
- [4] M. Ehsani, "Repair of corroded/damaged metallic pipelines using fiber-reinforced polymer composites," in *Rehabilitation of Pipelines Using Fiber-reinforced Polymer (FRP) Composites*, V. M. Karbhari, Ed., Cambridge: Woodhead Publishing, 2015, pp. 39-59.
- [5] H. Toutanji and S. Dempsey, "Stress modeling of pipelines strengthened with advanced composites materials," *Thin-Walled Structures* vol. 39, no. 2, pp. 153-165, 2001.
- [6] A. S. Tijsseling, "Fluid-structure interaction in liquid-filled pipe systems: A review," *Journal of Fluids and Structures* vol. 10, no. 2, pp. 109-146, 1996.
- [7] Y. A. Cengel and J. M. Cimbala, *Fluid Mechanics: Fundamentals and Applications, Second Edition in SI Units*. Boston: McGraw-Hill, 2010.
- [8] E. J. Finnemore and J. B. Franzini, *Fluid Mechanics with Engineering Applications, Tenth Edition*. New York: McGraw-Hill, 2002.
- [9] O. R. Fossmark, *Roterende maskiner*. Stavanger: Institutt for maskinteknikk og materialteknologi, 1999.
- [10] J. Záruba, *Water Hammer in pipe-line systems*. Amsterdam: Elsevier, 1993.
- [11] K. Brautaset, *Innføring i oljehydraulikk*. Oslo: Universitetsforlaget, 1987.
- [12] OMEGA Engineering inc. *Waterhammer: A complex phenomenon with a simple solution*, 2016. [Online]. Available: <http://www.omega.com/techref/waterhammer.html> (read 26.04.2016).
- [13] D. G. Pavlou, "Design challenges of steel pipelines in unsteady flow conditions," *Journal of Pipeline Engineering* vol. 14, no. 3, pp. 157-162, 2015.

- [14] J. E. Shepherd and K. Inaba, "Shock Loading and Failure of Fluid-Filled Tubular Structures," in *Dynamic Failure of Materials and Structures*, A. Shukla, G. Ravichandran, Y. D.S. Rajapakse, Eds., New York: Springer, 2010, pp. 153-190.
- [15] D. G. Pavlou, *Composite Materials in Piping Applications*. Lancaster, CA: DEStech Publications, 2013.
- [16] L. P. Kollár and G. S. Springer, *Mechanics of Composite Structures*. West Nyack, NY: Cambridge University Press, 2003.
- [17] P. K. Mallick, *Fiber-reinforced composites: Materials, manufacturing, and design – 2nd ed. rev. and expanded*. New York: Marcel Dekker, 1993.
- [18] W. A. Bruce and W. E. Amend, "Advantages of Steel Sleeves over Composite Materials for Pipeline Repair," in *Evaluation, Rehabilitation & Repair of Pipelines*, Clarion Technical Conferences and Tiratsoo Technical, Berlin, Germany, 2010. Available: http://www.dnvusa.com/Binaries/Advantages%20of%20Steel%20Sleeves%20over%20Composite%20Materials%20for%20Pipeline%20Repair_tcm153-574206.pdf (read 01.05.2016).
- [19] C. Alexander and B. Francini, "State of the Art Assessment of Composite Systems Used to Repair Transmission Pipelines," in *2006 International Pipeline Conference, Volume 1*, Calgary, Alberta, Canada, 2006, pp. 823-830.
- [20] M. Shamsuddoha, et al., "Effectiveness of using fibre-reinforced polymer composites for underwater steel pipeline repairs," *Composite Structures* vol. 100, pp. 40-54, 2013.
- [21] Clock Spring. *The Original Clock Spring Repair Sleeve*, 2015. [Online]. Available: <http://www.clockspring.com/wp-content/uploads/2015/10/CS-Standard-2015.pdf> (read 02.05.2016).
- [22] A. Y. L. Leong, et al., "Overwrap composite repairs of offshore risers at topside and splash zone," in *The 18th International Conference on Composite Materials*, Jeju, Korea, 2011.
- [23] Premier Corrosion Protection Services, Inc. *Pipe Wrap*. [Online]. Available: <http://www.premier-florida.com/projects/pipe-wrap/> (read 02.05.2016).
- [24] R. T. Fenner, *Engineering Elasticity*. Chichester, West Sussex: Ellis Horwood, 1986.
- [25] B. Massey and J. Ward-Smith, *Mechanics of Fluids, Eighth edition*. Abingdon, Oxon: Taylor & Francis, 2006.

- [26] E. B. Wylie and V. L. Streeter, *Fluid Transients*. Ann Arbor, Michigan: FEB Press, 1983.
- [27] M. S. Ghidaoui, et al., "A Review of Water Hammer Theory and Practice," *Applied Mechanics Reviews* vol. 58, no. 1, pp. 49-76, 2005.
- [28] T. E. Simkins, "The Influence of Transient Flexural Waves on Dynamic Strains in Gun Tubes," Technical Report ARCCB-TR-89020, U.S. Army Armament Research, Development and Engineering Center, Benet Laboratories, Watervliet, NY, 1989.
- [29] R. A. Leishear, "Derivations for Hoop Stresses Due to Shock Waves in a Tube," in *ASME 2007 Pressure Vessels and Piping Conference, Volume 3: Design and Analysis*, San Antonio, Texas, USA, 2007, pp. 185-194.
- [30] D. G. Pavlou, "Dynamic response of multi-layered FRP cylindrical shell under unsteady loading conditions," *Engineering Structures* vol. 112, pp. 256-264, 2016.
- [31] R. Skalak, "An extension to the theory of water hammer," *Transactions of the ASME* vol. 78, pp. 105-116, 1956.
- [32] A. S. Tijsseling, "Exact solution of linear hyperbolic four-equation system in axial liquid-pipe vibration," *Journal of Fluids and Structures* vol. 18, no. 2, pp. 179-196, 2003.
- [33] A. S. Tijsseling, "Water hammer with fluid-structure interaction in thick-walled pipes," *Computers & Structures* vol. 85, no. 11-14, pp. 844-851, 2007.
- [34] S. Timoshenko and S. Woinowsky-Krieger, *Theory of Plates and Shells, Second Edition*. New York: McGraw-Hill, 1959.
- [35] A. P. Boresi and R. J. Schmidt, *Advanced Mechanics of Materials, Sixth Edition*. New York: Wiley, 2003.
- [36] K. Rege, "Undamped Vibration of Fibre-Reinforced Polymer Overwrapped Pipes under Fluid Hammer Conditions," *Oil and Oil Products Pipeline Transportation: Science & Technology*, to be published.
- [37] R. Bærheim, *Laplacetransformasjon*. Stavanger: University of Stavanger, 2012.
- [38] H. Edwards and D. E. Penney, *Elementary differential equations with boundary value problems, Sixth Edition*. Upper Saddle River, N.J: Pearson, 2009.
- [39] G. B. Thomas, Jr., et al., *Thomas' Calculus, Tenth Edition*. Boston: Addison-Wesley, 2001.

- [40] L. Lorentzen, et al., *Kalkulus – med én og flere variable*. Oslo: Universitetsforlaget, 2003.
- [41] R. C. Hibbeler, *Mechanics of Materials, Eighth Edition in SI Units*. Singapore: Prentice Hall, 2011.
- [42] V. I. Gulyaev, et al., "Propagation of Harmonic Waves in a Cylindrical Shell (Timoshenko Model)," *International Applied Mechanics* vol. 39, no. 4, pp. 472-478, 2003.
- [43] ThyssenKrupp. *Material data sheet X52_L360xx*, 2011. [Online]. Available: http://www.s-k-h.com/media/de/Service/Werkstoffblaetter_englisch/Leitungsrohre/X52_L360xx_engl.pdf (read 30.05.2016).
- [44] M. Ehsani, "Latest Advances in Pipeline Renovation with Fiber Reinforced Polymer (FRP)," in *Water Distribution Systems Analysis 2010*, Tucson, AZ, USA, 2010, pp. 200-208.
- [45] D. Fan and A. Tijsseling, "Fluid-Structure Interaction With Cavitation in Transient Pipe Flows," *Journal of Fluids Engineering* vol. 114, no. 2, pp. 268-274, 1992.

Appendix A: MATLAB program

Overview

A MATLAB program has been written, which may be used to calculate the dynamic and radial deflection of a pipeline subjected to water hammer. The pipeline could either be solely made of metal, solely made of laminated fibre-reinforced polymer (FRP), or it could be a metal pipe with a FRP overwrap. The intention has been to make a user-friendly program, and the scripts are therefore quite long.

The different files which are needed in the program are shown in figure A.1. The program consists of 8 functions, which are placed in a subfolder called "WHToolbox", 8 scripts, and one Excel spreadsheet which is used to define the input variables. All scripts may be run from the script "MainMenu.m", which brings up the menu shown in figure A.2.

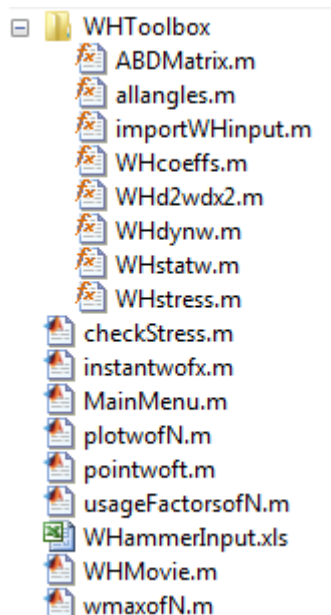


Figure A.1: MATLAB files.

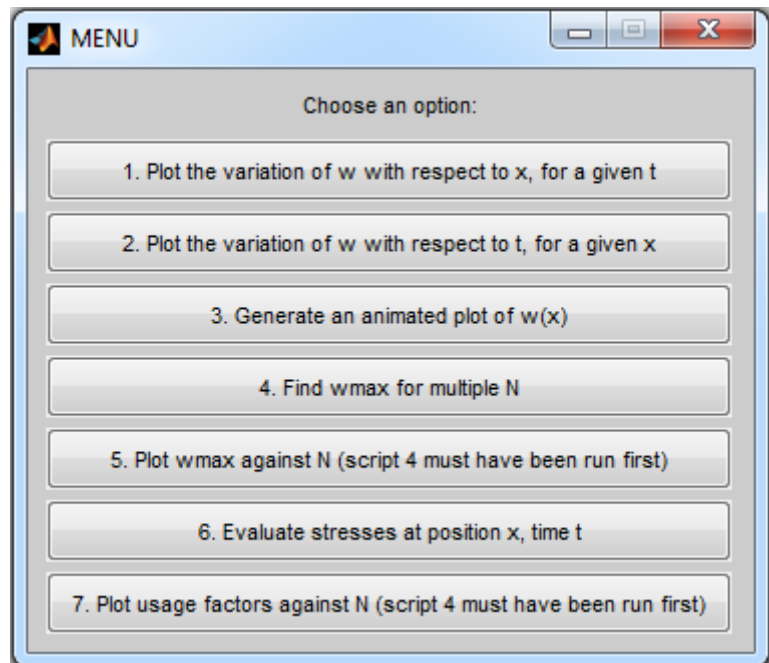


Figure A.2: The main menu

- Script 1 in the main menu generates plots similar to figure 8 and 9, page 49.
- Script 2 generates plots similar to figure 12, page 53.
- Script 3 generates an animation which shows how the deformation pattern of the pipe (figure 8) changes with time.
- Script 4 generates the data which is needed to generate plots like those shown in figures 13-19.
- Script 5 generates plots similar to figure 13, page 56.
- Script 6 calculates the pipe wall stresses at position x , time t , and checks whether the metal yields or the FRP laminate fails at this combination of x and t .
- Script 7 generates plots similar to figure 14, page 56.

Defining the input

The Excel spreadsheet in which the inputs are defined is shown in figure A.3. It is important that all the inputs are written in the columns and rows shown in the figure, and that the spreadsheet is saved in xls-format.

The following is worth noting regarding the spreadsheet:

- The defined names of the materials are only used in the figures, and do not contain any other information.
- A pipe made solely of metal may be calculated by setting $N = 0$.
- A pipe made solely of laminated FRP may be calculated by setting $hM = 0$.
- The answer to "Is the laminate symmetric?" should either be YES or NO.
- The field "Approximate static solution" has two options:
 - NO – Calculates the radial deflection due to the static pressure p_0 by using the Fourier sine series expression (3.100).
 - YES – Calculates the radial deflection due to the static pressure p_0 by using the approximate expression (3.94).
- The same notation is used as in the rest of the thesis, except that the subscript "st" has been replaced by "M", as the pipe material may be any metal, not just steel.

Each time a new pipe is going to be calculated, a new copy of the spreadsheet should be made, with a new name, like "Case1.xls", "Case2.xls". To run the calculation of this pipe, the name of the spreadsheet (Case1, etc., *without* the filename extension .xls) is typed in the MATLAB Command Window when asked for, when "Mainmenu.m" is run. The program will then save the calculated data in a text file with the same name. All the spreadsheets must be in the same folder as the MATLAB scripts.

The functions

The functions are saved in the subfolder "WHToolbox", and are used by the scripts.

importWHinput.m

```
function [WHdata, angles, settings, symconfig] = importWHinput(project)
%IMPORTWHINPUT Imports data from an Excel sheet with the required input
%data.
% SYNTAX
% [WHdata, angles, settings] = importWHinput(project)
% [WHdata, anglesrep, settings, symconfig] = importWHinput(project)
% DESCRIPTION
% Imports the numerical input data for calculation of the undamped
% vibration of a metal pipe, repaired with a fibre-reinforced polymer
% (FRP) overwrap, subjected to water hammer conditions. 'project' is
% the name of the spreadsheet, which is placed in the current MATLAB
% directory. This function only supports Excel sheets in the .xls
% format.
% WHdata is an array of the following parameters:
% WHdata=[rhoM, EM, nuM, MR, hM, L, rhola, E1, E2, G12, nu12, hla, N,
% rho, K, V, p0]. All units are SI units.
% angles is an array consisting of the angles of the fibres for each
% laminae, starting from the inner one.
% settings is a cell containing different information from the
% spreadsheet.
%
% If the optional output symconfig is not included, angles will carry
% the fibre directions of all N laminae in the laminate.
% If the optional output symconfig is included, angles will only carry
% the fibre directions of the recurring group of fibre directions.
% symconfig is a parameter which is equal to 1 if the laminate is
% symmetric, and otherwise equal to 0.
%
% This function depends on the function 'allangles.m'.
%
% Kristen Rege
% Created: 2016-04-07
% Modified: 2016-05-24

filename = ([project, '.xls']); % The name of the spreadsheet.

[numdata,txt] = xlsread(filename); % Reading numerical values from the
% spreadsheet.
rhoM = numdata(1,1); % Density of the metal.
EM = numdata(2,1)*10^9; % Modulus of elasticity of the metal.
nuM = numdata(3,1); % Poisson's ratio for the metal.
MR = 0.5*numdata(5,1)*10^(-3); % Outer radius of the metal pipe.
hM = numdata(6,1)*10^(-3); % Thickness of the metal pipe.

L = numdata(7,1); % Length of the pipe.

rhola = numdata(1,6); % Density of the FRP.
E1 = numdata(2,6)*10^9; % Modulus of elasticity, princ.dir.1, FRP
E2 = numdata(3,6)*10^9; % Modulus of elasticity, princ.dir.2, FRP
G12 = numdata(4,6)*10^9; % Shear modulus of the FRP.
nu12 = numdata(5,6); % Poisson's ratio for the FRP.
hla = numdata(6,6)*10^(-3); % Thickness of each FRP lamina.
N = numdata(7,6); % Total number of laminae.

rho = numdata(17,1); % Density of the conducted fluid.
K = numdata(18,1)*10^9; % Bulk modulus of elasticity of fluid.
V = numdata(19,1); % Steady-state velocity of fluid.
p0 = numdata(20,1)*10^5; % Steady-state pressure.

% Collecting these paramters in an array:
WHdata=[rhoM, EM, nuM, MR, hM, L, rhola, E1, E2, G12, nu12, hla, N, rho, K, V, p0];

% Number of different fibre angles in the repeated group of laminae:
repeatedlayers=length(numdata(13,:)) - 4;
```

```

% Extracting the repeated group of fibre angles:
anglesrep=zeros(1,repeatedlayers);
for k1 = 1:repeatedlayers
    anglesrep(k1) = numdata(12, 4+k1);
end

% Variable which is equal to 1 if the laminate is symmetric:
symconfig = strcmp(txt(19,7),'YES');

if nargout == 3
    % Generating full angles array if 3 outputs are called for:
    angles = allangles(anglesrep, N, symconfig);
elseif nargout == 4
    % Writing an array with only the repeated group of fibre angles if 4
    % outputs are called for:
    angles = anglesrep;
end

settings = cell(1,7);
settings{1,1} = numdata(18,6)*10^(-6); % Saving dt to settings.
settings{1,2} = numdata(17,6)*10^(-3); % Saving dx to settings.
settings{1,3} = txt(8,3); % Saving name of material 1.
settings{1,4} = txt(8,8); % Saving name of material 2.
settings{1,5} = numdata(19,6)/100; % Saving tstart to settings.
settings{1,6} = strcmp(txt(28,8),'YES'); % Saving static calc method.
settings{1,7} = numdata(21,6); % Saving number of half round trips.

end

```

allangles.m

```

function angles = allangles(anglesrep, N, symconfig)
%ALLANGLES Generates an array of angles from a repeated group of angles.
% SYNTAX
% angles = allangles(anglesrep, N, symconfig)
% DESCRIPTION
% Generates an array angles containing the fibre directions of N
% laminae in a laminate.
% anglesrep is an array containing the fibre directions of a group of
% layers which is repeated throughout the laminate.
% N is the total number of laminae.
% symconfig is equal to 1 if the laminate is symmetric, and otherwise
% equal to 0.
%
% Kristen Rege
% Created: 2016-04-23
% Modified: 2016-05-24

angles=zeros(1,N);

numrep=length(anglesrep); % Number of laminae in the repeated group.

if symconfig == 0
    for k2=1:numrep
        for k3=k2:numrep:N
            angles(k3)=anglesrep(k2);
        end
    end
elseif symconfig == 1
    if mod(N,2)~=0 % Displaying an error message if N is odd.
        disp('Error: Laminates with odd number of laminae are not supported.')
        disp('Let N be an even number.')
        angles=NaN;
    elseif mod(N,2*numrep)~=0
        error('Error: N must be a multiplum of 2x the number of repeated laminae.')
    else
        for k2=1:numrep
            for k3=k2:numrep:N/2
                angles(k3)=anglesrep(k2); % Building array above mid-plane.
            end
            for k3=N/2+k2:numrep:N
                angles(k3)=anglesrep(numrep+1-k2); % array below mid-plane.
            end
        end
    end
end
end

```

```

end

if mod(sum(angles), 90) ~=0 % Displaying error if the laminate is not
    error('Error: The laminate is not balanced.') % balanced.
end

end

```

ABDMatrix.m

```

function ABD = ABDMatrix(EM, nuM, hM, E1, E2, G12, nu12, hla, N, angles)
%ABDMATRIX Generates the laminate stiffness matrix ABD for the input data.
% SYNTAX
%     ABD = ABDMatrix(rhoM, EM, nuM, hM, rhola, E1, E2, G12, nu12, hla,
%                   N, angles)
% DESCRIPTION
%     Generates the 6x6 ABD matrix for a laminate consisting of one
%     isotropic bottom layer, and several anisotropic layers on top, from
%     the material properties specified as input. The input data is
%     specified as follows:
%     EM = Elastic modulus of the isotropic material.
%     nuM = Poisson's ratio for the isotropic material.
%     hM = Thickness of the isotropic material.
%     E1 = Modulus of elasticity, princ.dir.1, anisotropic material.
%     E2 = Modulus of elasticity, princ.dir.2, anisotropic material.
%     G12 = Shear modulus for the anisotropic material.
%     nu12= Poisson's ratio 1-2 for the anisotropic material.
%     hla = Thickness of each anisotropic lamina.
%     N = Number of anisotropic laminae.
%     angles = Array with the fibre directions of each of the N laminae
%     The isotropic layer may be omitted by setting hM=0, while the
%     anisotropic layers may be omitted by setting N = 0.
%
%     Kristen Rege
%     Created: 2016-04-08
%     Modified: 2016-05-29

GM = EM/(2*(1+nuM)); % Defining the shear modulus of the isotropic material

% Reduced stiffnesses for the isotropic material, assuming plane stress:
Q11M = EM / (1-nuM^2);
Q22M = Q11M;
Q12M = nuM*Q11M;
Q66M = GM;

nu21 = nu12 * E2/E1; % Poisson's ratio in the other principal direction for
                    % the anisotropic laminae.
% Reduced stiffnesses for the anisotropic material, assuming plane stress:
Q11 = E1 / (1 - nu12*nu21);
Q12 = nu12*E2 / (1 - nu12*nu21);
Q22 = E2 / (1 - nu12*nu21);
Q66 = G12;

% Defining the size of each quarter of the ABD matrix:
A = zeros(3,3);
B = zeros(3,3);
D = zeros(3,3);

z = -(hla*N+hM)/2; % z is the coordinate normal to the laminate, being
                  % equal to zero at the mid-surface of the laminate.
% Defining the laminate stiffness:
for k = 1:N+1
    if k == 1 % Transformed reduced stiffnesses for the isotropic layer:
        Q_(1,1) = Q11M;
        Q_(1,2) = Q12M;
        Q_(1,3) = 0; % Q_16
        Q_(2,2) = Q22M;
        Q_(2,3) = 0; % Q_26
        Q_(3,3) = Q66M; % Q_66
        h = hM; % Thickness of layer is defined.
    else % The other layers are anisotropic:
        m = cos(angles(k-1)*pi/180); % Cosine of angle between x and princ.dir.1
        n = sin(angles(k-1)*pi/180); % Sine of angle between x and princ.dir.1
    end
end

```



```

% Transformed reduced stiffnesses for the anisotropic layer:
Q_(1,1) = Q11*m^4 + 2*(Q12 + 2*Q66)*(n^2)*m^2 + Q22*n^4;
Q_(1,2) = (Q11 + Q22 - 4*Q66)*(n^2)*m^2 + Q12*(n^4 + m^4);
Q_(1,3) = (Q11 - Q12 - 2*Q66)*n*m^3 + (Q12 - Q22 + 2*Q66)*m*n^3; % Q_16
Q_(2,2) = Q11*n^4 + 2*(Q12 + 2*Q66)*(n^2)*m^2 + Q22*m^4;
Q_(2,3) = (Q11 - Q12 - 2*Q66)*m*n^3 + (Q12 - Q22 + 2*Q66)*n*m^3; % Q_26
Q_(3,3) = (Q11 + Q22 - 2*Q12 - 2*Q66)*(n*m)^2 + Q66*(n^4 + m^4); % Q_66
h = hla; % Thickness of layer is defined.
end

% The transformed reduced stiffness matrix is symmetric:
Q_(2,1) = Q_(1,2); Q_(3,1) = Q_(1,3); Q_(3,2) = Q_(2,3);

% The three sub-matrices are built up from the stiffness of each layer:
for i = 1:3
    for j = 1:3
        A(i,j) = A(i,j) + Q_(i,j) * ((z + h) - z);
        B(i,j) = B(i,j) + (1/2)*Q_(i,j) * ((z + h)^2 - z^2);
        D(i,j) = D(i,j) + (1/3)*Q_(i,j) * ((z + h)^3 - z^3);
    end
end

z = z + h; % z-value of next layer.
end

ABD = [A B; B D]; % The ABD matrix.

% Deviation from axial symmetry:
dev = (D(1,3) + D(2,3))/D(3,3);
disp(['"Deviation" from axial symmetry, when N = ' num2str(N) ': ' num2str(dev*100) ' %'])
disp(' ')
end

```

WHcoeffs.m

```

function [NF, dp, alpha, omega, Omega, p, Omega0] = WHcoeffs(WHdata, angles)
%WHCOEFFS Generates all the coefficients required to calculate the dynamic
%response of a pipeline to water hammer conditions.
% SYNTAX
% [NF, dp, alpha, omega, Omega, p, Omega0] = WHcoeffs(WHdata, angles)
% DESCRIPTION
% This function calculates all the coefficients required to calculate
% the dynamic response of a pipeline to water hammer conditions.
% WHdata and angles are input data as described in the function
% 'importWHdata.m'. The output is the required number of terms in the
% sum NF, the pressure rise dp, the pressure wave velocity alpha, the
% angular frequency of the wave omega, in addition to three arrays,
% Omega, p and Omega0 (for the static response), each containing NF
% coefficients for the calculation of w.
%
% This function depends on the function 'ABDMatrix.m'.
%
% Kristen Rege
% Created: 2016-04-19
% Modified: 2016-05-29

% Applying the input data to their corresponding names:
WHdatacell = num2cell(WHdata);
[rhoM, EM, nuM, MR, hM, L, rhola, E1, E2, G12, nu12, hla, N, rho, K, V, p0]=WHdatacell{:};

% Defining the various radii:
IR = MR - hM; % Inner radius of the pipe.
OR = MR + N*hla; % Outer radius of the composite pipe.
R = (OR+IR)/2; % Mean radius of the complete pipe.

h = hM+N*hla; % Thickness of the complete pipe.

% Mean density of the pipe wall:
rhom = ((MR^2-IR^2)*rhoM + (OR^2-MR^2)*rhola) / (OR^2 - IR^2);

% The ABD matrix is found with the tailor-made function:
ABD = ABDMatrix(EM, nuM, hM, E1, E2, G12, nu12, hla, N, angles);
A22 = ABD(2,2);
B12 = ABD(1,5);

```

```

B22 = ABD(2,5);
D11 = ABD(4,4);
D12 = ABD(5,4);

% Coefficients for the solution:
lambda1 = D11;
lambda2 = D12/(R^2) - 2*B12/R;
lambda3 = A22/(R^2) - B22/(R^3);

% The velocity of the pressure wave:
alpha = sqrt(1 / (rho/K + 2*R*rho/A22));

dp = rho * V * alpha; % The magnitude of the pressure wave.

% The required number of terms required is found from estimates:
if (lambda2+rhom*h*alpha^2)^2 < 4*lambda1*lambda3
    % If the denominator doesn't reach zero:
    NF = round(1.5*(L/pi)*sqrt((lambda2 + rhom*h*alpha^2)/(2*lambda1)));
else
    % If the denominator reaches zero:
    NF = round(1.1*sqrt((lambda2 + rhom*h*alpha^2 + sqrt((lambda2 + rhom*h*alpha^2)^2 -
4*lambda1*lambda3))/(2*lambda1*(pi/L)^2)));
end

omega = pi * alpha / L; % A constant.

% The coefficients Omega0_n Omega_n and p_n are calculated for each n:
Omega0=zeros(1, NF);
Omega=zeros(1, NF);
p=zeros(1, NF);
for n=1:1:NF;
    omegan = sqrt((pi*n/L)^2);
    Omega0(n) = sqrt((lambda1*omegan^4 - lambda2*omegan^2 + lambda3));
    Omega(n) = Omega0(n)/sqrt(rhom*h);
    p(n) = dp*L/(rhom*h*n*pi);
end

assignin('base', 'lambda3', lambda3); % Exporting lambda3 to workspace.

% Calculating and saving the critical pressure wave speed to workspace:
alphacr = sqrt((2*sqrt(lambda1*lambda3) - lambda2)/(rhom*h));
assignin('base', 'alphacr', alphacr);

end % End of function.

```

WHstatw.m

```

function w0 = WHstatw(NF, Omega0, p0, L, x)
%WSTATW Calculates the radial displacement at x due to the internal
%pressure p0.
% SYNTAX
% w0 = WHstatw(NF, Omega0, p0, L, x)
% DESCRIPTION
% This function calculates the radial deformation of a pipeline
% subjected to a static internal pressure p0, at position x. L is the
% length of the pipe. The other input data are calculated with and
% described in the function 'WHcoeffs.m'.
%
% Kristen Rege
% Created: 2016-05-20
% Modified: 2016-05-20

% Producing an error if x is chosen outside the length of the pipe:
if x<0 || x>L
    error(['ERROR: x must be in the interval 0 <= x <= L! Currently, x = ', num2str(x), ',
and L = ', num2str(L), '.'])
end

ws = 0; % w is a sum. ws saves the sum after each term.
for n=1:1:NF; % The NF terms are calculated and added together.
    ws = ws + (2*p0/(n*pi)) * ((1-cos(n*pi))/((Omega0(n))^2)) * sin(n*pi*x/L);
end

w0 = ws; % w0 is saved.

end % End of function.

```

WHdynw.m

```
function w = WHdynw(NF, omega, Omega, p, L, x, t)
%WHDYNW Calculates the radial displacement at x,t due to water hammer.
% SYNTAX
%   w = WHdynw(NF, omega, Omega, p, L, x, t)
% DESCRIPTION
%   This function calculates the radial deformation of a pipeline
%   subjected to water hammer, at position x, at time t. The function
%   is only applicable to the first round trip of the pressure
%   wave. L is the length of the pipe. The other input data are
%   calculated by and described in the function 'WHcoeffs.m'.
%
%   Kristen Rege
%   Created: 2016-04-15
%   Modified: 2016-05-22

% Producing an error if x is chosen outside the length of the pipe:
if x<0 || x>L
    error(['ERROR: x must be in the interval 0 <= x <= L! Currently, x = ', num2str(x), ',
and L = ', num2str(L), '.'])
end

% Producing an error if t is chosen outside the first round trip.
if t<0 || t>2*pi/omega % = 2*L/alpha
    error(['ERROR: t must be in the interval 0 <= t <= ', num2str(1000*pi/omega) ' ms!
Currently, t = ', num2str(1000*t), ' ms.'])
end

ws = 0; % w is a sum. ws saves the sum after each term.
if t<=pi/omega % First half of the round trip.
    for n=1:1:NF; % The NF terms are calculated and added together.
        ws = ws + (2*p(n)/L)*( (cos(Omega(n)*t) - cos(n*omega*t))/((Omega(n))^2 -
(n*omega)^2) + (1-cos(Omega(n)*t))/((Omega(n))^2))*sin(n*pi*x/L);
    end
else % Second half of the round trip.
    for n=1:1:NF; % The NF terms are calculated and added together.
        ws = ws + (2*p(n)/L)*( (cos(Omega(n)*t) - cos(n*(2*pi-omega*t)))/((Omega(n))^2 -
(n*omega)^2) + (1-cos(Omega(n)*t))/((Omega(n))^2))*sin(n*pi*x/L);
    end
end

w = ws; % w is saved.

end % End of function.
```

WHd2wdx2.m

```
function d2w = WHd2wdx2(NF, omega, Omega, Omega0, p, p0, L, x, t)
%WHD2WDX2
% SYNTAX
%   d2w = WHd2wdx2(NF, omega, Omega, Omega0, p, p0, L, x, t)
% DESCRIPTION
%   This function calculates the radial curvature of a pipe wall, at
%   position x from the valve and time t from valve closure, due to
%   water hammer conditions. The function is only applicable to the
%   first round trip of the pressure wave. L is the length of the pipe,
%   and p0 is the internal static pressure. The other input data are
%   calculated by and described in the function 'WHcoeffs.m'.
%
%   Kristen Rege
%   Created: 2016-05-24
%   Modified: 2016-05-25

% Producing an error if x is chosen outside the length of the pipe:
if x<0 || x>L
    error(['ERROR: x must be in the interval 0 <= x <= L! Currently, x = ', num2str(x), ',
and L = ', num2str(L), '.'])
end

% Producing an error if t is chosen outside the first round trip.
if t<0 || t>2*pi/omega % = 2*L/alpha
    error(['ERROR: t must be in the interval 0 <= t <= ', num2str(1000*pi/omega) ' ms!
Currently, t = ', num2str(1000*t), ' ms.'])
end
```

```

d2ws = 0; % d2w/dx2 is a sum. ws saves the sum after each term.
if t<=pi/omega % First half of the round trip.
    for n=1:1:NF; % The NF terms are calculated and added together.
        % The dynamic term:
        d2ws = d2ws - ((n*pi/L)^2) * (2*p(n)/L)*( (cos(Omega(n)*t) -
cos(n*omega*t))/((Omega(n))^2 - (n*omega)^2) + (1-
cos(Omega(n)*t))/((Omega(n))^2))*sin(n*pi*x/L);
        % The static term:
        if p0 ~=0
            d2ws = d2ws - ((n*pi/L)^2) * (2*p0/(n*pi)) * ((1-cos(n*pi))/((Omega0(n))^2)) *
sin(n*pi*x/L);
        end
    end
else % Second half of the round trip.
    for n=1:1:NF; % The NF terms are calculated and added together.
        % The dynamic term:
        d2ws = d2ws - (n*pi/L)^2 * (2*p(n)/L)*( (cos(Omega(n)*t) - cos(n*(2*pi-
omega*t)))/((Omega(n))^2 - (n*omega)^2) + (1-cos(Omega(n)*t))/((Omega(n))^2))*sin(n*pi*x/L);
        % The static term:
        if p0 ~=0
            d2ws = d2ws - ((n*pi/L)^2) * (2*p0/(n*pi)) * ((1-cos(n*pi))/((Omega0(n))^2)) *
sin(n*pi*x/L);
        end
    end
end
end

d2w = d2ws; % w is saved.

end % End of function.

```

WHstress.m

```

function [sigmaM, sigmaxyFRPi, sigma12FRPi, sigmaxyFRPo, sigma12FRPo] = WHstress(project, x,
t, N)
%WHSTRESS Calculates the stress in a pipe subjected to water hammer
%conditions.
% SYNTAX
% [sigmaM, sigmaxyFRPi, sigma12FRPi, sigmaxyFRPo, sigma12FRPo] = WHstress(project, x, t)
% [sigmaM, sigmaxyFRPi, sigma12FRPi, sigmaxyFRPo, sigma12FRPo] = WHstress(project, x, t,
N)
% DESCRIPTION
% Calculates the critical stress components in a metal pipe and its
% FRP overwrap, subjected to water hammer conditions, at position x
% and time t from valve closure.
% project is the name of a Excel sheet containing the required data.
% N is the number of FRP laminae, if it differs from that found in the
% Excel sheet.
% sigmaM is a vector containing the three stress components sigma_x,
% sigma_y and tau_xy at the inner surface of the metal pipe.
% sigmaxyFRPi is a vector containing the three stress components
% sigma_x, sigma_y and tau_xy at the inner surface of the FRP
% overwrap.
% sigma12FRPi is a vector containing the three stress components
% sigma_1, sigma_2 and tau_12 at the inner surface of the FRP
% overwrap, in the principal directions of the lamina.
% sigmaxyFRPo is a vector containing the three stress components
% sigma_x, sigma_y and tau_xy at the outer surface of the FRP
% overwrap.
% sigma12FRPo is a vector containing the three stress components
% sigma_1, sigma_2 and tau_12 at the outer surface of the FRP
% overwrap, in the principal directions of the lamina.
%
% This function depends on the functions 'importWHinput.m',
% 'WHcoeffs.m', 'allangles.m', 'WHstatw.m' and 'WHdynw.m'.
%
% Kristen Rege
% Created: 2016-05-28
% Modified: 2016-06-04

% Importing data:
if nargin == 3
    [WHdata, angles, settings] = importWHinput(project);
elseif nargin == 4
    [WHdata, anglesrep, settings, symconfig] = importWHinput(project);
end

```

```

% Extracting required information:
WHdatacell = num2cell(WHdata);
[rhoM, EM, nuM, MR, hM, L, rhola, E1, E2, G12, nu12, hla, Nint, rho, K, V, p0]=WHdatacell{:};

% Alternative value for N:
if nargin == 3
    N = Nint;
elseif nargin == 4
    WHdata(13) = N;
    angles = allangles(anglesrep, N, symconfig);
end

% Defining the various radii:
IR = MR - hM;           % Inner radius of the pipe.
OR = MR + N*hla;       % Outer radius of the composite pipe.
R = (OR+IR)/2;         % Mean radius of the complete pipe.

h = hM+N*hla;          % Thickness of the complete pipe.

% Calculating required coefficients:
[NF, dp, alpha, omega, Omega, p, Omega0] = WHcoeffs(WHdata, angles);

% Calculating the total radial deflection:
if p0 == 0 % If static pressure is equal 0:
    w = WHdynw(NF, omega, Omega, p, L, x, t);
else % If static pressure /= 0:
    w = WHstatw(NF, Omega0, p0, L, x) + WHdynw(NF, omega, Omega, p, L, x, t);
end

% Calculating the curvature:
d2w = WHd2wdx2(NF, omega, Omega, Omega0, p, p0, L, x, t);

% Stresses at the inner surface of the metal pipe:
sigmaxM = (EM/(1-nuM^2)) * (0.5*h*d2w + nuM*(w/R)*(1+0.5*h/R));
sigmayM = (EM/(1-nuM^2)) * ((w/R)*(1+0.5*h/R) + nuM*0.5*h*d2w);
sigmaM = [sigmaxM, sigmayM, 0];

if N > 0 % FRP stresses are only calculated if there are any FRP lamina.
    % Strains in the innermost FRP lamina:
    exyFRP(1,1) = -(-h/2 + hM)*d2w;
    exyFRP(2,1) = (w/R)*(1 - (-h/2 + hM)/R);
    exyFRP(3,1) = 0;

    % Poisson's ratio in the other principal direction for the FRP lamina:
    nu21 = nu12 * E2/E1;

    % Reduced stiffnesses for the FRP material, assuming plane stress:
    Q11 = E1 / (1 - nu12*nu21);
    Q12 = nu12*E2 / (1 - nu12*nu21);
    Q22 = E2 / (1 - nu12*nu21);
    Q66 = G12;

    m = cos(angles(1)*pi/180); % Cosine of angle between x and princ.dir.1
    n = sin(angles(1)*pi/180); % Sine of angle between x and princ.dir.1

    % Transformed reduced stiffnesses for the innermost FRP lamina:
    Q_(1,1) = Q11*m^4 + 2*(Q12 + 2*Q66)*(n^2)*m^2 + Q22*n^4;
    Q_(1,2) = (Q11 + Q22 - 4*Q66)*(n^2)*m^2 + Q12*(n^4 + m^4);
    Q_(1,3) = (Q11 - Q12 - 2*Q66)*n*m^3 + (Q12 - Q22 + 2*Q66)*m*n^3; % Q_16
    Q_(2,2) = Q11*n^4 + 2*(Q12 + 2*Q66)*(n^2)*m^2 + Q22*m^4;
    Q_(2,3) = (Q11 - Q12 - 2*Q66)*m*n^3 + (Q12 - Q22 + 2*Q66)*n*m^3; % Q_26
    Q_(3,3) = (Q11 + Q22 - 2*Q12 - 2*Q66)*(n*m)^2 + Q66*(n^4 + m^4); % Q_66

    % The transformed reduced stiffness matrix is symmetric:
    Q_(2,1) = Q_(1,2); Q_(3,1) = Q_(1,3); Q_(3,2) = Q_(2,3);

    % The stresses are given by matrix multiplication of stiffness and strains:
    sigmaxyFRPi = Q_ * exyFRP;

    % Transformation matrix for the stresses between xy and 12 coord. systems:
    T = [m^2, n^2, 2*m*n
        n^2, m^2, -2*m*n
        -m*n, m*n, m^2-n^2];

```

```

% Transforming the lamina stresses from the xy system to the 12 system:
sigma12FRPi = T*sigmaxyFRPi;

% Strains in the outermost FRP lamina:
exyFRP(1,1) = -0.5*h*d2w;
exyFRP(2,1) = (w/R)*(1 - 0.5*h/R);
exyFRP(3,1) = 0;

m = cos(angles(end)*pi/180); %Cosine of angle between x and princ.dir.1
n = sin(angles(end)*pi/180); % Sine of angle between x and princ.dir.1

% Transformed reduced stiffnesses for the innermost FRP lamina:
Q_(1,1) = Q11*m^4 + 2*(Q12 + 2*Q66)*(n^2)*m^2 + Q22*n^4;
Q_(1,2) = (Q11 + Q22 - 4*Q66)*(n^2)*m^2 + Q12*(n^4 + m^4);
Q_(1,3) = (Q11 - Q12 - 2*Q66)*n*m^3 + (Q12 - Q22 + 2*Q66)*m*n^3; % Q_16
Q_(2,2) = Q11*n^4 + 2*(Q12 + 2*Q66)*(n^2)*m^2 + Q22*m^4;
Q_(2,3) = (Q11 - Q12 - 2*Q66)*m*n^3 + (Q12 - Q22 + 2*Q66)*n*m^3; % Q_26
Q_(3,3) = (Q11 + Q22 - 2*Q12 - 2*Q66)*(n*m)^2 + Q66*(n^4 + m^4); % Q_66

% The transformed reduced stiffness matrix is symmetric:
Q_(2,1) = Q_(1,2); Q_(3,1) = Q_(1,3); Q_(3,2) = Q_(2,3);

% The stresses are given by matrix multiplication of stiffness and strains:
sigmaxyFRPo = Q_ * exyFRP;

% Transformation matrix for the stresses between xy and 12 coord. systems:
T = [m^2, n^2, 2*m*n
     n^2, m^2, -2*m*n
     -m*n, m*n, m^2-n^2];

% Transforming the lamina stresses from the xy system to the 12 system:
sigma12FRPo = T*sigmaxyFRPo;

else
sigmaxyFRPi = [0; 0; 0];
sigma12FRPi = [0; 0; 0];
sigmaxyFRPo = [0; 0; 0];
sigma12FRPo = [0; 0; 0];
end

assignin('base', 'w', w); % Exporting w to workspace.
assignin('base', 'd2w', d2w); % Exporting d2w to workspace.

end

```

The scripts

MainMenu.m

```
%MainMenu.m
% Main menu for the whole set of MATLAB scripts, which enables the user
% to run the scripts easily from a menu.
%
% Kristen Rege
% Created: 2016-04-22
% Modified: 2016-06-05

clc, clear, close % Initiating.

% The name of the project used last time is saved, so that it isn't needed
% to type it each time.
if exist(fullfile(cd, 'WHToolbox/Save.txt'), 'file') ~= 2
    project = input('Enter name of project (should be the name of an Excel worksheet, for
example: Casel): ', 's');
    saved = fopen('WHToolbox/Save.txt','wt');
    fprintf(saved, project); % A file for saving last project is made, if
fclose(saved); % it doesn't exist already.
else
    saved = fopen('WHToolbox/Save.txt','r');
    project = fgetl(saved); % Importing the name of last project.
    fclose(saved);

    % The user gets the choice to continue with last project or not:
    projectn = menu(['Continue with last project, ' project, '?'], 'Yes', 'No');

    if projectn == 2 % Type the name of the new project, if not.
        project = input('Enter name of project (should be the name of an Excel worksheet, for
example: Casel): ', 's');
        saved = fopen('WHToolbox/Save.txt','wt');
        fprintf(saved, project);
        fclose(saved);
    end
end

% Handle to make sure the current project name is taken into account when
% running the other scripts:
menuentry = 1;

% A menu where the user may choose between the 5 different scripts:
script = menu('Choose an option:', '1. Plot the variation of w with respect to x, for a given
t', '2. Plot the variation of w with respect to t, for a given x', '3. Generate an animated
plot of w(x)', '4. Find wmax for multiple N', '5. Plot wmax against N (script 4 must have
been run first)', '6. Evaluate stresses at position x, time t', '7. Plot usage factors
against N (script 4 must have been run first)');
switch script
    case 1
        run instantwofx
    case 2
        run pointwofT
    case 3
        run WHMovie
    case 4
        run wmaxofN
    case 5
        run plotwofN
    case 6
        run checkStress
    case 7
        run usageFactorsofN
end

% The handle is removed, so that the wrong project isn't initiated when
% running one of the scripts next time:
clear('menuentry');
% Option to return to the main menu:
returns = menu('Do you want to return to the menu?', 'Yes', 'No');
if returns == 1;
    run MainMenu
end
```

instantwofx.m

```
%instantwofx.m
% This script generates a plot of the instantaneous radial deflection of
% a pipeline, due to water hammer conditions, as a function of the
% position along the pipe.
%
% Kristen Rege
% Created: 2016-04-08
% Modified: 2016-05-30

clc, close % Initiating.

if exist('menuentry', 'var') == 1 % If program is started from main menu,
    project = project; % that project name is used.
else
    clear % If not, the data is taken from the
    project = 'WHammerInput'; % Excel sheet WHammerInput.
end

addpath('WHToolbox') % Adds the toolbox with the required functions.

% Importing data:
[WHdata, angles, settings] = importWHinput(project);

% Extracting required information:
L = WHdata(6);
hM = WHdata(5);
N = WHdata(13);
MR = WHdata(4);
p0 = WHdata(17);

% Calculating required coefficients:
[NF, dp, alpha, omega, Omega, p, Omega0] = WHcoeffs(WHdata, angles);

% Menu allowing the user to choose x0 and x1:
section = menu('Should the radial deflection along the whole length of the pipe be printed?',
'Yes', 'No, just a section');
switch section
    case 1
        x0 = 0;
        x1 = L;
    case 2
        x0 = input(['Enter a x-position from 0 to ', num2str(L), ' meters from which the plot
should be started: ']);
        error=1; % A while-loop enables the user to retry if a lower
        while error==1 % x1 than x0 is chosen.
            x1 = input(['Enter a x-position from ', num2str(x0), ' to ', num2str(L), ' meters
at which the plot should end: ']);
            if x1<x0
                disp(' ')
                disp(['ERROR: x1 must be larger than x0! Currently, x1 = ', num2str(x1), ' m,
and x0 = ', num2str(x0), ' m.'])
                disp(' ')
            else
                error=0;
            end
        end
        disp(' ')
end

% Menu allowing the user to choose the instant at which to plot:
time = menu('How far along the length of the pipe should the pressure wave have come? The
closest 0.1 millisecond is chosen.', '25% of L', '50% of L', '75% of L', '100% of L', '125%
of L (returned 25%)', '150% of L (returned 50%)', 'Other');
if time < 7 % Common values may be directly chosen from the menu:
    t = (round(0.25*time*10000*L/alpha)) * 10^(-4);
else % Other values may be typed:
    perc = input('Enter the percentage of the pipe which the pressure wave should have
travelled (e.g. 42): ');
    t = (round(perc*100*L/alpha)) * 10^(-4);
    disp(' ')
end
```



```

% Displaying the stacking sequence used in the calculations, to enable
% verification with intended stacking sequence.
disp('A plot is made for a pipe with an overwrap with the following fibre directions (from
the inner lamina and outwards):')
disp(['[' , num2str(angles), '']])
disp('Please check that this is the intended stacking sequence.')

% Extracting settings:
dx = settings{1,2}; % Length step.
matr1 = char(settings{1,3}); % Material of pipe.
matr2 = char(settings{1,4}); % Material of overwrap.
apprstatic = settings{1,6}; % Approximate static solution (1) or not (0).

% Executing the calculation:
% A matrix with proper dimension is established to save the deformation:
if p0 == 0
    w = zeros(1, floor((x1-x0)/dx)+1);
else
    if apprstatic == 1; % The approximate static solution is equal in all
        w = ones(1, floor((x1-x0)/dx)+1) * p0/lambda3; % points.
    else
        w = zeros(1, floor((x1-x0)/dx)+1);
        xx = 1; % Fourier solution for the static displacement:
        for x = x0:dx:x1
            w(xx) = WHstatw(NF, Omega0, p0, L, x);
            xx = xx + 1;
        end
    end
end
end

xx = 1; % A counter for x-position.
for x = x0:dx:x1 % w is calculated for every dx for x0 <= x <= x1.
    w(xx) = w(xx) + WHdynw(NF, omega, Omega, p, L, x, t);
    xx = xx + 1; % Increment in position.
end

x=x0:dx:x1; % Array with the points at which the deflection is calculated.

% Generating the plot:
plot(x, w*1000)
xlabel('Position x [m]')
ylabel('Radial deflection w [mm]')
ymax=ylim;
text(0.75*(x1-x0), 0.92*ymax(2), ['Time: t = ' num2str(t*1000) ' ms'])
title(['Radial deflection of a ' num2str(MR*2000) 'mm ' matr1 ' pipe, ' num2str(hM*1000) 'mm
thick,'] [' with ' num2str(N) ' laminae of ' matr2])

```

pointwoft.m

```
%pointwoft.m
% This script generates a plot of the radial vibration at one point
% along a pipeline, due to water hammer conditions, as a function of
% time.
%
% Kristen Rege
% Created: 2016-04-18
% Modified: 2016-05-30

clc, close % Initiating.

if exist('menuentry', 'var') == 1 % If program is started from main menu,
    project = project; % that project name is used.
else
    clear % If not, the data is taken from the
    project = 'WHammerInput'; % Excel sheet WHammerInput.
end

addpath('WHToolbox') % Adds the toolbox with the required functions.

% Importing data:
[WHdata, angles, settings] = importWHinput(project);

% Extracting required information:
L = WHdata(6);
hM = WHdata(5);
N = WHdata(13);
MR = WHdata(4);
p0 = WHdata(17);
nhalfrounds = settings{1,7}; % Number of half rounds to compute.

% Calculating required coefficients:
[NF, dp, alpha, omega, Omega, p, Omega0] = WHcoeffs(WHdata, angles);

% Menu allowing the user to choose the position at which to plot:
position = menu('Please select the position along the pipe to plot the radial vibration
for:', '1% of L', '25% of L', '50% of L', '75% of L', '99% of L', 'Other');
if position < 5 && position > 1 % Common values may be directly chosen from
    x = 0.25*(position-1)*L; % the menu:
elseif position == 1
    x = 0.01*L;
elseif position == 5
    x = 0.99*L;
else % Other values may be typed:
    x = input('Enter the position along the pipe to plot the radial vibration for (as a
percentage of L, e.g. 42): ')*L/100;
    disp(' ')
end

% Menu allowing the user to choose t0 and t1:
if nhalfrounds ==1
    interval = menu('Should the radial vibration be plotted for a full half round trip?',
'Yes', 'No, just a part of it');
else
    interval = menu('Should the radial vibration be plotted for a full round trip?', 'Yes',
'No, just a part of it');
end
switch interval
    case 1
        t0 = 0;
        t1 = nhalfrounds*L/alpha;
    case 2
        t0 = input(['Enter t0 [ms] from which to plot, between 0 and ',
num2str(nhalfrounds*1000*L/alpha), ' ms: ']) * 10^(-3);
        error=1; % A while-loop enables the user to retry if a lower
        while error==1 % t1 than t0 is chosen.
            t1 = input(['Enter t1 [ms] at which to stop the plot, between ',
num2str(1000*t0), ' ms and ', num2str(nhalfrounds*1000*L/alpha), ' ms: ']) * 10^(-3);
            if t1<t0
                disp(' ')
                disp(['ERROR: t1 must be larger than t0! Currently, t1 = ', num2str(1000*t1),
' ms, and t0 = ', num2str(1000*t0), ' ms.'])
                disp(' ')
            else
                disp(' ')
            end
        end
    end
end
```

```

        error=0;
    end
end
disp(' ')
end

% Displaying the stacking sequence used in the calculations, to enable
% verification with intended stacking sequence.
disp('A plot is made for a pipe with an overwrap with the following fibre directions (from
the inner lamina and outwards):')
disp([' ', num2str(angles), ''])
disp('Please check that this is the intended stacking sequence.')

% Extracting settings:
dt = settings{1,1};           % Time step.
matr1 = char(settings{1,3});  % Material of pipe.
matr2 = char(settings{1,4});  % Material of overwrap.
apprstatic = settings{1,6};  % Approximate static solution (1) or not (0).

% Executing the calculation:
% A matrix with proper dimension is established to save the deformation:
if p0 == 0
    w = zeros(1, floor((t1-t0)/dt)+1);
else
    if apprstatic == 1; % The approximate static solution is equal in all
        w = ones(1, floor((t1-t0)/dt)+1) * p0/lambda3; % points.
    else
        w = zeros(1, floor((t1-t0)/dt)+1);
        tt = 1; % Fourier solution for the static displacement:
        for t = t0:dt:t1
            w(tt) = WHstatw(NF, Omega0, p0, L, x);
            tt = tt + 1;
        end
    end
end
end

tt = 1; % A counter for time.
for t = t0:dt:t1 % w is calculated for every dx for x0 <= x <= x1.
    w(tt) = w(tt) + WHdynw(NF, omega, Omega, p, L, x, t);
    tt = tt + 1; % Increment in time.
end

t=t0:dt:t1; % Array with the instants at which the deflection is calculated

% Generating the plot:
plot(t*1000, w*1000)
xlabel('Time t [ms]')
ylabel('Radial deflection w [mm]')
ymax=yli;
text(30*(t1-t0), 0.92*ymax(2), ['Position: x = ' num2str(x) ' m'])
title(['Radial deflection of a ' num2str(MR*2000) 'mm ' matr1 ' pipe, ' num2str(hM*1000) 'mm
thick,'] [' with ' num2str(N) ' laminae of ' matr2])

```

WHMovie.m

```

%WHMovie.m
% This script generates an animation, illustrating the vibration of a
% pipeline due to water hammer conditions. Its maximum radial
% displacement during the first (or half of the first) round trip is also
% found. The user is able to save the animation, either as images or a
% movie file. The quality of the movie will depend on the user's
% operating system, and available video codecs however.
%
% Kristen Rege
% Created: 2016-04-19
% Modified: 2016-05-24

clc, close % Initiating.

if exist('menuentry', 'var') == 1 % If program is started from main menu,
    project = project; % that project name is used.
else
    clear % If not, the data is taken from the
    project = 'WHammerInput'; % Excel sheet WHammerInput.
end

```

```

addpath('WHToolbox') % Adds the toolbox with the required functions.

% Importing data:
[WHdata, angles, settings] = importWHinput(project);

% Extracting required information:
L = WHdata(6);
hM = WHdata(5);
N = WHdata(13);
MR = WHdata(4);
p0 = WHdata(17);

% Calculating required coefficients:
[NF, dp, alpha, omega, Omega, p, Omega0] = WHcoeffs(WHdata, angles);

% Menu to enable saving of the movie:
save = menu('Do you want to save the movie?', 'No', 'Yes, as images', 'Yes, as an avi-file');

% Displaying the stacking sequence used in the calculations, to enable
% verification with intended stacking sequence.
disp('A plot is made for a pipe with an overwrap with the following fibre directions (from
the inner lamina and outwards):')
disp(['[' , num2str(angles), ']'])
disp('Please check that this is the intended stacking sequence.')

% Extracting settings:
dt = settings{1,1}; % Time step.
dx = settings{1,2}; % Length step.
matr1 = char(settings{1,3}); % Material of pipe.
matr2 = char(settings{1,4}); % Material of overwrap.
apprstatic = settings{1,6}; % Approximate static solution (1) or not (0).
nhalfrounds = settings{1,7}; % Number of half rounds to compute.

% Defining the limits of the calculation:
x0 = 0;
x1 = L;
t0 = 0;

% Rounding t1 off to the nearest lower time step:
t1 = nhalfrounds * dt*floor(L/(alpha*dt));

wmax = 0; % Making space for the determination of the max deformation.
xp=x0:dx:x1; % Array with the points at which the deflection is calculated.

if save==2
    c = clock;
    folderN=(['WH-', num2str(c(1)), '-', num2str(c(2)), '-', num2str(c(3)), '-',
num2str(c(4)), '-', num2str(c(5))]);
    mkdir(folderN); % Creating a new folder with current date and time as
% name, to save the images.
end

if save==3 % Naming the movie with current date and time.
    c = clock;
    movname=(['WH-', num2str(c(1)), '-', num2str(c(2)), '-', num2str(c(3)), '-',
num2str(c(4)), '-', num2str(c(5)), '-', num2str(c(6)), '.avi']);
    aviobj = avifile(movname,'compression','None', 'FPS', 1/(dt*10000));
end % Initiating movie recording.

% A matrix with proper dimension is established to save the deformation:
if p0 == 0
    w = zeros(round((t1-t0)/dt)+1, round((x1-x0)/dx)+1);
else
    if apprstatic == 1;% The approximate static solution is equal for all x
        w = ones(round((t1-t0)/dt)+1, round((x1-x0)/dx)+1) * p0/lambda3;
    else
        wst = zeros(1, round((x1-x0)/dx)+1);
        xx = 1; % Fourier solution for the static displacement:
        for x = x0:dx:x1 % Calculated for one time step:
            wst(1, xx) = WHstatw(NF, Omega0, p0, L, x);
            xx = xx + 1;
        end % The calculated static deflection is copied to all time steps:
        w = repmat(wst, round((t1-t0)/dt)+1, 1);
    end
end
end

```

```

% These couple of lines generates the last image frame (but hidden), so
% that the required upper and lower limits of the y-axis may be found:
xx = 1; % A counter for x-position.
wtrial = zeros(1, round((x1-x0)/dx)+1);
for x = x0:dx:x1 % w is calculated for every dx for x0 <= x <= x1.
    winst = WHdynw(NF, omega, Omega, p, L, x, t1/nhalfrounds);
    wtrial(xx) = w(1,xx) + winst;
    xx = xx + 1; % Increment in position
end
plot(xp, wtrial*1000); % The plot is made, but not shown.
ymax=ylim; % The limits of the y-axis are extracted.
if nhalfrounds > 1 % Modifier for second half of the round trip:
    ymax=[-ymax(2)+2000*w(1,round(0.5*L)), ymax(2)];
end

tt=1; % Starting at the first row in the matrix.

% Executing the calculation:
for t = t0:dt:t1 % The plot is made for all time steps.
    xx = 1; % A counter for x-position.

    for x = x0:dx:x1 % w is calculated for every dx for x0 <= x <= x1.
        winst = WHdynw(NF, omega, Omega, p, L, x, t); % Calc. of w.
        w(tt,xx) = w(tt,xx) + winst; % Current w is saved in the matrix.

        if w(tt,xx)>wmax
            wmax = w(tt,xx); % wmax is updated if current w is larger.
            xc = x; % Position for wmax is saved.
            tc = t; % Time for occurrence of wmax is saved.
        end

        xx = xx + 1; % Increment in position.
    end

    % Generating the plot:
    plot(xp, w(tt,:)*1000);
    xlabel('Position x [m]')
    ylabel('Radial deflection w [mm]')
    ylim(ymax); % Using the limits of the y-axis found earlier.
    text(0.8*(x1-x0), 0.92*ymax(2), ['t = ' num2str(t*1000) ' ms'])
    title(['Radial deflection of a ' num2str(MR*2000) ' mm ' matr1 ' pipe, ' num2str(hM*1000)
'mm thick,'] [' with ' num2str(N) ' laminae of ' matr2]))
    drawnow % The plot is shown.

    if save==2 % The images are named from 0001 and upwards:
        if (tt >= 1) && (tt <= 9)
            imgname = ['000', num2str(tt)]; % Zeros are added as necessary
        elseif (tt >= 10) && (tt <= 99) % to get the images sorted.
            imgname = ['00', num2str(tt)];
        elseif (tt >= 100) && (tt <= 999)
            imgname = ['0', num2str(tt)];
        else
            imgname = num2str(tt);
        end % The image is saved as a jpg-file, if so chosen.
        saveas(gcf,fullfile(folderN, imgname), 'jpeg');
    end

    if save==3 % The plot is added to the movie, if so chosen:
        aviobj = addframe(aviobj,gcf);
    end

    tt = tt + 1; % Increment in time.
end

if save==3 % The movie is closed and properly saved:
    aviobj = close(aviobj);
end

disp(' ') % Displaying wmax in the command window:
disp(['The maximum displacement is ', num2str(1000*wmax), ' mm, and occurs at x = ',
num2str(xc), ' m, when t = ', num2str(1000*tc), ' ms.'])

```

wmaxofN.m

```
%wmaxofN.m
% This script allows the user to calculate mean and maximum radial
% deflections of the pipeline, for an user-defined set of N. N is the
% number of FRP laminae added to the metallic pipe. It may be preferable
% to calculate different sets of N in different instances of MATLAB, so
% that multiple processors can be used for the calculation, which is very
% time consuming for long pipes.
%
% Kristen Rege
% Created: 2016-04-21
% Modified: 2016-05-28

clc, close % Initiating.

if exist('menuentry', 'var') == 1 % If program is started from main menu,
    project = project; % that project name is used.
else
    clear % If not, the data is taken from the
    project = 'WHammerInput'; % Excel sheet WHammerInput.
end

addpath('WHToolbox') % Adds the toolbox with the required functions.

% Importing data:
[WHdata, anglesrep, settings, symconfig] = importWHinput(project);

% Extracting required information:
L = WHdata(6);
hM = WHdata(5);
MR = WHdata(4);
hla = WHdata(12);
p0 = WHdata(17);

% Extracting settings:
dt = settings{1,1}; % Time step.
dx = settings{1,2}; % Length step.
matr1 = char(settings{1,3}); % Material of pipe.
matr2 = char(settings{1,4}); % Material of overwrap.
tstart = settings{1,5}; % Alternative start time.
apprstatic = settings{1,6}; % Approximate static solution (1) or not (0).
nhalfrounds = settings{1,7}; % Number of half rounds to compute.

% Defining the limits of the calculation:
x0 = 0;
x1 = L;

% Finding maximum number of laminae, to remain inside thin-walled shell
Nmax = round((2*MR-41*hM)/(39*hla)); % theory.

N0 = -1;
while N0 < 0 || N0 > Nmax % User enters lowest number of laminae:
    N0 = input(['Enter the lowest value of N to calculate wmax for (minimum 0, maximum ',
    num2str(Nmax), '): ']);
end
disp(' ')

N1 = -1;
while N1 < N0 || N1 > Nmax % User enters highest number of laminae:
    N1 = input(['Enter the highest value of N to calculate wmax for (minimum ', num2str(N0),
    ', maximum ', num2str(Nmax), '): ']);
end
disp(' ')

dN = -1;
if N1 == N0 % If only one lamina is to be calculated, dN is set equal to
    dN = 1; % one for simplicity.
else
    while dN < 1 || dN > N1-N0 % User enters the interval for N.
        dN = input(['Enter the magnitude of the intervals between each N (minimum ',
    num2str(1+symconfig), ', maximum ', num2str(N1-N0), '): ']);
    end
    disp(' ')
end
```

```

% t0 is chosen from a menu:
starttt = menu('Calculate for all t?', 'Yes', ['No, only for t > ' num2str(tstart*100) '% of
full time']);
if starttt == 1
    t0 = 0;
end

% User may choose to show an illustration of the deflection during calcs:
showimg = menu('Do you want to view the deformation pattern as it is calculated?', 'No', 'Yes
(increased computational time)');

if showimg == 2
    xp=x0:dx:x1; % Array with the points at which the defl. is calculated.
else % A progress bar is initiated, if illustrations are not to be shown:
    progress= waitbar(0, ['Progress for N = ', num2str(N0)]);
end

duration = 0; % Variable for saving the time used to calculate.

for N = N0:dN:N1 % A for-loop for all N.
    tic; % Recording of passed time starts.
    WHdata(13) = N; % N is entered to the data.

    % Constructing the array of angles:
    angles = allangles(anglesrep, N, symconfig);

    % Calculating required coefficients:
    [NF, dp, alpha, omega, Omega, p, Omega0] = WHcoeffs(WHdata, angles);

    % Rounding t1 off to the nearest lower time step:
    t1 = nhalfrounds * dt*floor(L/(alpha*dt));

    if starttt == 2
        t0 = dt*round(tstart*t1/dt);
    end

    wmax = 0; % Making space for the determination of the max deformation.

    % A matrix with proper dimension is established to save the deformation
    if p0 == 0
        w = zeros(round((t1-t0)/dt)+1, round((x1-x0)/dx)+1);
    else % The approximate static solution is equal for all x:
        if apprstatic == 1;
            w = ones(round((t1-t0)/dt)+1, round((x1-x0)/dx)+1) * p0/lambda3;
        else
            wst = zeros(1, round((x1-x0)/dx)+1);
            xx = 1; % Fourier solution for the static displacement:
            for x = x0:dx:x1 % Calculated for one time step:
                wst(1, xx) = WHstatw(NF, Omega0, p0, L, x);
                xx = xx + 1; % The calculated static deflection is copied
            end
            % to all time steps:
            w = repmat(wst, round((t1-t0)/dt)+1, 1);
        end
    end

    if showimg == 2 % These couple of lines generates the last image frame
        % (but hidden), so that the required upper and lower limits of the
        % y-axis may be found:
        xx = 1; % A counter for x-position.
        wtrial = zeros(1, round((x1-x0)/dx)+1);
        for x = x0:dx:x1 % w is calculated for every dx for x0 <= x <= x1.
            winst = WHdynw(NF, omega, Omega, p, L, x, t1/nhalfrounds);
            wtrial(xx) = w(1,xx) + winst;
            xx = xx + 1; % Increment in position
        end
        plot(xp, wtrial*1000); % The plot is made, but not shown.
        ymax=yylim; % The limits of the y-axis are extracted.
        if nhalfrounds > 1 % Modifier for second half of the round trip:
            ymax=[-ymax(2)+2000*w(1,round(0.5*L)), ymax(2)];
        end
    else
        progint=0; % Resets and writes current N to the progress bar:
        waitbar(progint/100, progress, ['Progress for N = ', num2str(N)]);
    end
end

```

```

tt=1; % Starting at the first row in the matrix.

% Executing the calculation:
for t = t0:dt:t1 % The plot is made for all time steps.
    xx = 1; % A counter for x-position.

    for x = x0:dx:x1 % w is calculated for every dx for x0 <= x <= x1.
        winst = WHdynw(NF, omega, Omega, p, L, x, t); % Calc. of w.
        w(tt,xx) = w(tt,xx) + winst; % Current w is saved in the matrix

        if w(tt,xx)>wmax
            wmax = w(tt,xx); % wmax is updated if current w is larger.
            xc = x; % Position for wmax is saved.
            tc = t; % Time for occurrence of wmax is saved.
        end

        xx = xx + 1; % Increment in position.
    end

    if showing == 2 % Generating the plot:
        plot(xp, w(tt,:)*1000);
        xlabel('Position x [m]')
        ylabel('Radial deflection w [mm]')
        ylim(ymax); % Using the limits of the y-axis found earlier.
        text(0.8*(x1-x0), 0.92*ymax(2), ['t = ' num2str(t*1000) ' ms'])
        title(['Radial deflection of a ' num2str(MR*2000) 'mm ' matr1 ' pipe, '
num2str(hM*1000) 'mm thick,'] [' with ' num2str(N) ' laminae of ' matr2]);
        drawnow % The plot is shown.
    else % The progress bar is updated for every percentage increment:
        if round(((t-t0)/(t1-t0))*100) > progint
            progint = round(((t-t0)/(t1-t0))*100);
            waitbar(progint/100, progress);
        end
    end

    tt = tt + 1; % Increment in time.
end % The entire matrix w has now been calculated for the specific N.

% The mean and maximum displacements are saved to a txt-file:
wmean = (dp+p0)/lambda3;
output = [N, wmean, wmax, xc, tc];
dlmwrite([project, '.txt'], output, '-append', 'delimiter', '\t')

disp(' ') % Displaying wmax and wmean in the command window:
disp(['The maximum deflection for N = ', num2str(N) ' is ', num2str(1000*wmax), ' mm, and
occurs at x = ', num2str(xc), ' m, when t = ', num2str(1000*tc), ' ms.'])
disp(['The mean radial deflection for N = ', num2str(N) ' is ', num2str(1000*wmean), '
mm.'])

duration = duration + toc; % The time passed since tic is saved.
if N<N1 % The remaining time is estimated, based on passed time:
    timeleft = ((N1-N)/(dN+N-N0))*duration;
    if timeleft < 181 % The remaining time is stated in seconds,
        disp(' ') % minutes or hours, as fitting.
        disp(['Estimated time remaining: ', num2str(round(timeleft)), ' s'])
    elseif timeleft/60 < 121
        disp(' ')
        disp(['Estimated time remaining: ', num2str(round(timeleft*100/60)/100), ' min'])
    else
        disp(' ')
        disp(['Estimated time remaining: ', num2str(round(timeleft/36)/100), ' h'])
    end
else % If the calculation is completed, the time passed is shown:
    disp(' ')
    disp(['Calculation completed after: ', num2str(round(duration*100/60)/100), ' min'])
end
end

if showing == 1 % The progress bar is closed.
    close(progress);
end

```


plotwofN.m

```
%plotwofN.m
% This script allows the user to plot the mean and maximum radial
% deflections of the pipeline, as a function of N, using the data
% calculated with the script maxwofN.m. N is the number of FRP laminae
% added to the metallic pipe.
%
% Kristen Rege
% Created: 2016-04-22
% Modified: 2016-06-03

clc, close % Initiating.

if exist('menuentry', 'var') == 1 % If program is started from main menu,
    project = project; % that project name is used.
else
    clear % If not, the data is taken from the
    project = 'WHammerInput'; % Excel sheet WHammerInput.
end

addpath('WHToolbox') % Adds the toolbox with the required functions.

% Importing data:
[WHdata, angles, settings] = importWHinput(project);
hM = WHdata(5); % Thickness of metal pipe.
MR = WHdata(4); % Radius of metal pipe.
matr1 = char(settings{1,3}); % Material of pipe.
matr2 = char(settings{1,4}); % Material of overwrap.

% Importing the data generated in maxwofN.m:
M = dlmread([project, '.txt']);
M = sortrows(M); % Sorting M after increasing values of N.
N = M(:,1);
wmean = M(:,2);
wmax = M(:,3);

% Plotting the figure:
plot(N, wmax*1000, 'xr-')
xlabel('Number of laminae N')
ylabel('Radial deflection w [mm]')
title(['Radial deflection of a ' num2str(MR*2000) 'mm ' matr1 ' pipe, ' num2str(hM*1000) 'mm
thick,'] [' with N laminae of ' matr2]))
hold on
plot(N, wmean*1000, '*b-')
legend('Max dynamic','Mean dynamic')
ylim([800*min(wmean) 1200*max(wmax)])
%print('FIG2','-depsc','-tiff') % To save fig in eps-format.
```

checkStress.m

```
%checkStress.m
% This script calculates the pipe wall stresses at position x, and time
% t, due to water hammer conditions. The stresses in both the steel pipe
% and the FRP overwrap are calculated. The stresses are then compared to
% the von Mises and Tsai-Wu failure criteria.
%
% Kristen Rege
% Created: 2016-05-26
% Modified: 2016-06-04

clc, close % Initiating.

if exist('menuentry', 'var') == 1 % If program is started from main menu,
    project = project; % that project name is used.
else
    clear % If not, the data is taken from the
    project = 'WHammerInput'; % Excel sheet WHammerInput.
end

addpath('WHToolbox') % Adds the toolbox with the required functions.

% Importing data:
[WHdata, angles, settings] = importWHinput(project);

% Importing failure stresses:
filename = ([project, '.xls']); % The name of the spreadsheet.
[numdata] = xlsread(filename); % Reading numerical values from the spreadsheet.
sigmaY = numdata(4,1)*10^6; % Yield strength of the metal.
sigma1T = numdata(24,1)*10^6;
sigma1C = numdata(25,1)*10^6;
sigma2T = numdata(26,1)*10^6;
sigma2C = numdata(27,1)*10^6;
tau12F = numdata(28,1)*10^6;

% Extracting required information:
L = WHdata(6); % Length of pipe.
nhalfrounds = settings{1,7}; % Number of half rounds to compute.

% Calculating required coefficients:
[NF, dp, alpha, omega, Omega, p, Omega0] = WHcoeffs(WHdata, angles);

% User enters values for x and t:
disp('The values of x and t giving the highest radial deflection should be found');
disp('by using one of the other scripts, and entered here. ');
x = input(['Enter a x-position from 0 to ', num2str(L), ' meters at which to calculate
stresses: ']);
t = input(['Enter the time t from 0 to ', num2str(floor(10000*nhalfrounds*L/alpha)/10), ' ms
at which to calculate stresses: '])*10^(-3);
disp(' ')

% Using the function WHstress to calculate the stress components:
[sigmaM, sigmaxyFRPi, sigma12FRPi, sigmaxyFRPo, sigma12FRPo] = WHstress(project, x, t);

% Extracting the stresses in the metal pipe:
sigmaxM = sigmaM(1);
sigmayM = sigmaM(2);

% Equivalent von Mises stress:
sigmaVM = sqrt(sigmaxM^2 - sigmaxM*sigmayM + sigmayM^2);

% Printing output:
disp(['von Mises stress in the metal pipe: ', num2str(round(sigmaVM*10^(-5))/10), 'MPa']);
disp(['Yield strength of the metal pipe: ', num2str(round(sigmaY*10^(-5))/10), 'MPa']);
if sigmaVM>sigmaY
    disp('The metal pipe is subjected to yielding.')
else
    disp(['Safety factor for the metal pipe: ', num2str(round(100*sigmaY/sigmaVM)/100)]);
end
disp(' ')

% Extracting the stresses in the innermost FRP lamina:
sigma1i = sigma12FRPi(1);
sigma2i = sigma12FRPi(2);
tau12i = sigma12FRPi(3);
```

```

% Extracting the stresses in the outermost FRP lamina:
sigma1o = sigma12FRPo(1);
sigma2o = sigma12FRPo(2);
tau12o = sigma12FRPo(3);

% Coefficients in the Tsai-Wu criterion:
F1 = 1/sigma1T + 1/sigma1C;
F2 = 1/sigma2T + 1/sigma2C;
F11 = -1/(sigma1T*sigma1C);
F22 = -1/(sigma2T*sigma2C);
F66 = (1/tau12F)^2;

% Calculating the Tsai-Wu criterion:
TWi = F1*sigma1i + F2*sigma2i + F11*sigma1i^2 + F22*sigma2i^2 + F66*tau12i^2 -
sqrt(F11*F22)*sigma1i*sigma2i;
TWO = F1*sigma1o + F2*sigma2o + F11*sigma1o^2 + F22*sigma2o^2 + F66*tau12o^2 -
sqrt(F11*F22)*sigma1o*sigma2o;

% Printing the results:
disp(['The Tsai-Wu expression for the innermost FRP lamina is equal to ',
num2str(round(TWi*100)/100), '.']);
disp(['The Tsai-Wu expression for the outermost FRP lamina is equal to ',
num2str(round(TWO*100)/100), '.']);
disp('Failure occurs when this value is equal to 1 or higher. ');

if TWi >= 1
    disp('The innermost FRP lamina is subjected to failure. ');
elseif TWO >= 1
    disp('The outermost FRP lamina is subjected to failure. ');
else
    disp('The laminate is intact, and does not fail. ');
    if TWi >= 0
        disp(['Safety factor for the innermost lamina: ', num2str(round(100/TWi)/100)]);
    end
    if TWO >= 0
        disp(['Safety factor for the outermost lamina: ', num2str(round(100/TWO)/100)]);
    end
end
end

```

usageFactorsofN.m

```

%usageFactorsofN.m
% This script calculates the usage factor (1/(safety factor)) for a steel
% pipe and its FRP overwrap, for different values of the number of FRP
% laminae, N.
%
% Kristen Rege
% Created: 2016-05-29
% Modified: 2016-06-04

clc, close % Initiating.

if exist('menuentry', 'var') == 1 % If program is started from main menu,
    project = project; % that project name is used.
else
    clear % If not, the data is taken from the
    project = 'WHammerInput'; % Excel sheet WHammerInput.
end

addpath('WHToolbox') % Adds the toolbox with the required functions.

% Importing data:
[WHdata, angles, settings] = importWHinput(project);
hM = WHdata(5); % Thickness of metal pipe.
MR = WHdata(4); % Radius of metal pipe.
matr1 = char(settings{1,3}); % Material of pipe.
matr2 = char(settings{1,4}); % Material of overwrap.

% Importing failure stresses:
filename = ([project, '.xls']); % The name of the spreadsheet.
[numdata] = xlsread(filename); % Reading numerical values from the
% spreadsheet.
sigmaY = numdata(4,1)*10^6; % Yield strength of the metal.
sigma1T = numdata(24,1)*10^6;
sigma1C = numdata(25,1)*10^6;

```

```

sigma2T = numdata(26,1)*10^6;
sigma2C = numdata(27,1)*10^6;
taul2F = numdata(28,1)*10^6;

% Importing the data generated in maxwofN.m:
M = dlmread([project, '.txt']);
M = sortrows(M); % Sorting M after increasing values of N.
Nused = M(:,1); % Number of laminae N.
xc = M(:,4); % Position for maximum radial deflection.
tc = M(:,5); % Time for maximum radial deflection.

usageM=zeros(1,size(Nused,1));
usageFRPi=zeros(1,size(Nused,1));
usageFRPo=zeros(1,size(Nused,1));

% Calculating usage factor for each N:
for n=1:size(Nused,1)

    N=Nused(n);
    x=xc(n);
    t=tc(n);

    % Using the function WHstress to calculate the stress components:
    [sigmaM, sigmaxyFRPi, sigma12FRPi, sigmaxyFRPo, sigma12FRPo] = WHstress(project, x, t,
N);

    % Extracting the stresses in the metal pipe:
    sigmaxM = sigmaM(1);
    sigmayM = sigmaM(2);

    % Equivalent von Mises stress:
    sigmaVM = sqrt(sigmaxM^2 - sigmaxM*sigmayM + sigmayM^2);

    usageM(n) = sigmaVM/sigmaY;

    % Extracting the stresses in the innermost FRP lamina:
    sigma1i = sigma12FRPi(1);
    sigma2i = sigma12FRPi(2);
    taul2i = sigma12FRPi(3);

    % Extracting the stresses in the outermost FRP lamina:
    sigma1o = sigma12FRPo(1);
    sigma2o = sigma12FRPo(2);
    taul2o = sigma12FRPo(3);

    % Coefficients in the Tsai-Wu criterion:
    F1 = 1/sigma1T + 1/sigma1C;
    F2 = 1/sigma2T + 1/sigma2C;
    F11 = -1/(sigma1T*sigma1C);
    F22 = -1/(sigma2T*sigma2C);
    F66 = (1/taul2F)^2;

    % Calculating the Tsai-Wu criterion:
    TWi = F1*sigma1i + F2*sigma2i + F11*sigma1i^2 + F22*sigma2i^2 + F66*taul2i^2 -
sqrt(F11*F22)*sigma1i*sigma2i;
    TTwo = F1*sigma1o + F2*sigma2o + F11*sigma1o^2 + F22*sigma2o^2 + F66*taul2o^2 -
sqrt(F11*F22)*sigma1o*sigma2o;

    usageFRPi(n) = TWi;
    usageFRPo(n) = TTwo;

end

% Plotting the figure:
plot(Nused, usageM, 'xr-')
xlabel('Number of laminae N')
ylabel('Usage factor')
title(['Usage factor of a ' num2str(MR*2000) 'mm ' matr1 ' pipe, ' num2str(hM*1000) 'mm
thick,'] [' with N laminae of ' matr2])
hold on
grid on
plot(Nused, usageFRPo, '*b-')
plot(Nused, usageFRPi, '+k-')
legend([matr1, ' pipe'], 'outermost FRP lamina', 'innermost FRP lamina')
ylim([0 1.3*max(usageM)])

```